A TCR MIMIC ANTIBODY TARGETS IMMUNOPROTEASOME-REGULATED PRAME PEPTIDE/HLA-I ANTIGENS FOR CANCER THERAPY

A Dissertation

Presented to the Faculty of the Weill Cornell Graduate School

of Medical Sciences

in Partial Fulfillment of the Requirements for the Degree of

Doctor of Philosophy

by

Aaron Y. Chang

May 2018

A TCR MIMIC ANTIBODY TARGETS IMMUNOPROTEASOME-REGULATED PRAME PEPTIDE/HLA-I ANTIGENS FOR CANCER THERAPY

Aaron Y. Chang, Ph.D.

Cornell University 2018

Preferentially expressed antigen in melanoma (PRAME) is a cancer-testis antigen that is expressed in many cancers and leukemias; in healthy tissue, PRAME is limited to the testes and ovaries, making it a highly attractive cancer target. PRAME is an intracellular protein that cannot currently be drugged. After proteasomal processing, the $PRAME^{300-309}$ peptide (ALY) is presented in the context of human lymphocyte antigen HLA-A*02:01 molecules, for recognition by the T cell receptor (TCR) of cytotoxic T cells. We describe Pr20, a TCR mimic (TCRm) human IgG1 antibody discovered through phage-display technology that recognizes the cell-surface ALY peptide/HLA-A2 complex; Pr20 is an immunological tool and potential therapeutic agent. Pr20 bound to ALY peptide-pulsed cells and PRAME+/HLA-A2+ cancers. An afucosylated Fc form (Pr20M) directed antibody-dependent cellular cytotoxicity against PRAME+/HLA-A2+ leukemia cells and was therapeutically active in human leukemia models *in vivo* as a monotherapy. Interestingly, in some tumors, Pr20 binding markedly increased upon IFNγ treatment, mediated by induction of the immunoproteasome catalytic subunit β5i. The immunoproteasome reduced internal destructive cleavages within the ALY epitope compared to the constitutive proteasome.

The ALY/HLA-A2 epitope expression is far lower than traditional mAb targets and therefore we explored strategies to enhance potency of Pr20M. We demonstrate that

combining Pr20M and CD47 ‘do not eat me’ signal blockade (using a SIRPα-variant peptide called CV1) led to enhanced antibody dependent cellular phagocytosis (ADCP) and dramatic therapeutic effects in leukemia xenograft models. We also engineer a bispecific T cell engager (BiTE) and chimeric antigen receptor (CAR) T cell using the Pr20 scFv. Pr20-BiTE and Pr20-CAR were both capable of potent redirected T cell lysis against PRAME+/HLA-A2+ leukemia *in vitro*, however these constructs also had off-target activities against HLA-A2+ cells despite undetectable binding of Pr20.

Finally, we confirm the MAPK pathway as an important regulator of HLA-I expression through a high-throughput small molecule inhibitor screen and describe mTOR as a potential regulator of HLA-I. We also discover that a 5-lipoxygenase inhibitor BW-B70c can enhance HLA-I expression through transcriptional regulation but through a mechanism independent of 5-lipoxygenase. BW-B70c treatment increases tumor-antigen presentation on HLA-I and sensitizes cells to TCRm-mediated ADCC. We also explore the use of the cytomegalovirus immunoevasin US6 to modulate antigen presentation on HLA-I with the goal of identifying strategies to protect engineered cellular therapeutics harboring foreign or synthetic transgenes from immunological attack.

The data provide rationale for developing TCRm antibodies as therapeutic agents for cancer, offer mechanistic insight on proteasomal regulation of tumor-associated peptide/HLA antigens, yield possible therapeutic solutions to these ultra-low surface presentation targets, and explore a strategy to protect genetically engineered cells harboring foreign genes from immunological attack.

BIOGRAPHICAL SKETCH

Aaron was born and raised in the San Jose, California area. He developed an interest in lab research through COSMOS, a high school summer program, where he learned DNA cloning and molecular biology techniques at the University of California, Davis. Having no prior exposure to the bioscience field, he was captivated by the possibilities of recombinant DNA technology, which to him might as well have been science fiction. His curiosity led him to pursue a BS in Molecular Biology at the University of California, San Diego. There, he grew to enjoy lab-work as an intern at The Scripps Research Institute. He developed a passion in translational research, dreaming of making discoveries or developing technologies that could help treat patients. Therefore he continued at UC San Diego for a MS in Immunology, studying dendritic cell dysfunction during viral infections in the lab of Dr. Elina Zuniga. His disease interests shifted to cancer: an ailment that strikes personally as his mother and father are both cancer survivors. He realized the amazing complexity of cancer as a disease and the need to understand more about cancer biology. He decided to pursue a PhD at Cornell University - Weill Graduate School of Medical Sciences, where he joined Dr. David Scheinberg's lab at Memorial Sloan Kettering Cancer Center. There, he studied novel antibody constructs and mechanisms of tumor-antigen presentation, fusing his interests in cancer biology with his background in immunology. Aaron contributed significantly to several exciting projects, which furthered his drive to continue pursuing research in immuno-oncology. He will be starting a postdoc position at Pfizer in June 2018 with Pfizer's Oncology Research Unit at Pearl River, NY where he hopes to uncover meaningful strategies to potentiate cancer immunotherapy.

To my parents and my sisters for their love and endless support throughout my pursuits. To my friends, Cornell classmates, and the Scheinberg lab members who continuously inspire me to break my own boundaries.

AKNOWLEDGEMENTS

The author would like to thank all scientists involved with the present work, both in the Scheinberg lab and collaborators, especially scientists from Eureka Therapeutics and the Garcia group at Stanford University. This work was funded by multiple grants including in part, the Office of Assistant Secretary of Defense for Health Affairs through the Peer Reviewed Cancer Research Program under award no. W81XWH-16-1-0242. Opinions, interpretations, conclusions, and recommendations are those of the author and are not necessarily endorsed by the Department of Defense.

The author would like to thank all past and present members of the Scheinberg lab for their intellectual curiosity, technical skills, and an infectious drive for scientific endeavor. Special acknowledgments must be given to Dr. Tao Dao, who initiated this project and entrusted me to develop it from an early stage; and Ron Gejman, for specialized assistance in bioinformatics analysis. Additional thanks must be given to Casey Jarvis, Andrew Scott, Melissa Mathias, Elliott Brea, Claire Oh, and Nick Veomett, who have helped develop assays and generated data and reagents. Thanks must also be given to Thomas Gardner, Martin Klatt, Heather Jones, Megan Dacek, Pedro Silberman, and Sungsoo (Mike) Mun for technical assistance and intellectual discussions. Additional acknowledgements are presented in the following chapters.

Most importantly, the author would like to thank Dr. David Scheinberg for encouraging creative scientific thinking and for the many lessons to be applied both in and out of the lab. Without his consistent enthusiasm and strong mentorship, this work would not have been possible. His scientific curiosity is truly contagious.

TABLE OF CONTENTS

LIST OF FIGURES

CHAPTER I: TARGETING IMMUNOPROTEASOME-REGULATED PRAME PEPTIDE/HLA-I ANTIGENS WITH A THERAPEUTIC ANTIBODY

LIST OF TABLES

LIST OF ABBREVIATIONS

5-LO	5-Lipoxygenase
ADCC	Antibody-dependent cellular cytotoxicity
ADCP	Antibody-dependent cellular phagocytosis
ALL	Acute lymphoblastic leukemia
ALL	Acute lymphoblastic leukemia
ALY	ALYVDSLFFL - PRAME peptide
AML	Acute myeloid leukemia
AML	Acute myeloid leukemia
BiTE	Bispecific T cell Engager
CAR	Chimeric Antigen Receptor
Cas9	CRISPR associated protein 9
CDR	Complementarity-determining regions
CML	Chronic myeloid leukemia
CRISPR	Clustered regularly interspaced short palindromic repeats
cTEC	cortical thymic epithelial cells
CTL	cytotoxic T lymphocytes
CTLA4	Cytotoxic T lymphocyte-associated protein 4
CV1	SIRPα Consensus Variant 1
Fab	Fragment, antigen binding
Fc	Fragment, crystallizable
FcR	Fragment, crystallizable receptor
GAPDH	Glyceraldehyde 3-phosphate dehydrogenase
HLA	Human leukocyte antigen
HSV-TK	Herpes simplex virus thymidine kinase

IFNγ	Interferon gamma
Ig	Immunoglobulin
IRF1	Interferon regulatory factor 1
mAb	monoclonal antibody
MAPK	Mitogen-activated protein kinase
MEK	MAPK/ERK Kinase
MHC	Major histocompatibility complex
mTOR	Mammalian target of rapamycin
NK	Natural killer
NPI	Normalized percent inhibition
NSG mouse	NOD.Cg-*Prkdc*^{scid} IL2rg^{tm1Wjl}/SzJ mice
Ova	Chicken ovalbumin protein
PBMC	Peripheral blood mononuclear cells
PD-1	Programmed cell death protein 1
PD-L1	Programmed death-ligand 1
pMHC	Peptide / MHC
POC	Percent of control
Pr20	anti-PRAME$^{300-309}$/HLA-A2 clone 20
Pr20M	Pr20 - Modified ADCC through Glycosylation Engineering
PRAME	Preferentially expressed antigen in melanoma
scFv	Single chain fragment variable
SIINFEKL	Chicken Ova$^{257-264}$
SIRPα	Signal regulatory protein alpha
STAT1	Signal transducer and activator of transcription 1
STING	Stimulator of interferon genes
TAP	Transporter associated with peptide processing

TBP	TATA-binding protein
TCR	T cell receptor
TCRm	T cell receptor mimic
TEIPP	T cell epitopes associated with impaired peptide processing
TLR	Toll like receptor
TNFα	Tumor Necrosis Factor alpha
UMP1	Proteasome maturation factor UMP1
US6	Unique short region protein 6
WT1	Wilms tumor protein 1
β2M	beta-2-microglobulin

INTRODUCTION

Monoclonal Antibodies for Cancer Therapy

Monoclonal antibodies (mAbs) are potent protein drugs that can modulate cellular signaling pathways in disease and redirect immunological attack[1–3]. Antibodies are produced naturally in the immune system for recognizing and neutralizing pathogens such as bacteria and viruses. They are produced in high amounts by differentiated B cells called plasma cells in several immunoglobulin (Ig) isotypes: IgG, IgM, IgE, IgA, and IgD[4], however the vast majority of therapeutic antibodies are of IgG isotype[3]. IgG are Y-shaped antibodies containing a two-armed fragment antigen-binding (Fab) component generating two antigen binding sites, and one fragment crystallizable (Fc) portion. The antigen binding sites typically have extremely high-affinity interactions with a target epitope (up to pM to nM range), while the Fc constant region mediates interactions with other immune effector proteins and cells. Structurally, IgG are comprised of 4 polypeptide subunits: 2 immunoglobulin light chains (~25 kD) and 2 immunoglobulin heavy chains (~50 kDa). The light chain comprises of a variable region (V_L) and a constant region (C_L)[4]. The heavy chain has 1 variable region (V_H) and several constant regions (C_H). Typically, each heavy chain is linked to a light chain through a disulfide bond between the C_L and C_H1 to form a dimer arm structure[4]. Meanwhile, the C_H2 region of this arm forms a disulfide bond with another C_H2 to generate a tetrameric two-armed structure[5]. Each variable region contains domains of hypervariable regions or complementarity determining regions (CDR1, CDR2, CDR3) where random somatic recombination of the V(D)J gene segments leads to generation of an extreme diversity of antibody paratopes[6]. Upon B cell activation, there is an additional process of somatic hypermutation at these regions resulting in a colossal antibody repertoire in addition to affinity maturation of specific

antibody clones[7]. The subtype of IgG determines Fc effector functionality such that IgG1 and IgG3 have stronger immune effector activation capability through activating Fc Receptors (FcR) compared to IgG2 and IgG4[4]. These properties are mediated by affinity to either activating or inhibitory FcR found on specific immune cells such as macrophages, dendritic cells, and natural killer (NK) cells. For cancer therapy, mAbs are typically designed to either block receptor signaling cascades required for cancer growth, stimulate signaling cascades that enhance anti-tumor effects and immunity, or bind to cancer cells and mark them for immune attack by macrophages and NK cells. These immune cells can recognize mAb-coated tumor cells through activating FcR to engage in antibody dependent cellular phagocytosis and cytotoxicity[3]. Whereas the natural antibody responses in mammals generates a pool of polyclonal antibodies that bind varies epitopes on an pathogen, modern molecular and cellular techniques have allowed the generation of monoclonal antibodies that are identical in molecular structure and target epitope allowing for exquisite control over the mechanism of action and preventing unintended and often unpredictable off-target engagement[8].

The majority of modern mAbs are generated through either hybridoma technology or phage-display technology. The hybridoma approach requires immunization of an animal, typically mice, with the target antigen, then harvesting the plasma cells before fusing them with a cancerous myeloma cell to cause immortalization of plasma cells – called hybridomas[9]. Each hybridoma clone secretes a unique mAb that can be grown indefinitely *in vitro*. Although most US Food and Drug Administration (FDA)-approved mAb drugs were produced through hybridoma technology, a major limitation is that the mAbs are murine of origin, which would lead to rapid clearance through an anti-murine immune response in humans. This typically would require subsequence processes to make chimeric (consisting of human Fc region with murine

Fab) or humanized (murine CDR sequences genetically grafted onto human antibody sequences). This can be circumvented through the use of transgenic mice that express human immunoglobulin genes such as the VelocImmune[10] mouse (Regeneron) and Xenomouse[11] (Amgen) technological platforms. The other major approach to generating mAbs is through phage-display library screening. In phage-display, a large genetic library of Fab regions is generated from donor B cells or a synthetic library is randomly generated through PCR techniques[9,12]. These libraries are then expressed as single chain variable fragments (scFv) in bacteriophage such that each phage displays only one unique scFv[9,12–14]. scFv are fusion proteins of the variable regions of the heavy (V_H) and light chains (V_L) of immunoglobulin, connected with a short linker peptide of ten to about 25 amino acids. Libraries can then be panned against a desired target such that reactive phages are bound while non-reactive phages are washed away. Sequences of desired clones are then cloned into a human IgG scaffold and expressed as full-length mAb and purified[15].

Indeed, mAbs have become an essential format in our armamentarium for cancer therapy. For example, the anti-CD20 mAb Rituximab for lymphoma and chronic lymphocytic leukemia[2,16] and anti-HER2 mAb Trastuzumab for HER+ breast cancer[17,18] have revolutionized the way we treat these diseases. Both Rituximab and Trastuzumab have multiple mechanisms of action. Rituximab binds CD20 on B-cell lymphomas to (1) initiate signaling cascades that lead to apoptosis, (2) recruit Fc-dependent complement cascade to lyse tumor cells, and (3) to recruit Fc-dependent immune actions such as antibody-dependent cellular cytotoxicity (ADCC) and antibody-dependent cellular phagocytosis (ADCP)[19]. Trastuzumab can (1) block essential HER2 receptor kinase signaling in breast cancer cells, (2) trigger HER2 degradation, and (3) recruit immune cells to mediate ADCC[20]. Indeed, the efficacy of

several mAb drugs against cancer is commonly attributed to the ability of mAbs to engage several independent mechanisms of action[21]. However, a major limitation of mAbs is that they are typically confined to only access cell-surface antigens while the vast majority of aberrations in cancers such as over-expressed tumor-associated antigens, point mutation proteins, and translocation products, are intracellular proteins[22] and not accessible to traditional mAbs. Recent advances have led to exciting developments of cell-penetrating mAbs[23] that can specifically target mutated oncogenic proteins such constitutively active KRas G12D[24], However, these cell-penetrating antibodies can suffer from low potency and do not activate immune engagement because the Fc portion is internalized into the cell and inaccessible to FcR-bearing cells such as macrophages and NK cells.

MHC Class I Antigen Presentation Pathway

Major histocompatibility complex (MHC) is a set of proteins that can complex with peptide fragments derived from other cellular and pathogenic proteins and functions to present these peptides on the cell-surface.[25] T cells can survey these peptide/MHC (pMHC) complexes and can distinguish healthy cells versus cells expressing foreign proteins (infected cells) or mutated genes (malignant cells)[25,26]. This process is an exquisite mechanism of adaptive immune surveillance against intracellular pathogens and cancer. MHC class I (MHC-I) molecules are heterodimers structurally comprised of two polypeptide chains: the MHC-I α chain and beta-2-microglobulin (β2M)[27]. A short peptide fragment (typically 8-10 amino acids) complexes with a peptide-binding pocket in MHC-I formed by α1 and α2 chain[26,27]. All three components: MHC-I, β2M, and a bound peptide, are required for MHC-I stability. The cell-surface presentation of these pMHC antigens is a complex and highly regulated process. Generally, cellular proteins are degraded through the proteasome into peptide fragments in the cytosol.

These peptides are then translocated into the endoplasmic reticulum (ER) through the transporter associated with antigen presentation (TAP) complex, which is an ATP-binding cassette family transporter[28,29]. TAP is a heterodimer made up of 2 subunit proteins: TAP1 and TAP2 both of which are required for function. The TAP complex associates with several other proteins in the peptide-loading complex such as tapasin, calreticulin, and calnexin[27]. Calnexin stabilizes MHC-I α chain until β2M is bound. As MHC-I is not stable without a bound peptide, calreticulin and other proteins act as chaperones that stabilize MHC-I until Tapasin recruits MHC-I/β2M heterodimers to the TAP complex to facilitate peptide loading[27,28]. These peptide/MHC-I complexes are then trafficked to and presented on the cell-surface where they can be surveyed and recognized by the T cell receptor (TCR) of cytotoxic T cells (Fig. 1.1). Upon successful engagement, the T cell will activate and release perforin and granzymes to lyse and kill the target cell[30]. As T cells develop through the process of thymic selection, mature T cells are selected for their inability to react to self-peptide and potential ability to recognize foreign peptides[31]. Cancerous cells are characterized by genomic instability and have acquired several mutated and aberrantly-expressed proteins leading to uncontrolled cell growth[32]. Such proteins can give rise to peptide that are recognized as 'foreign' neo-antigens because they are not found on healthy cells[30,33]. In addition, there are exciting discoveries that antigenic peptides can also be presented on MHC-I as phosphopeptides[34] or derived from alternative sources such as introns[35,36] or proteasome-spliced peptide products[37]. If these neo-antigens and tumor-associated antigens form stable complexes with MHC-I, they can be presented on the cell-surface to be recognized by T cells. Therefore, T cells provide the immune system a fined-tuned mechanism to distinguish between self and foreign peptides to ultimately recognize and kill infected or neoplastic cells. This is particularly important when

foreign or tumor-associated proteins are not expressed as membrane proteins on the cell surface and are not accessible to antibodies or humoral immunity.

MHC-I in humans is known as human leukocyte antigen (HLA) encoded by three loci: HLA-A, HLA-B, and HLA–C for HLA class I (HLA-I), leading to six alleles per person due to the diploid nature[38]. HLA-I is highly polymorphic and there are several thousand annotated alleles generating a multitude of HLA-I proteins with varying peptide-binding pockets and unique sets of associated peptides[39]. The large diversity of HLA alleles likely resulted from the evolutionary advantage of presenting a larger repertoire of peptides allowing protection against more pathogens[40]. Nomenclature of HLA alleles consists of allele family (2 digit code) followed by subtype (third and fourth digit), then further subtypes with synonymous nucleotide polymorphisms or differences in introns or translated regions[41]. Although polymorphisms in the peptide binding cleft results in a range of specificities for different peptide motifs, the majority of variable residues lie toward the middle of the cleft, while conserved large aromatic residues constitute the ends. This leads to conserved peptide 'anchor residues' at the N-terminal and C terminal ends (typically second and last position of a peptide) that face into the HLA peptide binding cleft[42]. Some HLA alleles are more common than others such as the HLA-A*02 superfamily where the HLA-A*02:01 allele is found in approximately 30-40% of the United States population[43–45]. HLA-A*02:01 (abbreviated here forth as HLA-A2) is one of the most common and well-studied HLA alleles and has shed light on several biochemical interactions and processes that define our understanding of peptide / MHC-I immunobiology. Peptides presented by HLA-A2 generally utilize position 2 and positions 9/10 as the N- and C-terminal anchor residues respectively. Position 2 is anchored most dominantly by Leucine, Methionine,

or Valine while position 9/10 is typically anchored by Leucine, Isoleucine, Methionine, Valine, or Alanine[46].

MHC class II molecules (HLA-DP, -DM, -DOA, -DOB, -DQ, -DR in humans) is an additional system to present longer peptides (in the range of 11-30 amino acids) derived from extracellular proteins[47]. Peptide / MHC-II complexes are recognized by CD4+ T cells to activate a helper T cell response which is important for stimulating B cells to generate antigen-specific antibodies[27]. However, expression of MHC-II is typically limited to professional antigen presenting cells while MHC-I are expressed on all nucleated cells and therefore represent a much broader system for directly targeting cancer cells from a wide range of histological origins[27].

T Cell and TCR-based Strategies to Therapeutically Target Peptide/MHC-I Complexes

The T cell receptor (TCR) of T cells recognize peptide / MHC complexes and allow T cells access to the universe of intracellular pathogen and cancer antigens. The enormous diversity of TCR specificities is generated through V(D)J recombination of two TCR chains, the TCR Vα and Vβ chains, which are linked as a pair through a disulfide bond[48]. Additionally, TCR are low-affinity and can be cross-reactive to several peptide / MHC epitopes allowing for the TCR repertoire to react against an even larger range of potential epitopes[49]. The attractive ability to target intracellular proteins has spurred the development of several strategies to use T cells and TCR-based agents in cancer therapy, many of which are in clinical evaluations. These include cancer vaccinations, adoptive T cell therapy, re-infusion of TCR-transduced T cells, or TCR-based protein agents[50]. Cancer vaccines rely on immunizing patients to antigens found in their tumors. This can be performed through immunization with

tumor antigen whole proteins, peptides, or genetic material along with immunostimulatory adjuvants with the goal of generating cytotoxic T cells that can lyse the cancer cells. Indeed, patients vaccinated with these approaches have generated functionally reactive antigen-specific T cells in patients leading to clinical benefits when an immune response develops after vaccination[51]. Adoptive T cell therapy relies on isolating patient T cells before stimulating them with a tumor-specific antigen *ex vivo* with the goal of activating and expanding a polyclonal population of tumor antigen-specific T cells. Expanded anti-tumor T cells are then re-infused into the patient[52]. TCR-transduced T cells rely on extracting T cells from a patient, transducing them with a monoclonal TCR construct directed against a tumor antigen, then re-infusing the T cells back into the patient[53]. Although these TCR-transduced T cells are endowed with anti-tumor lysis capabilities, they can lead to autoimmunity due to unpredictable cross-reactivity upon mis-pairing of the endogenous TCR Vα- or Vβ-chain with the transgenic TCR[53].

The Constitutive Proteasome and Immunoproteasome

The proteasome is a compartmentalized protease with a barrel structure that is important for cellular homeostasis. It functions to degrading proteins marked for catabolism – including misfolded or unneeded proteins[54]. The proteasome regulates several important biochemical pathways, achieved through using ubiquitin as a signal to slate proteins for proteasome degradation. Ubiquitin is a small (8.5 kDa) protein which can be enzymatically conjugated to typically a Lysine residue on a targeted protein through the action of ubiquitin-activating enzymes, ubiquitin-conjugating enzymes, and ubiquitin ligases[55]. Ubiquitination is an important protein post-translational modification that has several functions in cellular processes including to

mark proteins for proteasomal degradation. Structurally, the 26S proteasome consists of a 20S proteolytic core that can be capped on both ends with a 19S regulatory particle[56]. Ubiquitinated proteins are delivered to the proteasome through Ub-dependent chaperones and shuttling factors[55]. The 19S regulatory particle contains receptors that recognize Ubiquitinated proteins, unfold the protein through ATPases, and translocate the protein into the 20S complex for proteolysis[55]. Inside the 20S complex, there are several catalytic subunits generating three distinct proteolytic activities: chymotryptic, tryptic, and caspase-like cleavage[57]. These are hydrolysis reactions that attack the peptide bonds generating peptides of between 4-25 amino acids in length[55]. Although a major function of the proteasome is to degrade proteins for regulation and homeostasis, it also generates peptides that upon further processing can complex with MHC-I molecules to be presented at the cell-surface[26,56].

The proteasome is a multi-subunit complex that can exist in two major forms: the constitutive proteasome and the immunoproteasome, which have altered cleavage specificities and thus generate unique repertoires of peptides[56,58]. They differ in 3 catalytic subunits: β1, β2, and β5 are found in the constitutive proteasome while β1i, β2i, and β5i comprise the immunoproteasome[56,58–60]. β1, β2, and β5 have caspase-like, trypsin-like, and chymotrypsin-like catalytic activity respectively while β1i, β2i, and β5i have chymotrypsin-like, trypsin-like, and chymotrypsin-like catalytic activities[57]. The increased chymotrypsin-like activity causes the immunoproteasome to generally favors cleavage after hydrophobic residues and enhances generation of peptides that can fit into the groove of HLA-I[56,57]. Several antigens are restricted to a specific proteasome form and such knowledge can help dictate immunotherapy strategies against these targets[61–63]. Basal expression of the immunoproteasome is typically restricted to immune cells, however most cell types can induce expression of the

immunoproteasome upon stimulation through pro-inflammatory cytokines such as IFNγ and TNFα[57]. Assembly of the 20s catalytic barrel is a highly regulated and complex process that proceeds sequentially and requires a chaperone protein UMP1[64]. The β subunits are initially translated as pro-peptides and function as their own intramolecular chaperones to assemble the 20s barrel. This is important because during immunoproteasome assembly, β1i enters the assembly pathway earlier than β1 during constitutive proteasome assembly[64]. This leads to favored β2i assembly because of β2i assembly is dependent on β1i. Finally, β5i is preferentially incorporated (over β5) into the intermediate containing β1i and β2i[64]. β5i-propeptide is required to ultimately process pro-β1i and pro-β2i into catalytically functional subunits. β5i also has a higher affinity to UMP1 than β5 and therefore preferentially incorporates into the 20s barrel[64]. Through these mechanisms, incorporation and maturation of the immunoproteasome subunits into the 20s barrel is a rapid process even in the presence of constitutive subunits.

A third proteasome known as the thymoproteasome has also been characterized. The thymoproteasome incorporates an alternative subunit known as β5t (in place of β5/ β5i) along with β1i and β2i, leading to reduced chymotrypsin-like activity and less peptide-bond cleavage after hydrophobic residues[65]. The thymoproteasome is exclusively expressed in the cortical thymic epithelial cells (cTECs) and has been demonstrated to play an important role in the positive selection process of CD8+ T cells[65,66]. Despite a fascinating biology, its restricted expression to cTECs makes thymoproteasome-generated peptides less directly attractive targets in cancer therapy.

The Cancer Testis Antigen "Preferentially Expressed Antigen in Melanoma" (PRAME)

Cancer-testis antigens are a group of tumor antigens that are over-expressed in many cancers, but exhibit limited expression in healthy adult tissue except for in the testes, ovaries, and endometrium[67]. The protein "preferentially expressed antigen in melanoma" (PRAME) is a cancer-testis antigen that was originally discovered as a melanoma antigen that elicited an immune response by a patients autologous cytotoxic T lymphocytes (CTL)[68]. PRAME is over-expressed in a broad range of cancer types including primary and metastatic melanoma (80-90% of cases) [67,69], breast cancer (27% of cases) [70], and neuroblastoma (>90% of cases) [70,71]. PRAME is also highly expressed in hematopoietic malignancies including acute myeloid leukemia (AML) (40-60% of cases) [72,73], acute lymphoblastic leukemia (ALL) (20-40% of cases) [67,73], myeloma (20-50% of cases) [67], and chronic myeloid leukemia (CML) (30-40% of cases) [67,74]. PRAME expression has been linked to poor prognosis in breast cancer [75] and neuroblastoma[71]. PRAME is also expressed in the stem cells of CML [76] suggesting that targeting PRAME could preferentially deplete the leukemia-initiating cell population. Although the biological function of PRAME is still not well elucidated, it is established that PRAME can inhibit retinoic acid receptor signaling and can prevent retinoic acid-mediated cellular differentiation, apoptosis, and cell cycle arrest. Biochemically, PRAME binds to the retinoic acid receptor preventing its interaction with a transactivator complex and thereby preventing transcription of retinoic acid-receptor-sensitive genes[67,77]. However, its function in cancers is complex and context dependent. In pediatric AML, higher PRAME mRNA expression correlated with favorable prognosis and prolonged survival[70]. However, in glioblastoma and premenopausal breast cancer, PRAME expression correlates with poor prognosis[70]. Although more careful studies will help to elucidate the biological role of PRAME in different contexts, its highly tumor-selective expression profile still makes PRAME an attractive therapeutic target.

PRAME is an intracellular protein[67,78,79] making it impossible to target using traditional antibodies directed at cell-surface proteins and it cannot currently be inhibited using small molecules. Its function in tumor progression is complex, and in some contexts, PRAME over-expression can reduce malignancy of leukemia *in vivo* [78]. Due to its context-dependent role to both promote and inhibit tumorigenesis, direct functional inhibition of the protein may not prove to be therapeutically effective. After proteasomal processing, however, PRAME-derived peptides including the PRAME$^{300-309}$ peptide ALYVDSLFFL (ALY) are presented on the cell surface in the context of HLA-A*02:01 (HLA-A2) molecules [80,81]. Several groups have demonstrated the ability to generate ALY/HLA-A2-specific CD8 cytotoxic T lymphocytes (CTLs) that can specifically lyse PRAME+/HLA-A2+ tumors and are reactive against primary leukemia [82–84] providing proof that this epitope is presented and can be targeted by immunotherapy.

RATIONALE FOR CURRENT WORK

Effective and safe cancer therapy is premised on the idea that neoplastic cells can be specifically identified and eliminated while healthy cells remain unharmed. Although a large number of cancer-specific changes in the cell have been identified, including tumor-specific mutations, glycosylation patterns and gene expression signatures, the vast majority of these cancer-specific markers and tumor-associated antigens cannot currently be targeted with either small molecule inhibitors or traditional antibodies. Recently, a strategy to target these heretofore-untargetable epitopes has been developed by use of T cell receptor mimic monoclonal antibodies (TCRm). TCRm have similar specificities as T cell receptors and are directed to peptides presented in

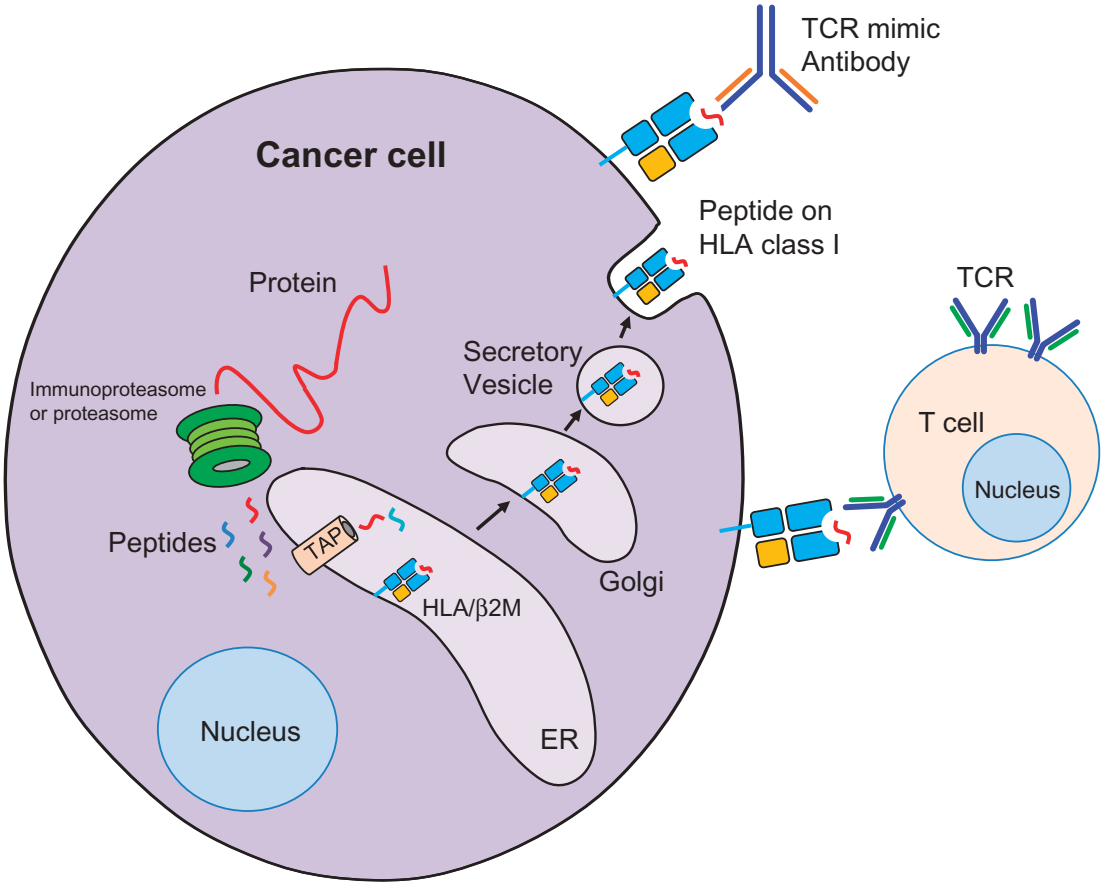

Figure 1.1. TCRm antibodies bind peptide/HLA class I complexes on cancer cells.*

Proteins expressed in a cancer cell can be degraded by the proteasome and processed into peptides. Peptides are then chaperoned into the ER through the TAP transporter complex, loaded onto HLA class I molecules, and shuttled to the cell surface where they can be recognized by TCR on cytotoxic T cells. TCRm, which mimic the specificity of TCR for peptide/HLA class I complexes, can be designed or discovered to target these intracellular or 'undruggable' proteins.

*Presented from Chang AY, Gejman R, Brea E, Oh C, Mathias M, Pankov D et al. Opportunities and challenges for TCR mimic antibodies in cancer therapy. Expert Opinion on Biological Therapy. 2016; DOI:10.1080/14712598.2016.1176138

complex with major histocompatibility complex (MHC) or human leukocyte antigen class I molecules (HLA-I) (Fig. 1.1). In contrast to other TCR-based therapies, TCRm can be delivered to patients as off-the-shelf pharmaceutical agents, in a variety of biological formats allowing for exquisite control over handling and pharmacology. In the present study, we designed a TCRm against the cancer-testis antigen PRAME and studied the regulation of the epitope expression. Monoclonal antibodies (mAbs) have demonstrated potent anti-tumor efficacy in the clinic. Despite promising results, a major limitation of currently marketed mAbs is that they bind exclusively to cell-surface and extracellular antigens, whereas the majority of aberrantly expressed proteins in cancer, including PRAME, are intracellular [43,67,78,79]. We hypothesized that a TCRm antibody directed against the peptide-HLA complex formed by ALY and HLA-A2 would be capable of specifically binding to PRAME-expressing tumors and would be a novel cancer therapeutic against a formerly un-targetable protein.

HLA-A2 is one of the most common HLA-I subtype found in approximately 30-40% of the United States population[43–45] and generating cancer immunotherapies against antigens presented by HLA-A2 such as PRAME would benefit a substantial population. Clinical trials have also demonstrated that patients vaccinated against PRAME can develop PRAME-specific CTLs[85] and helper T cells [86]. However, there are several major constraints to cellular and vaccine based strategies. CTL-based therapies are patient-specific and often require laborious manipulation before reinfusion while vaccines may be less potent and responses are difficult to predict or control, depending on the patient's immune repertoire and immunological status [87].

Additionally, a TCRm antibody has substantially lower peptide/HLA-I target density compared to traditional antibody epitopes, potentially limiting therapeutic efficacy

especially when immune effector molecules or cells are required for cytotoxicity. Therefore, in developing the technology, it would be important to determine strategies to augment therapeutic efficacy. One strategy is to combine TCRm with agents that enhance antibody effector mechanisms such as ADCP. Blockade of the CD47 / SIRPα 'do-not-eat me' signal axis has been demonstrated to enhance ADCP[88]. Therefore, it is important to determine whether CD47 blockade could synergize with ADCP activity of TCRm. In addition, alternative biological platforms could be utilized to enhance efficacy of a TCR mimic antibody. TCRm can be engineered into potent therapeutic formats such as a bispecific T cell engager (BiTE)[89,90] or transduced as a chimeric antigen receptor (CAR)[91,92] to redirect T cells against cancer cells. An additional strategy to enhance therapeutic potential of TCRm is through pharmacological regulation of HLA-I on target cancer cells. Increased expression of target peptide/HLA-I may enhance TCRm-mediated ADCC. Because HLA-I is a central mediator of immune recognition in cancer, increasing cell-surface HLA-I could also be used to potentiate a broad range of other immunotherapies including checkpoint blockade therapy, cancer vaccines, or TCR-transduced T cells.

In the following chapters, we report several novel findings. First, we report the discovery and characterization of Pr20, the first TCRm monoclonal antibody against PRAME, which we have generated to recognize the ALY peptide in complex with cell-surface HLA-A2. We characterized the ability of Pr20 to bind PRAME+/HLA-A2+ cancers and mediate cytotoxicity against PRAME-expressing malignancies *in vitro* and *in vivo*. In addition, we studied the role of the constitutive proteasome and immunoproteasome and their pharmacologic manipulation in generating the ALY peptide epitope, which may be important in the therapeutic use of this and other TCR-based agents. Next, we report the first combination therapy study of TCRm and CD47

axis blockade to demonstrate that dramatic therapeutic efficacy can be achieved despite low-density peptide/HLA-I targets. We also evaluate activities of the potent BiTE and CAR constructs with the Pr20 scFv-targeting moiety. Finally, we explore pharmacological and biological methods to modulate HLA-I expression aiming to identify strategies to augment TCRm and other immunotherapies, and strategies to protect engineered cellular therapeutics from host immunological attack.

CHAPTER I: TARGETING IMMUNOPROTEASOME-REGULATED PRAME PEPTIDE/HLA-I ANTIGENS WITH A THERAPEUTIC ANTIBODY[*,†]

INTRODUCTION

PRAME is a cancer-testis antigen overexpressed in a broad range of luekemias and solid tumors. It is an adaptor protein and not an enzyme and therefore direct inhibition with a small molecule inhibitor is challenging. It also has a complex and context-dependent biological function to either promote or inhibit tumor malignancy. Therefore, function inhibition may not necessarily lead to therapeutic benefit. Instead, its tumor-associated expression makes PRAME a prime candidate for immunotherapy approaches. Specific peptides from PRAME including $PRAME^{300-309}$ (ALY) are processed and presented on HLA-A2 molecules. HLA-A2 is the most common HLA-I haplotype in the US. Therefore, developing an effective TCRm against the PRAME ALY/HLA-A2 complex would benefit a large portion of leukemia and solid tumor patients in the US. In addition, elucidating biochemical mechanisms required for cell-surface presentation of ALY/HLA-A2 will shed light on what types of tumors may respond to immunotherapy against PRAME. The proteasome is a major determinant of HLA-I peptide processing and therefore we explore the role of the two major proteasome forms: the constitutive proteasome and the immunoproteasome, in the generation of the PRAME-derived ALY/HLA-A2 complex.

---

* Modified from Chang AY, Dao T, Gejman RS, Jarvis CA, Scott A, Dubrovsky L et al. A therapeutic T cell receptor mimic antibody targets tumor-associated PRAME peptide/HLA-I antigens. J Clin Invest 2017; 127: 2705–2718. DOI:10.1172/JCI92335.

† Some experiments were designed and conducted by or in collaboration with Cheng Liu from Eureka Therapeutics (Phage Display Panning and Screening and Fig. 1.2) Tao Dao (Fig. 1.3), Ronald C. Hendrickson, and Ron Gejman (Fig. 3.10)

MATERIALS AND METHODS

Selection and Characterization of scFv Specific for PRAME Peptide/HLA-A2 Complexes

A human scFv antibody phage display library was used for the selection of mAb clones. In order to reduce the conformational change of HLA-A2 complex introduced by immobilization onto plastic surfaces, a solution panning method was used in place of conventional plate panning. In brief, biotinylated negative antigens RHAMM-R3/HLA-A2 were first mixed with the human scFv phage library ($7x10^{10}$ clones), then the antigen-scFv phage antibody complexes were pulled down by streptavidin-conjugated Dynabeads M-280 through a magnetic rack and discarded. This step removed phage that bound to HLA-A2 along or HLA-A2 in complex with an irrelevant peptide. A repeat of this process on the positive ALY/HLA-A2 monomers was then conducted. ALY/HLA-A2-bound clones were then eluted and were used to infect *E. Coli* XL1-Blue. The scFv phage clones were expressed in the bacteria and were purified [93]. Panning was performed for 3-4 cycles to enrich scFv phage clones binding to ALY/HLA-A2 complex specifically. Positive phage clones were determined by standard ELISA method against biotinylated single chain HLA-A2/ALY peptide complexes. A total of 25 positive clones that possessed unique DNA coding sequences were subjected to further characterization. Binding to peptide/HLA-A2 complexes on live cell surfaces was determined using a TAP-deficient, HLA-A2+ cell line, T2. T2 cells were pulsed with peptides (50 μg/mL) in the serum-free RPMI1640 medium, in the presence of 20 μg/mL β2M overnight. The cells were washed, and the staining was performed in following steps. The cells were first stained with purified scFv phage clones, and followed by staining with a mouse anti-M13 phage coat protein mAb (Invitrogen MA1-12900), and finally the goat F(ab)2 anti-

mouse IgG conjugated to A488 (Invitrogen A11017) before flow cytometry. Each step of the staining was done between 30-60 minutes on ice and the cells were washed twice between each step of the staining. 4 clones (Pr8, Pr17, Pr20, Pr29) showed robust and specific binding to T2 cells pulsed with ALY peptide but not to T2 cells left unpulsed or pulsed with the irrelevant control RHAMM-3 peptide, and were engineered into full length human mAb.

Engineering Full Length mAb Using the Selected scFv Fragments.

Full-length human IgG1 of the selected phage clones were produced in HEK293 and Chinese hamster ovary (CHO) cell lines, as described [94]. In brief, antibody variable regions were sub-cloned into mammalian expression vectors, with matching human lambda or kappa light chain constant region and human IgG1 constant region sequences. Afucosylated Pr20M was produced in a similar method except in modified CHO cells as described [95]. Molecular weights of the purified full-length IgG antibodies were measured under both reducing and non-reducing conditions by electrophoresis.

Selection of Pr20 as Lead mAb Clone

4 full-length human IgG1 clones (Pr8, Pr17, Pr20, Pr29) were assayed for binding to HLA-A2+ healthy donor PBMC populations and PRAME+/HLA-A2+ leukemia cell lines AML14 and BV173. Pr20 was chosen as the lead TCRm mAb clone due to robust binding to cell lines without substantial binding to healthy PBMC populations. Other clones were not pursued due to either non-specific binding to HLA-A2+ healthy donor PBMC populations or inability to bind or mediate ADCC against PRAME+/HLA-A2+ tumor cells, suggesting that these clones did not bind endogenously processed and presented ALY/HLA-A2 complexes which may have

subtle structural constraints compared to exogenously-loaded ALY on HLA-A2 in the T2 cell assay or monomers folded *in vitro*.

Peptides

All peptides were purchased and synthesized by Genemed Synthesis Inc. The peptides were dissolved in dimethyl sulfoxide and frozen at −80°C. Peptide pulsing experiments were performed by incubating TAP-deficient T2 cells overnight with 50 μg/mL of peptide with 20 μg/mL β2M in either serum-free media or in the presence of 5% dialyzed FBS overnight. Control peptides used were established HLA-A2 binding peptides RHAMM-R3 (ILSLELMKL) and EW (QLQNPSYDK). Experimental peptides included the ALY peptide (ALYVDSLFFL) and the elongated 20-mer ALY-precursor peptide (LQCLQALYVDSLFFLRGRLD).

Cells

PBMC from HLA-typed healthy donors were obtained by Ficoll density centrifugation. Cell lines were maintained at Sloan Kettering and were originally obtained from the American type culture collection and frozen as aliquots in liquid nitrogen. BV173 was kindly provided by H. J. Stauss (University College London). The following cell lines were gifts from the listed labs at Memorial Sloan Kettering Cancer Center, New York, NY: AML14 was a gift from Ross Levine, SET2 was a gift from Richard J. O'Reilly. SK-Mel5 and SK-Mel37 were gifts from Jedd D. Wolchok, and SUDHL1 and SUDHL4 were gifts from Anas Younes. SKLY16, PC9, SK-Mel30, and SK-Mel2 were from cell line banks at Memorial Sloan Kettering Cancer Center. THP1, U266, A375, SW480, BJAB, NCI-H2228, MDA-MB231, T2, and HL60 were obtained from the American Type Culture Collection. UACC257 and UACC62 were obtained from the NCI. MAC1 and MAC2A were gifts from Mads H. Andersen

(University of Copenhagen, Copenhagen, Denmark). Cell lines of unknown HLA were HLA typed by the Department of Cellular Immunology at Memorial Sloan Kettering Cancer Center. All cell lines were cultured in RPMI 1640 supplemented with 10% FCS, 1% penicillin, 1%streptomycin, 2 mM L-glutamine, and 10 mM HEPES at 37°C and 5% CO_2.

Flow Cytometry

For cell surface staining, cells were blocked using FcR blocking reagent (Miltenyi 130-059-901) at the manufactures recommended dilution for 15 minutes on ice, then incubated with appropriate fluorophore -conjugated mAbs for 30 min on ice and washed twice before resuspension in a viability dye (either DAPI or propidium iodide at 1 μg/mL). Antibodies used include anti-HLA-A2 clone BB7.2-APC (ebioscience 17-9876-42), BB7.2-FITC (MBL K0186-4), anti-CD3-PerCP clone 7D6 (Invitrogen MHCD0331), anti-CD19-PE-Cy7 clone 1D3 (eBioscience 25-0193-81), anti-CD33-BV711 clone WM53 (Biolegend 303423), CD14-PE clone 61D3 (eBioscience 12-0149-42). Pr20 or its human IgG1 isotype control (Eureka Therapeutics ET901) was conjugated to APC using the lightning-link kit (Innova Bioscience 705-0010) and staining was performed at 3 μg/mL, which was determined to be a saturating concentration. Flow cytometry data were collected on a LSRfortessa (Beckton Dickinson) or an Accuri C6 (Beckton Dickinson) and analyzed with FlowJo V10 software.

Antibody-dependent Cellular Cytotoxicity

Cancer cell lines used as ADCC target cells were incubated with 50 μCi of ^{51}Cr for 1 hour at 37 °C and washed 3 time to remove free ^{51}Cr. Indicated concentrations of Pr20M or matched isotype control hIgG1 (afucosylated Eureka Therapeutics ET901)

were incubated with target cells and fresh PBMCs at effector:target ratios of 50:1 for 6 hours at 37 °C. The assay was performed in 96-well format with 5000 target cells per well and 250,000 PBMC. The supernatant was harvested, and the cytotoxicity was measured by scintillation counting. For flow-based ADCC assays, PBMC and GFP+ tumor target cells were incubated at effector:target ratio of 30:1 overnight with 1 μg/mL of Pr20M and flow cytometry was used to determine depletion of GFP+ tumor percentage. PBMC were also incubated alone with 1 μg/mL Pr20M to measure potential autologous toxicity to PBMC populations.

Western Blot and qPCR Analysis

Total cell lysate was extracted using RIPA buffer and quantified using the DC protein assay (Biorad). 15-30 μg of protein was loaded and run on 4-12% SDS PAGE gels. After 1 hr block with 5% milk at room temperature, immunoblotting was performed using the following antibodies (Enzo Life Science): anti-20s β5i (BML-PW8845-0025), anti-20s β2i (BML-PW8350-0025), anti-20s β1i (BML-PW8840-0025), anti-PRAME (Sigma-Aldrich HPA045153). Antibodies were probed at manufacturers recommended dilution overnight at 4°C before a secondary antibody conjugated to HRP was used for imaging. Replicate samples were probed using the indicated antibodies when noted, or blots were stripped with Restore™ Western Blot Stripping Buffer (ThermoFisher Scientific 21063), re-blocked with 5% milk, and re-probed with an anti-GAPDH-HRP direct conjugated antibody (Cell Signaling Technology 3683) as a loading control. qPCR was performed using the Taqman real-time PCR system. RNA was extracted using the Qaigen RNeasy, 1 μg of RNA was reverse transcribed into cDNA using qScript cDNA SuperMix (Quanta Biosciences) TaqMan probes and primers were designed from 'assay-on-demand' gene expression products (Applied Biosystems). Primer and probes were PRAME (assay ID number: Hs01022301_m1)

and the endogenous reference gene control was TATA-box binding protein (TBP) (assay ID number: HS99999910). The results are presented as relative differences in expression vs the endogenous reference control gene ($2^{-\Delta Ct}$), or fold changes based on the differences of normalized Ct values compared to control samples, assuming optimal primer efficiency ($2^{-\Delta\Delta Ct}$). Samples that did not amplify after 40 cycles or amplified at an equal or later Ct value compared to a water sample were considered negative and are not plotted with a value.

CRISPR knock-out Studies

LentiCRISPRv2 (Addgene plasmid #52961) [96] was a gift from Feng Zhang (Broad Institute, Cambridge, MA). Guide RNA sequences targeting the immunoproteasome subunits were as follows: (β2i: GTCCCTCACGCACGCAAGAC, β5i: GTGCAGCAGACTGTCAGTAC, β1i: GGTGCCTTGCAGGGATGCTG). Cells were transduced with LentiCRISPRv2 and transduced cells were selected using 1-4 μg/mL puromycin for 48 hours. Successful knockout was confirmed by western blot analysis.

Animals

Eight- to ten-week-old NOD.Cg-*Prkdc*^{scid} IL2rg^{tm1Wjl}/SzJ mice, known as NSG, were purchased from The Jackson Laboratory or obtained from the MSKCC animal breeding facility. Female mice were used for the BV173 and SET2 models while male mice were used for the AML14 model. C57BL/6 and B6.Cg-Tg(HLA-A/H2-D)Enge/J (HLA-A2 transgenic mice) (6 to 8 weeks old) for biodistribution experiments were also purchased from The Jackson Laboratory and bred at MSKCC.

Therapeutic trials of Pr20M

GFP/luciferase-transduced AML14 cells were passaged once in NSG mice and bone marrow was harvested to generate a sub-culture line that engrafted more consistently *in vivo*. Using this AML14 sub-culture line, 3 million cells were injected intravenously into two groups of NSG mice. On day 7, tumor engraftment between the two groups was confirmed by luciferase imaging to have minimal inter-group variation. Groups were blindly assigned to either treatment groups (Pr20M or Isotype-treated). 50 μg of Pr20M or an afucosylated isotype control human IgG1 (afucosylated Eureka Therapeutics ET901) was injected intravenously twice weekly (every 3 or 4 days) starting on day 7 until the experiment endpoint on day 29. Tumor growth was assessed by weekly bioluminescent imaging and bone marrow was harvested on day 29 for flow cytometric analysis. For BV173 and SET2 therapy experiments, $0.5x10^6$ SET2 cells and $3x10^6$ BV173 were engrafted into NSG mice through tail vein injection. Mice were treated with 50 μg of Pr20M on day 6, 10, 13, and 17 after engraftment or left untreated (control) and tumor burden was assessed by bioluminescent imaging on the indicated days.

Pharmacokinetic and Biodistribution Studies

Pr20 antibody was labeled with ^{125}I (PerkinElmer) using the chloramine-T method. 100 μg of antibody was reacted with 1mCi ^{125}I and 20 mg chloramine-T, quenched with 200 mg Na metabisulfite, then separated from free ^{125}I using a 10-DG column equilibrated with 2% bovine serum albumin in PBS. Specific activities of products were in the range of 4 to 8 mCi/mg. 2.5 μg of radiolabeled mAb was administered intravenously into each mouse through retro-orbital injection, and blood and/or organs were collected at indicated time points, weighed, and measured on a gamma-counter.

***In vitro* Proteasome Digestion and LC-MS/MS Mass Spectrometry Analysis**

A 20-mer PRAME sequence peptide (LQCLQALYVDSLFFLRGRLD) termed the "precursor peptide," encompassing the ALY epitope and elongated by 5 residues on each end was synthesized by Genemed and ensured to be over 95% pure by HPLC. The precursor peptide was dissolved in DMSO and stored at -80°C. Purified constitutive proteasome and immunoproteasome were purchased from Boston Biochem (E-360 and E-370 respectively). 10 μg of precursor peptide was mixed with either 5 μg of constitutive or immunoproteasome in 100 μL of assay buffer per replicate. Assay buffer consisted of 2 nM $MgAc_2$, 1 mM DTT, 20 mM HEPES/KOH at a pH of 7.8. The reaction was incubated at 37°C and at each time point, a 20 μL aliquot was removed and quenched with 2 μL of 10% TFA in water. Samples were stored frozen at -80°C until MS analysis. Each sample was analyzed separately by microcapillary LC with electrospray ionization coupled with tandem MS. We used a NanoAcquity LC System (Waters) with a 100-μm inner diameter × 10-cm length C18 analytical column (1.7 μm BEH130; Waters) configured with a 180-μm × 2-cm trap column coupled to a Q-Exactive Plus mass spectrometer (Thermo Fisher Scientific). A nanoelectrospray source (Proxeon, Thermo Scientific) set at 1800 V and a 25-micron (with 10-micron orifice) fused silica nano-electrospray needle (New Objective, Woburn, MA) was used to complete the nanoelectrospray interface. For each time point, the sample was diluted 1:20 in HPLC grade water with 0.1% (v/v) formic acid and 1 μL was loaded onto the trap column, washed with 3x loop volume of buffer A (Water with 0.1% (v/v) formic acid) and the flow was reversed through the trap column and the peptides eluted with a 90 min linear gradient from 1-50 % buffer B (Acetonitrile with 0.1% (v/v) formic acid) at 300 nL / min. The QE Plus was operated in automatic, data-dependent MS/MS acquisition mode with one MS full scan (400–1800 *m*/*z*) at 70,000 mass resolution and up to ten concurrent MS/MS scans for the ten most intense peaks selected from each survey scan. Survey scans were acquired in profile mode and MS/MS scans were acquired in centroid mode

at 17500 resolution and isolation window of 1.5 amu and normalized collision energy of 27. AGC was set to 1 x 10^6 for MS1 and 5 x 10^4 and 100ms IT for MS2. Charge exclusion of unassigned and greater than 6 enabled with dynamic exclusion of 15s. Degradation products were identified and quantified by *in silico* analysis of mass spectrometry data. Briefly, all HPLC peaks were identified using the "findpeaks" method in the "pracma" R package. For each retention time during which a HPLC peak appeared, the ms1 spectra was analyzed to identify series of peaks. Identified peak series were matched to a database of all possible precursor peptide degradation products. Total intensity of each degradation product was quantified by adding up the intensities of each product ion. If two degradation products yielded the same peak series (e.g. FFL and LFF), intensity was assigned to each product in proportion to the a2 and b2 product ions.

Statistical Analysis

Values reported represent means ± SEM unless otherwise noted. P-values were calculated with GraphPad Prism 6 (GraphPad Software Inc), using the paired Wilcoxon signed-rank test where appropriate, or student's t-test (unpaired, two-tailed) with $P < 0.05$ (*), $P < 0.01$ (**), $P < 0.001$ (***), and $P < 0.0001$ (****) considered significant. Binding affinity of Pr20 was determined on AML14 cells using Scatchard analysis after linear-transformation of [bound] and [bound]/[free] Pr20. The two-phase exponential decay model was used for analyzing Pr20M pharmacokinetics. Experiments were performed at least 3 times unless otherwise noted.

Study Approval

All animal studies were conducted in accordance with IACUC-approved protocols. After informed consent on Memorial Sloan Kettering Cancer Center Institutional Review Board approved protocols, peripheral blood mononuclear cells (PBMC) from

HLA-typed healthy donors were obtained by Ficoll density centrifugation. Frozen cells from AML patients were obtained under specific biospecimen banking protocols at Memorial Sloan Kettering after informed consent and research authorization.

RESULTS

Pr20 binds to ALY/HLA-A2 complexes in PRAME/HLA-A2 expressing leukemias

TCRm clones reactive with ALY/HLA-A2 complexes were identified through a phage-display library screen as described previously [43]. We aimed to identify a TCRm antibody that recognized ALY/HLA-A2, but not HLA-A2 alone or in complex with irrelevant HLA-A2-binding peptides. Briefly, single phage clones selective for the ALY/HLA-A2 complex were picked by a positive panning strategy on *in vitro*-folded ALY/HLA-A2 monomers and a negative panning against RHAMM-R3/HLA-A2 irrelevant peptide control monomers. Specificity of phage clones was further screened on live cells using the TAP-deficient HLA-A2+ T2 cells, (which have low levels of endogenously presented HLA-A2 peptides) pulsed with or without ALY or an irrelevant peptide. A more detailed description of phage-display library panning, positive clone screening, and scFv characterization can be found in the Supplemental Information: Methods. Four phage clones that selectively bound ALY-peptide pulsed T2 cells were engineered into full-length human IgG1. Pr20 IgG1 was selected as the lead clone after it was determined to have a low nM affinity (approximately 4-5 nM K_D) as measured by a binding assay with HLA-A2/ALY monomers using ForteBio, and by Scatchard analysis of binding PRAME+/HLA-A2+ AML14 cells (Fig. 1.2). mAb clones Pr8, Pr17, and Pr29 were not pursued due to non-specific binding to HLA-A2+ healthy donor peripheral blood mononuclear cells (PBMC), lower

estimated affinity, or inability to bind to target cells, possibly due to subtle structural differences between *in vitro*-folded ALY/HLA-A2 and endogenously-presented ALY/HLA-A2.

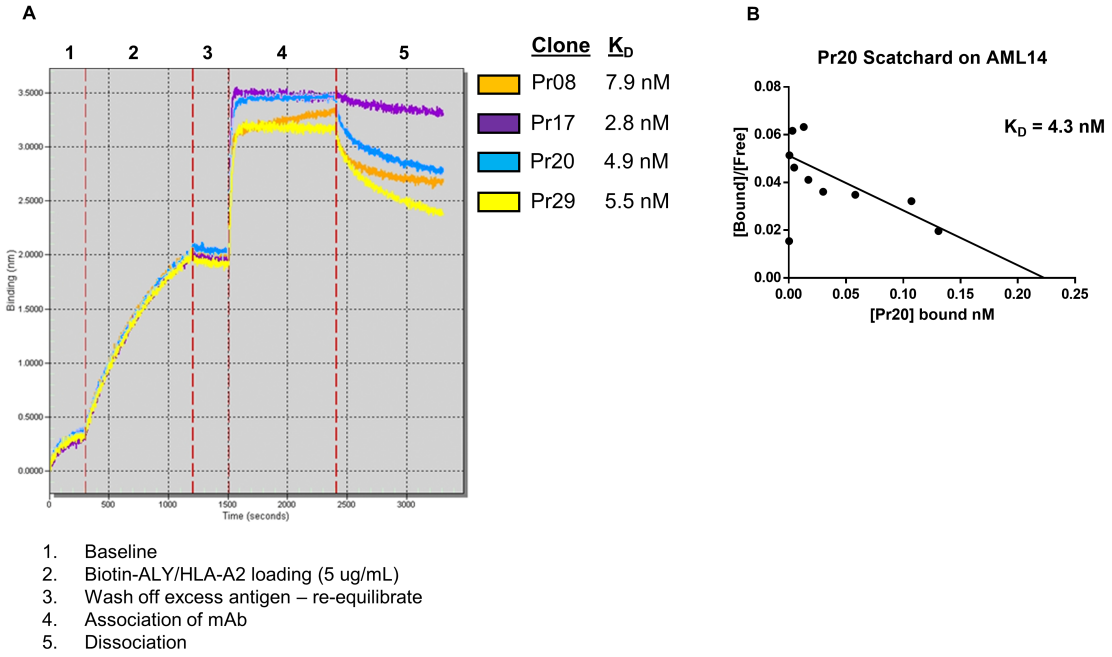

Figure 1.2. Pr20 exhibits a low nM affinity for ALY/HLA-A2.
(A) A Fortebio device was used to determine the affinity of Pr20 for the target protein complex ALY/HLA-A2 monomer. After biotinylated ALY/HLA-A2 monomers were loaded (2), excess antigen was washed off and the instrument was re-equilibrated (3). The association phase (4) and dissociation phase (5) data are shown. (B) Scatchard analysis was performed on the PRAME+/HLA-A2+ AML14 cells using increasing concentrations of I^{125}-Pr20. Affinity of Pr20 to the complex and avidity of Pr20 TCRm to AML14 was confirmed to be in the low nM range by the assays, respectively. Experiment in (A) was performed once and experiment in (B) was performed 2 times with 3 technical replicates per experiment.

To determine the specificity of Pr20, T2 cells were pulsed with ALY peptide or with the irrelevant control EW peptide (Fig. 1.3A). Pr20 did not bind T2 cells pulsed with EW peptide but readily bound T2 cells pulsed with ALY peptide as measured by flow cytometry, demonstrating that Pr20 bound to the ALY/HLA-A2 complex and not to

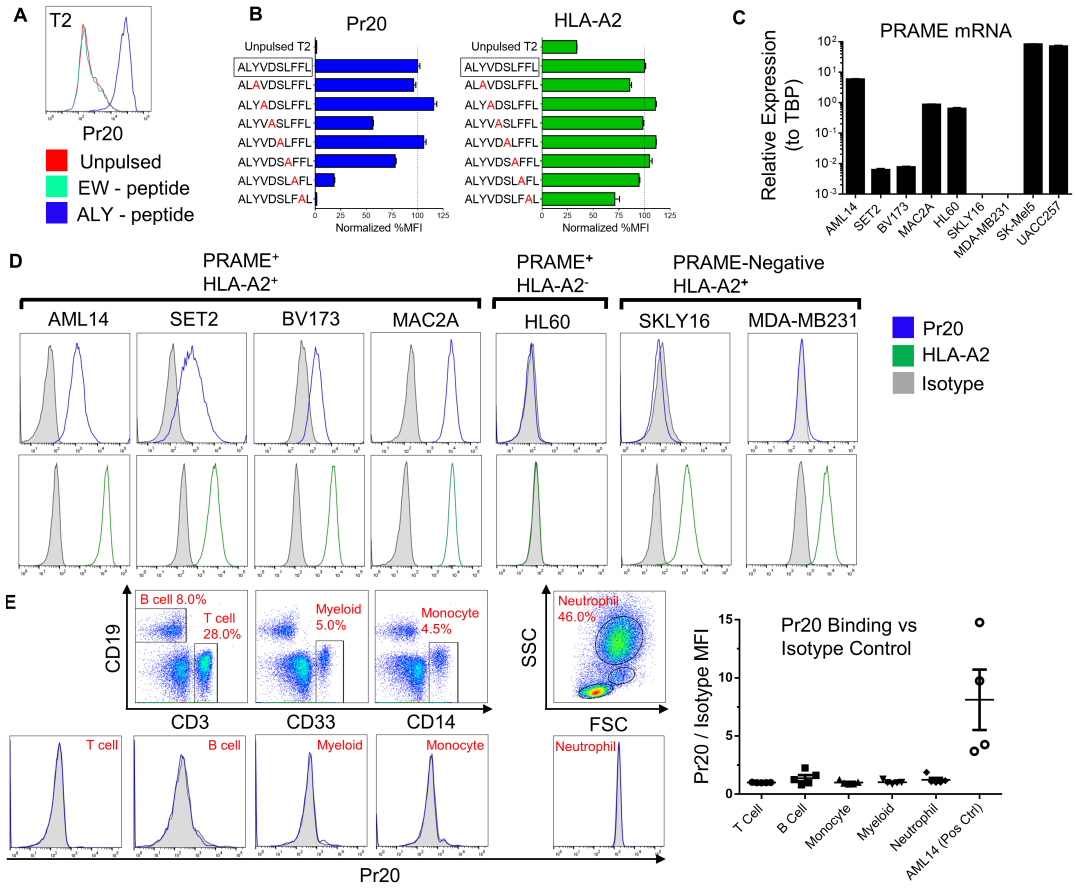

Figure 1.3. Pr20 binds ALY/HLA-A2 complexes and PRAME+ / HLA-A2+ leukemia.

Pr20 was directly labeled by conjugation to the fluorophore APC. (A) TAP-deficient T2 cells were pulsed overnight with 50 µg/mL of ALY peptide, irrelevant control EW peptide, or left unpulsed. Flow cytometry was used to determine P20 binding. (B) Each non-anchor residue in the ALY peptide was substituted for alanine and peptides were pulsed onto T2. Pr20 binding was determined by flow cytometry relative to native ALY peptide-pulsed T2. Cell-surface HLA-A2 was also measured by flow cytometry to ensure altered peptides maintained the ability to bind and stabilize HLA-A2 compared to unpulsed T2. (C) PRAME mRNA expression was determined by qPCR and samples that did not amplify after 40 cycles were considered negative. (D) The indicated cell lines were stained with Pr20 or an isotype control antibody and binding was determined by flow cytometry. Surface HLA-A2 was also assessed compared to an isotype control. All data from (A-D) are representative of at least 3 experiments. (E) Whole blood populations from HLA-A2+ healthy donors were stained with Pr20 to determine possible cross-reactivity. Representative gating strategy and Pr20 histogram compared to isotype control is shown and data from all HLA-A2+ healthy donors (n=5) is summarized. Staining was performed once independently for each healthy donor and an AML14 PRAME+HLA-A2+ leukemia–positive control was included in each assay to ensure assay reliability.

HLA-A2 alone or an irrelevant peptide/HLA-A2 complex. To more carefully map the TCRm epitope, each residue on the ALY peptide was replaced with alanine (except the canonical anchor residues on position 2 and 10 which are important for binding to HLA-A2) and Pr20 binding was assessed on peptide-pulsed T2 cells (Fig. 1.3B). Single alanine residue substitutions on positions 5, 7, 8, and 9 reduced or abrogated Pr20 binding at a saturating concentration of Pr20, suggesting that Pr20 primarily contacted the ALY peptide's C-terminal half (Fig. 1.3B left panel). Decrease in Pr20 binding was not due to instability of peptide/HLA-A2 complexes as each peptide increased surface HLA-A2 over un-pulsed T2 cells in the assay indicating that the peptides complexed with and stabilized HLA-A2 (Fig. 1.3B right panel). The data demonstrated that specific changes to the native peptide sequence can abrogate Pr20 binding, consistent with other reported TCRm [43,97].

After the preliminary biochemical and specificity characterization, we sought to test if Pr20 could recognize cancer cells expressing endogenous PRAME protein. PRAME mRNA expression was assessed by qPCR and surface HLA-A2 expression and Pr20 binding were assessed by flow cytometry across a panel of HLA-A2+ hematopoietic and solid tumor cell lines, several of which have been reported to express PRAME by other groups (Table 1.1 and Fig. 1.3C). Pr20 binding was readily detected in PRAME+/HLA-A2+ leukemia AML14, SET2, BV173 and the T cell lymphoma MAC2A demonstrating that Pr20 can detectably bind endogenously processed and presented peptides (Fig. 1.3D). Pr20 did not bind the PRAME+/HLA-A2- AML cell line HL60 indicating that the epitope was restricted by HLA-A2. In addition, Pr20 did not bind PRAME negative/HLA-A2+ tumors of various histological types including SKLY16 lymphoma, MDA-MB231 breast adenocarcinoma, and NCI-H2228 lung carcinoma. (Fig. 1.3D and Table 1.1). We detected minimal or no Pr20 binding on T,

B, myeloid, monocyte or neutrophil populations in whole blood taken from HLA-A2+ healthy donors (Fig. 1.3E).

Table 1.1. PRAME expression, Pr20 binding, and surface HLA-A2 expression on cancer cell lines.
PRAME expression in a panel of cell lines was determined by qPCR and expression was binned into the follow groups based on relative expression to the constitutive gene TBP as calculated by standard $2^{-\Delta Ct}$ method based on a standard 40-cycle qPCR: negative(-) = no amplification, low(+) = <0.01, medium(++) = <5, and high(+++) = >5. Surface HLA-A2 expression and Pr20 binding was determined by flow cytometry with the following bins determined by MFI relative to an isotype control. Pr20 binding was binned based on Pr20 MFI / Isotype MFI: negative(-) = <2, low(+) = <5, medium(++) = <10, and high(+++) = >10. Surface HLA-A2 was binned based on HLA-A2 MFI / Isotype MFI: negative(-) = <2, low(+) = <10, medium(++) = <50, and high(+++) = >50.

Cell line	Tumor origin	*PRAME* mRNA	Pr20 binding	Surface HLA-A2
BV173	B-ALL	+	+	+++
AML14	AML	++	+++	+++
SET2	AML	+	++	++
THP-1	AML	++	+	+
U266	Myeloma	++	+	+++
MAC1	T lymphoma	++	+++	+++
MAC2A	T lymphoma	++	+++	+++
SK-Mel5	Melanoma	+++	+	+++
SK-Mel30	Melanoma	+	–	+
SK-Mel2	Melanoma	+++	–	+++
SK-Mel37	Melanoma	+++	–	++
UACC257	Melanoma	+++	–	++
UACC62	Melanoma	+++	–	+
A375	Melanoma	++	–	+
SW480	Colon adenocarcinoma	+	–	++
B-JAB	Burkitt lymphoma	+	–	++
SUDHL1	Lymphoma	+	–	++
SUDHL4	B lymphoma	+	–	++
PC9	Non–small cell lung	+	–	+
NCI-H2228	Non–small cell lung	–	–	++
SKLY16	B lymphoma	–	–	++
MDA-MB231	Breast adenocarcinoma	–	–	++
HL60	AML	++	–	–

Fc-enhanced Pr20 (Pr20M) mediates ADCC against PRAME+ leukemia

Therapeutic mAbs can mediate cytotoxicity by various mechanisms including direct cytotoxicity and antibody-dependent cellular cytotoxicity (ADCC), but low expression of peptide/HLA-I epitopes can reduce activity of the TCRm. To study whether Pr20 could be cytotoxic against leukemia, we engineered an afucosylated Fc form of the antibody (designated *Pr20M*) that provides enhanced effector recruitment properties via increased FcR affinity. Such Fc sugar modifications are well-established to enhance mAb-mediated ADCC [98–101]. Pr20M's ability to mediate ADCC *in vitro* was assessed on PRAME+ leukemia in the presence of healthy human donor PBMC effectors. We demonstrated that Pr20M could direct ADCC against PRAME+/HLA-A2+ leukemia AML14, SET2, BV173, and lymphoma line MAC2A in a dose-dependent manner *in vitro* (Fig. 1.4A). Pr20M did not mediate substantial ADCC against the PRAME+/HLA-A2 negative HL60 leukemia or the PRAME negative/HLA-A2+ lymphoma SKLY16, confirming Pr20M specificity. To determine if Pr20M would direct cytotoxicity against healthy cells, we performed overnight autologous killing assays on HLA-A2+ PBMC in the presence of Pr20M. Pr20M did not mediate depletion of T cells (CD3+), B cells (CD19+), myeloid cells (CD33+), or monocytes (CD14+) in healthy HLA-A2+ PBMC *in vitro* (Fig. 1.4B), indicating the lack of toxicity to the major normal hematopoietic lineages. As a positive control in the same assay, PRAME+/HLA-A2+ lymphoma cells (MAC2A) were depleted by approximately 50%.

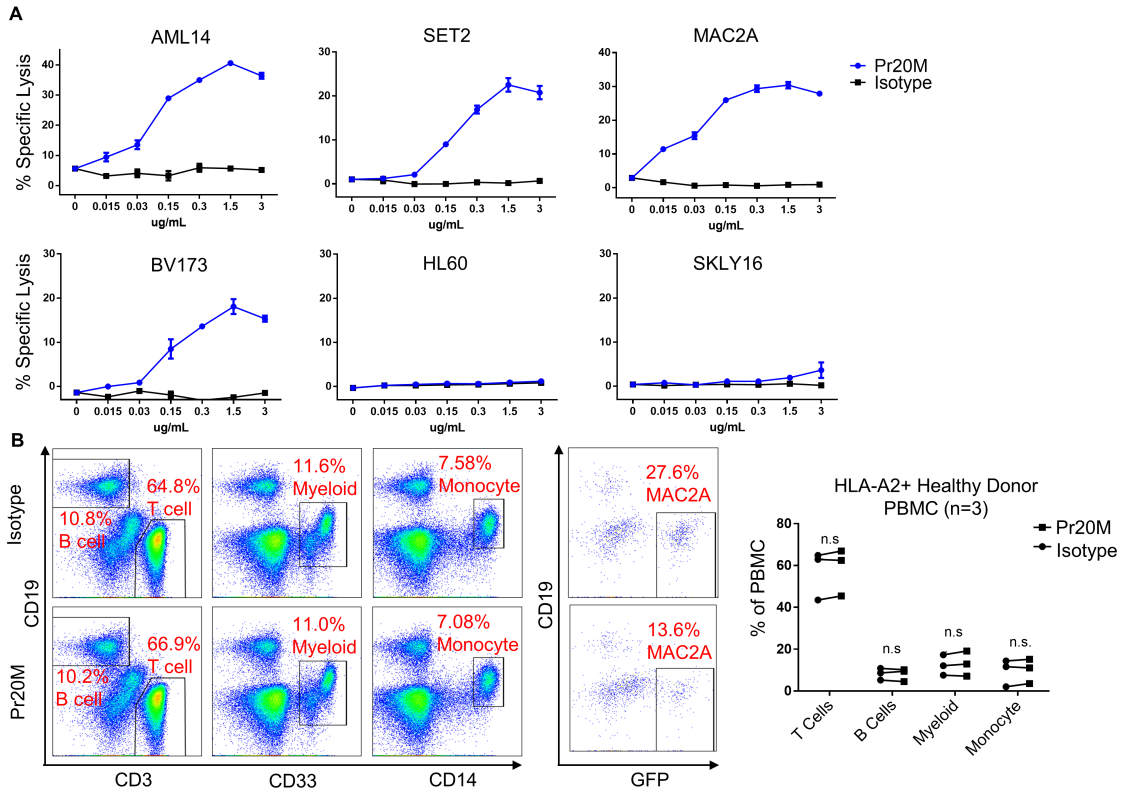

Figure 1.4. Pr20M mediates Antibody dependent cellular cytotoxicity *in vitro* on PRAME+/HLA-A2+ leukemias and lymphoma.

(A) ADCC assay was performed on hematopoietic cancers, ^{51}Cr-labeled target leukemia or lymphoma cells were incubated with healthy donor peripheral blood mononuclear cells (PBMC) at an effector:target ratio of 50:1. Pr20M or an afucosylated isotype control antibody was added at the indicated concentration. Supernatant was collected after 6 hours and scintillation counting was used to determine % specific lysis. Data represent at least 3 experiments for each cell line except SKLY16 and MAC2A (done twice). (B) Healthy donor PBMC were incubated overnight with 1 µg/mL of Pr20M or afucosylated isotype control. Flow cytometry was used to determine populations of B cells ($CD19^+CD3^-$), T cells ($CD3^+CD19^-$), monocytes ($CD14^+CD19^-$), and myeloid cells ($CD33^+CD19^-$). 1 representative analysis (n=3) is shown including a positive control to demonstrate that PBMCs in all assays were capable of depleting a PRAME+/HLA-A2+ lymphoma ($CD19^-$ and transduced with GFP). Data from HLA-A2+ healthy donor PBMC (n=3) performed independently are summarized and plotted. Data analyzed by paired Wilcoxon signed-rank test.

TCRm antibodies have been observed to mediate direct cytotoxicity using effector-independent mechanisms such as triggering caspase-mediated apoptosis [102]. To investigate if Pr20M mediated direct cytotoxicity, we incubated Pr20M with PRAME+/HLA-A2+ leukemia *in vitro* for 48 or 72 hours and assayed for metabolically viable cells. Pr20M did not substantially affect viability or cause growth inhibition *in vitro*, (Fig. 1.5) suggesting that Pr20M does not mediate direct cytotoxicity and requires immune effector cells for redirected lysis.

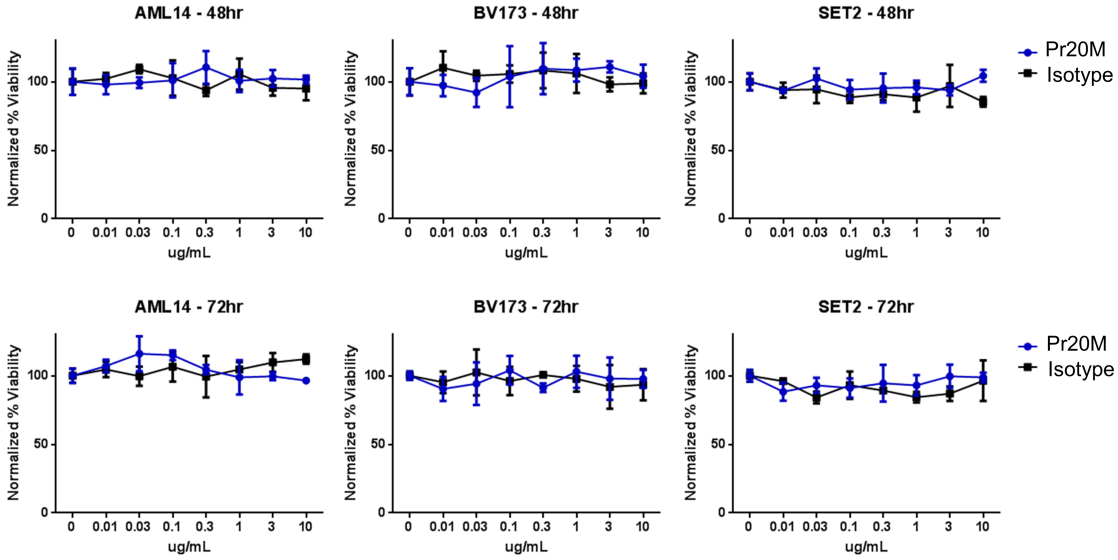

Figure 1.5. Pr20M does not mediate direct cytotoxicity or growth inhibition on PRAME+/HLA-A2+ leukemia.
PRAME+/HLA-A2+ leukemia cells were incubated with the indicated concentration of Pr20M for 48 or 72 hours. An ATP-based viability assay (Promega – CellTiter Glo) was used to determine relative cell viability compared to cells incubated with an isotype control antibody. The assay was performed as recommended by manufacturer. Data is representative of 3 experiments with 3 technical replicates for each dose and time point.

Pr20M is therapeutically active against disseminated leukemia models *in vivo*

To determine the therapeutic utility of the afucosylated Pr20M TCRm, pharmacokinetics and bio-distribution were examined *in vivo*. Pr20M exhibited a blood serum pharmacokinetic half-life of approximately 4.5 days in C57BL6 mice, similar to other reported TCRm, demonstrating that Pr20M was stable *in vivo* (Fig. 1.6A). This serum half-life was similar to other reported TCRm[99]. Although murine PRAME protein does not contain the ALY peptide, HLA-A2 transgenic mice can be used for potential off-target binding and toxicity studies, as the HLA-A2 can present potential cross-reactive murine protein-derived epitopes that might be shared with the human proteome. Bio-distribution studies in HLA-A2 transgenic mice showed that at

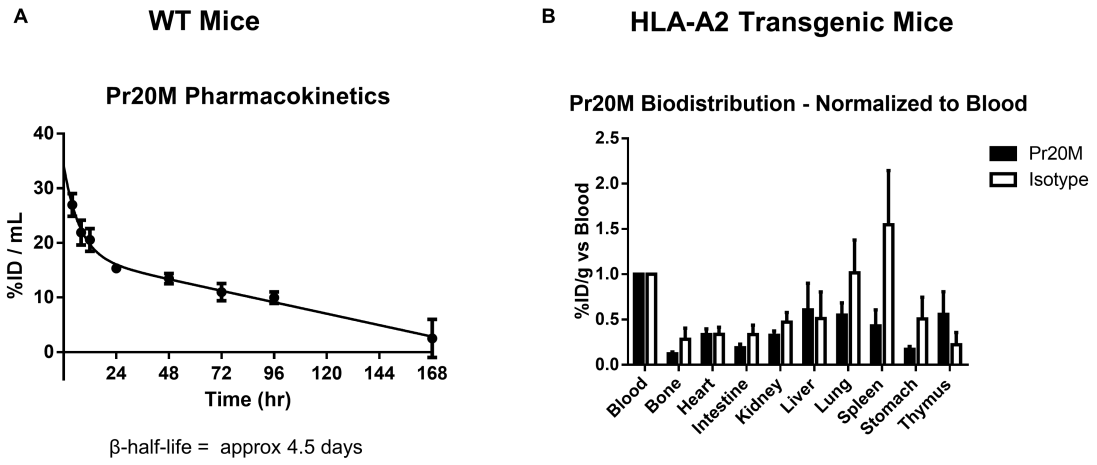

Figure 1.6. Pr20M demonstrates favorable blood pharmacokinetics and does not obviously accumulate in major organs *in vivo.*

Pr20M was radiolabeled with ^{125}I. (A) WT C57BL/6J mice (n=3) were injected retro-orbitally with trace amounts (2.5 μg) of radiolabeled Pr20M. Peripheral blood was collected at the indicated time points, scintillation counting was used to determine amount of Pr20M, and % initial dose (ID) / mL is graphed. Experiment was performed once. (B) HLA-A2 transgenic mice were injected retro-orbitally with 2.5 μg of radiolabeled Pr20M (n=3 per treatment group). 24 hours later, indicated organs were harvested and the % injected dose/g normalized to each mouse's % injected dose/g in blood is graphed. Experiment was performed once.

24 hours, there was no substantial antibody sink in any organ examined compared to isotype control antibody (Fig. 1.6B), suggesting no organ-specific or widely HLA-A2 presented murine peptide sequences were recognized by Pr20. While the mouse and human proteome are not identical, they are homologous. Taken together, our data suggest that Pr20 is relatively specific to the ALY sequence and that potential cross-reactive sequences are not processed or presented in normal mouse tissues.

To determine if Pr20M could be therapeutically active against leukemia models, B, T and NK cell-deficient non-obese diabetic/severe combined immunodeficiency/IL-2 receptor gamma deficient (NSG) mice [103] were xenografted with HLA-A2+/PRAME+ human leukemias BV173 (ALL), SET2 (AML) and AML14 (AML), which were transduced to express GFP and luciferase. Mice were treated twice a week with 50 μg of Pr20M from day 6 or 7 until the experiment end-point. Pr20M significantly reduced the growth of BV173, SET2, and AML14 as measured by bioluminescent imaging (BLI) (Fig. 1.7A, B, C) *in vivo*. In the BV173 model, Pr20M-treated mice at day 13 had reduced leukemia burden compared to day 6 (Fig. 1.7A). In the AML14 model, 3 out of 4 mice in the isotype-treated group succumbed to severe hind-leg paralysis by day 29, whereas none of the Pr20M-treated mice displayed such clinical signs. On day 29, recurrent AML14 leukemia was examined in the bone marrow. Bone marrow leukemia burden was significantly reduced in mice treated with Pr20M as measured by flow cytometry (Fig. 1.7D). No down-modulation of HLA-A2 or the Pr20-epitope was detected in AML14 cells harvested Pr20M-treated mice compared to the isotype-treated mice (Fig. 1.7E). Target down-regulation was therefore not a major mechanism of resistance to Pr20M in these models, confirming previously described observations with other TCRm therapies [104]. Our data demonstrates that Pr20M has broad therapeutic activity against several human leukemias.

Figure 1.7. Pr20M is therapeutically active against ALL and AML *in vivo* and target epitope down-regulation is not a mechanism of Pr20M resistance.
BV173 (ALL), SET2 (AML), and AML14 (AML) were transduced to express luciferase and GFP. NSG mice were engrafted though tail vein injection and on day 6 or 7, mice were randomized into groups and treated with 50 μg of Pr20M twice a week, left untreated (control for BV173 and SET2), or treated with an afucosylated isotype control antibody (AML14). Tumor burden was determined by BLI for BV173 (n=5 mice) (A), SET2 (n=5 mice) (B), and AML14 (n=4 mice) (C) once a week throughout the experiment and the BLI data is summarized below the images. The scale for day 7 and 14 for AML14 is lowered to indicate engraftment and early tumor growth. Total flux (photos/sec) was normalized to each mouse's total flux on day 6 or 7 immediately before initiation of Pr20M therapy and summarized with mean ± SEM. (D) Mice from the AML14 experiment were sacrificed on day 29 and bone marrow was harvested to determine tumor burden by flow cytometry for GFP+/HLA-A2+ AML14 cells. Representative plots (n=4 mice per group) are shown and data is summarized. (E) MFI of AML14 for HLA-A2 and Pr20 was determined by flow cytometry. Because Pr20M-treated mice presumably had Pr20M already bound on tumor cells, staining was performed by an additional Pr20 stain on all samples followed by a secondary PE-conjugated anti-human antibody (n=4 mice per group). Experiments were performed once per model. Differences were evaluated using the unpaired T tests on indicated times and samples. AML14 BLI data is representative of 3 similar experiments while SET2 and BV173 BLI data is from 1 experiment each.

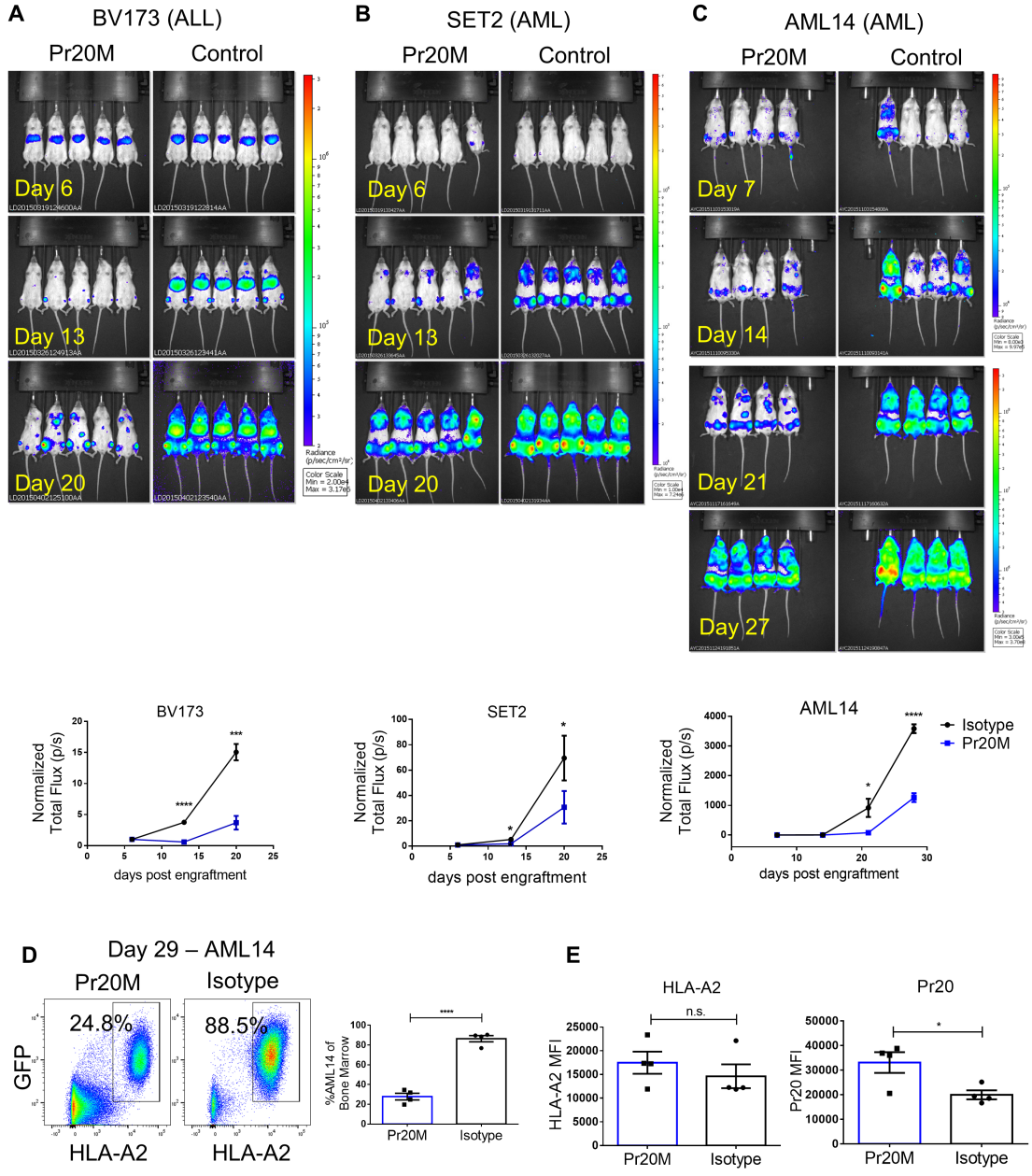
A
BV173 (ALL)
Pr20M
Control
Day 6
Day 13
Day 20
B
SET2 (AML)
Pr20M
Control
Day 6
Day 13
Day 20
C
AML14 (AML)
Pr20M
Control
Day 7
Day 14
Day 21
Day 27
BV173
SET2
AML14
Normalized Total Flux (p/s)
days post engraftment
Isotype
Pr20M
D
Day 29 – AML14
Pr20M
Isotype
24.8%
88.5%
GFP
HLA-A2
HLA-A2
%AML14 of Bone Marrow
Pr20M
Isotype
E
HLA-A2
n.s.
HLA-A2 MFI
Pr20M
Isotype
Pr20
Pr20 MFI
Pr20M
Isotype

PRAME protein expression alone is not sufficient for Pr20 binding, but IFNγ can enhance Pr20 binding in PRAME+ solid tumors and enhance ADCC

Interestingly, neither PRAME mRNA levels nor PRAME protein levels correlate with Pr20 cell surface binding. Several HLA-A2+ cancers that expressed high levels of PRAME, such as the melanoma cell lines SK-Mel5, UACC257, and A375, did not readily bind Pr20 (Table 1.1). Therefore, we hypothesized that PRAME and HLA-A2 expression alone is necessary but not sufficient to generate the ALY/HLA-A2 complex. Hematopoietic cells are well known to express an alternative form of the proteasome called the immunoproteasome[58], and indeed, most PRAME positive leukemias bound Pr20. We hypothesized that the immunoproteasome is important for processing the ALY peptide. Although not highly expressed in most tissues, the immunoproteasome can be up-regulated by pro-inflammatory cytokines such as IFNγ and TNFα [60].

PRAME+ melanoma cell lines SK-Mel5, UACC257, and A375, and a PRAME+ colon adenocarcinoma SW480, were treated with IFNγ for 72hr to induce immunoproteasome expression. Upon IFNγ treatment, these cell lines showed dramatically increased binding to Pr20 (Fig. 1.8A top panels). As IFNγ can cause up-regulation of HLA-I, it was possible that the increased Pr20 binding was partly driven by increased cell surface HLA-A2. However, Pr20 binding increased far more (up to 10 fold) than HLA-A2 (2-6 fold) (Fig. 1.8A Bottom panels), suggesting that increases in HLA-A2 were not the dominant cause of the increased Pr20 binding. Importantly, pre-treatment of the tumor cells with IFNγ led to enhanced Pr20M-mediated ADCC *in vitro,* indicating that up-regulation of the target epitope might enhance therapeutic utility (Fig. 1.8B). Increased Pr20 binding was not observed on several samples of HLA-A2+ healthy donor PBMC populations after IFNγ treatment (Fig. 1.9). PRAME

mRNA and protein expression did not increase after IFNγ treatment, and indeed, decreased slightly (Fig. 1.8C), suggesting that IFNγ-mediated regulation of PRAME protein expression was not the cause of increased ALY peptide presentation. Protein expression of the immunoproteasome subunits β1i, β2i, and β5i increased after IFNγ treatment (Fig. 1.8D) possibly leading to enhanced generation of the ALY peptide.

The immunoproteasome catalytic subunit β5i is important for IFNγ-mediated regulation of Pr20 binding

We hypothesized that IFNγ could enhance generation of the ALY peptide by altering the proteasome components. To determine if increased Pr20 binding was due to immunoproteasome up-regulation, we generated CRISPR knockouts of each immunoproteasome subunit in the SK-Mel5 melanoma. After knockout by Cas9, β1i, β2i, and β5i were not measurable by western blot analysis compared to a vector control (Fig. 1.10A). The immunoproteasome subunit knockouts were treated with IFNγ for 72 hours and Pr20 binding was assessed by flow cytometry (Fig. 1.10B). β5i knockout led to significantly less Pr20 binding, demonstrating that β5i plays an important role in IFNγ-mediated processing of the ALY peptide epitope. CRISPR

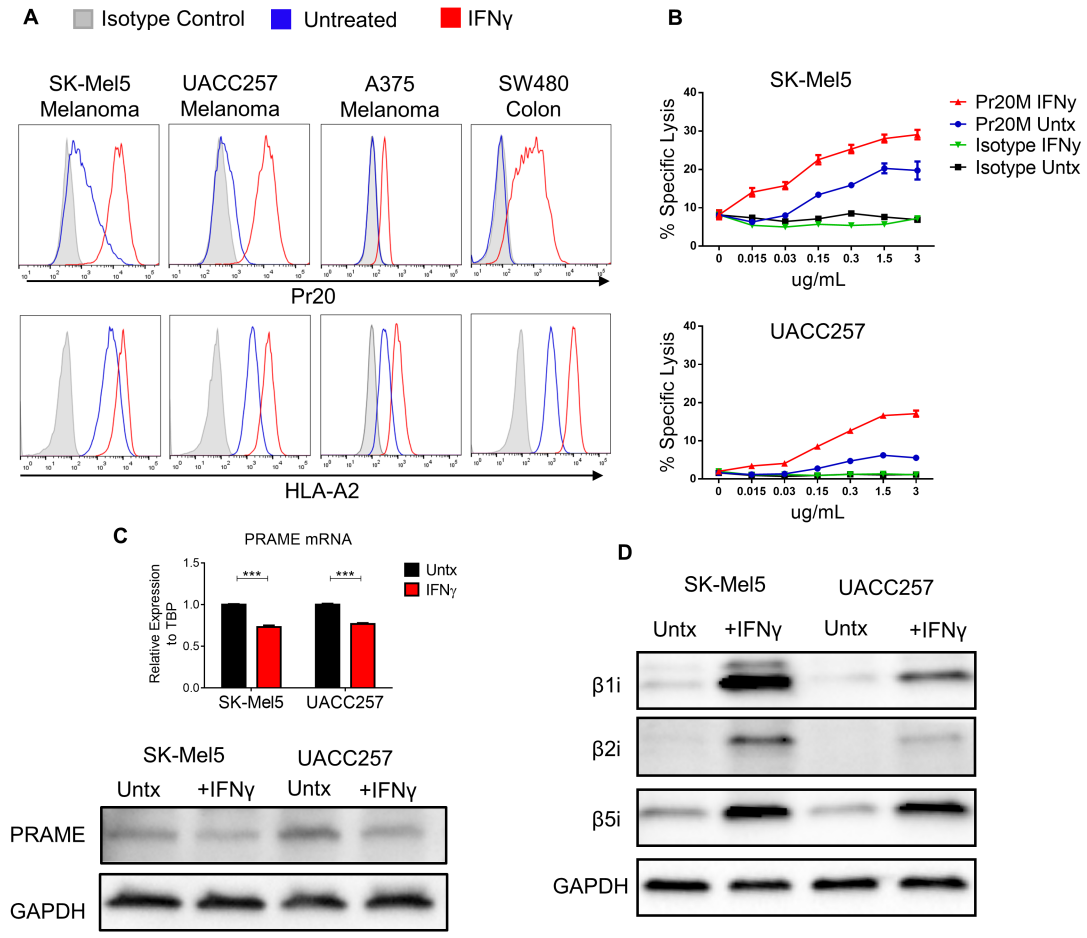

Figure 1.8. Melanomas and other solid tumors do not readily bind Pr20, but treatment with IFNγ induces immunoproteasome expression and dramatically increases Pr20 binding.

(A) HLA-A2+ melanomas and a colon adenocarcinoma that expressed PRAME by qPCR (Table 1) were either left untreated (blue) or treated with 10 ng/mL of IFNγ for 72 hours (red) and stained with Pr20 compared to untreated cells stained with an isotype control antibody (grey). HLA-A2 staining was performed in parallel. Data represents 3 independent experiments. (B) Melanomas were pre-treated with 10 ng/mL IFNγ for 72 hours or left untreated before ^{51}Cr-ADCC assay was used to determine specific lysis by Pr20M. Samples were assayed in 3 technical replicates and data is representative of 3 experiments per cell line. (C) PRAME expression after 72 hours of IFNγ treatment was also measured by qPCR and western blot analysis. qPCR data was analyzed by unpaired T test and is representative of 3 experiments with 3 technical replicates per experiment where mean ± SEM are plotted. Western blot data is representative of 3 experiments. (D) The expression of each immunoproteasome subunit was also determined after IFNγ treatment by western blot analysis. Data is representative of 3 experiments.

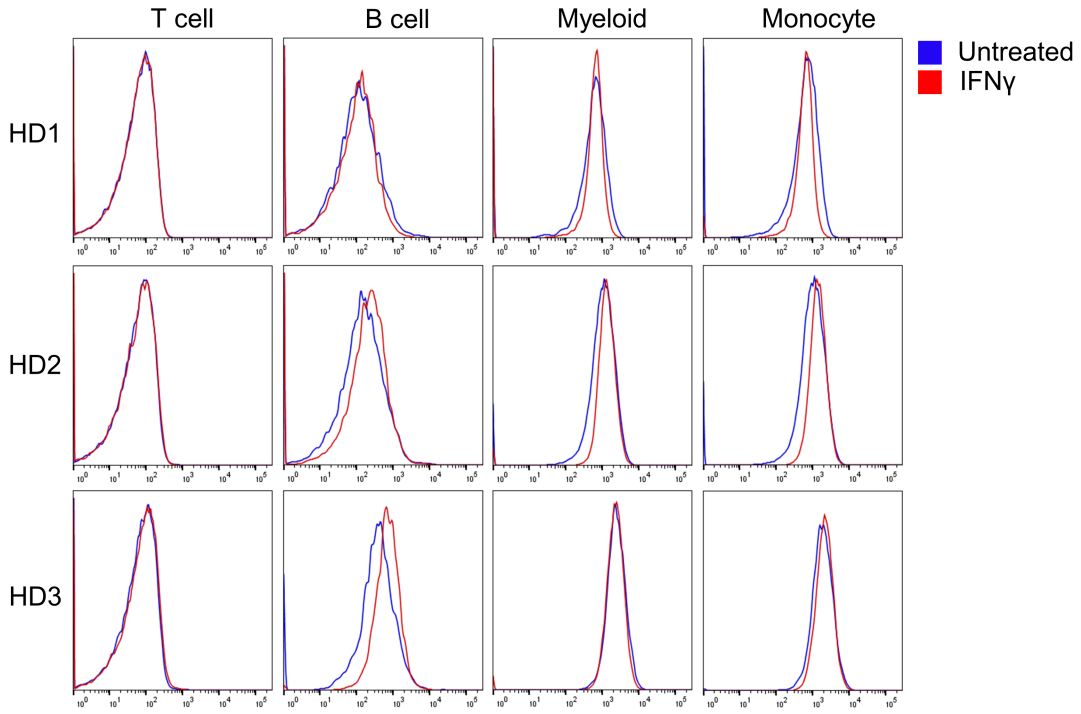

Figure 1.9. IFNγ does not induce substantial Pr20 binding in HLA-A2+ healthy donor PBMC populations.
HLA-A2+ healthy donor (HD) PBMC were left untreated or incubated with 10 ng/mL IFNγ for 72 hours. Flow cytometry was used to determine Pr20 binding in major PBMC populations (T, B, myeloid, and monocyte). Gating strategy was performed as in figure 2B. The experiment was performed on PBMC from n=3 HLA-A2+ healthy donors.

knockout of β5i yielded the same effect in UACC257, another HLA-A2+/PRAME+ melanoma (Fig. 1.10B Bottom Panel), and SW480, an HLA-A2+/PRAME+ colon adenocarcinoma (Fig. 1.11). Surface HLA-A2 expression was not affected by β5i knock out in the SK-Mel5 model and only minimally decreased in the UACC257 model (Fig. 1.10B). ONX-0914, a selective inhibitor of β5i was used to provide orthogonal validation that the immunoproteasome is important for generation of ALY/HLA-A2. SK-Mel5 and UACC257 were treated with IFNγ for 72 hours with or

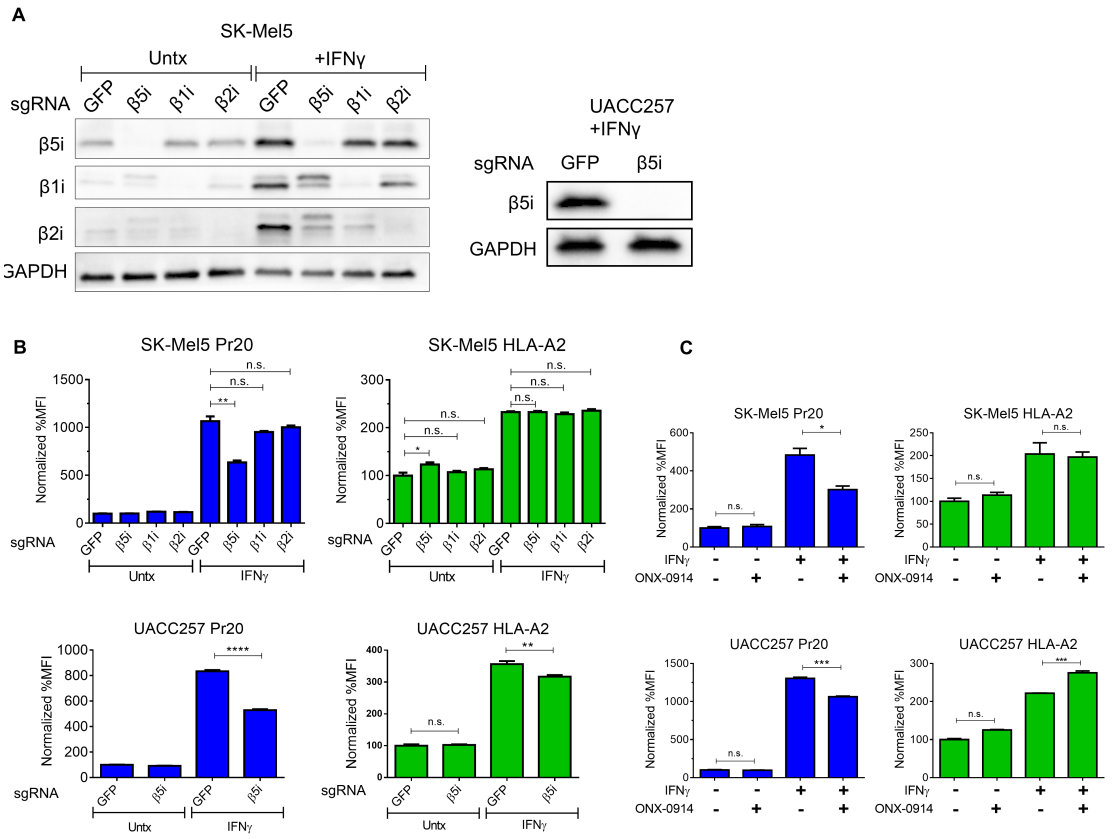

Figure 1.10. Immunoproteasome catalytic subunit β5i is important for IFNγ-mediated Pr20 binding in melanomas and other solid tumors.
β1i, β2i, and β5i were knocked out in the SK-Mel5 melanoma line using a CRISPR approach. A CRISPR construct against GFP was used as a vector control. (A left panel) Cells were treated with 10 ng/mL IFNγ for 72 hours and western blot analysis was used to demonstrate successful knock-outs. Blots were derived from replicate samples run on parallel gels with the GAPDH loading control shown from the β2i blot. (B) Flow cytometry was used to determine Pr20 binding and surface HLA-A2 on the indicated knock-outs (sgRNA against β1i, β2i, and β5i) untreated or treated with IFNγ for 72 hrs. (B top panels) Data is normalized to MFI of untreated GFP sgRNA CRISPR control. (B lower panels) β5i CRISPR knock-out experiments were performed in the same manner on the UACC257 melanoma line. Successful knock-out was determined by western blot (A right panel) and Pr20 binding and surface HLA-A2 was determine by flow cytometry (B lower panel). (C) SK-Mel5 and UACC257 cells were left untreated or treated with 10 ng/mL IFNγ for 72 hours in the presence or absence of 200 nM of the β5i inhibitor ONX-0914. Flow cytometry was used to determine MFI relative to untreated cells. All data are representative of 3 experiments with 3 technical replicates per experiment and mean ± SEM plotted. Statistical significance was determined by unpaired T test compared to control.

without the presence of ONX-0914. ONX-1014 was used at 200 nM, a concentration reported to have potent biochemical inhibition of β5i but minimal inhibition of other proteasome catalytic subunits [59]. As expected, cells treated with ONX-0914 had reduced Pr20 binding compared to cells treated with IFNγ alone (Fig. 1.10C). Taken together, our data suggest the shift from the constitutive proteasome to the immunoproteasome is an important mechanism for increased epitope presentation and Pr20 binding. Furthermore, SK-Mel5 cells treated with bortezomib alone, a potent inhibitor of the constitutive proteasome β5 subunit and to a lesser extent the β1 subunit [105], did not substantially alter binding to Pr20 at doses that were not cytotoxic. We also explored the use of demethylating agents in an attempt to increase the level of PRAME protein expression and thereby possibly peptide epitope on the surface. We observed only modest increases in Pr20 binding after decitabine treatment (Fig 1.12).

The constitutive proteasome mediates internal destructive cleavage of the ALY peptide

Proteasomal degradation can regulate the generation of a specific HLA-I associated peptide through enhancing the required N or C-terminal cleavages, or through reducing destructive internal cleavages. Several tumor-associated antigens exhibit restriction to the immunoproteasome because the peptide is largely destroyed by the constitutive proteasome and thus intact peptide cannot be presented [61,63]. To elucidate the differing proteolytic mechanisms between the constitutive and immunoproteasome involved in generating increased ALY peptide epitope on the surface, an elongated 20-mer ALY-precursor peptide was synthesized with 5 residues extending from each terminus ($PRAME^{295-314}$). The ALY-precursor peptide was incubated with either purified constitutive proteasome or immunoproteasome *in vitro* and digest fragments

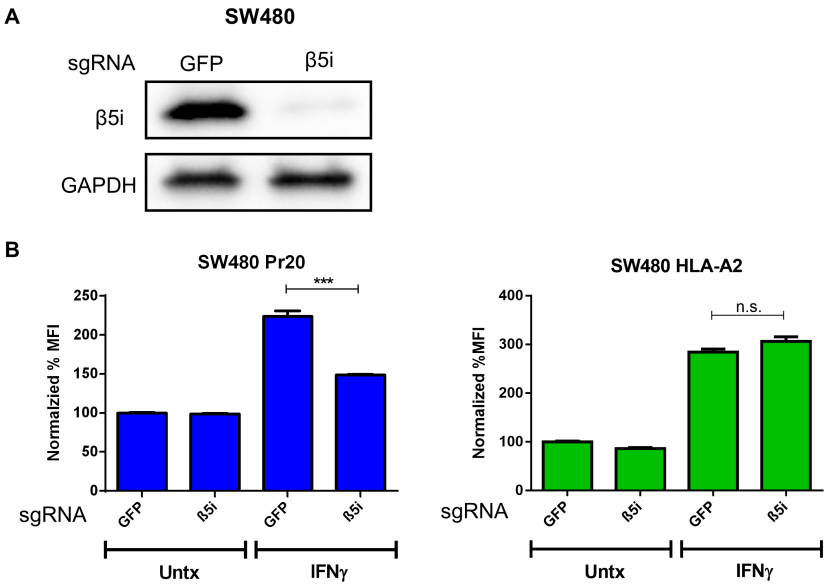

Figure 1.11. β5i knock-out by CRISPR abrogates IFNγ-mediated Pr20 binding in colon adenocarcinoma SW480.
CRISPR constructs against the immunoproteasome subunit β5i or the irrelevant GFP was generated and transduced as described in figure 4. (A) Western blot analysis was used to confirm successful knock-out. (B) SW480 cells transduced with the CRISPR construct against β5i or GFP were treated with 10 ng/mL IFNγ for 72 hours and Pr20 binding and surface HLA-A2 expression was measured by flow cytometry. Normalized %MFI is plotted with and without treatment. Experiment was performed 3 times with 3 technical replicates per experiment. Mean ± SEM are plotted from one representative experiment. Differenced analyzed by unpaired T test.

were analyzed by mass spectrometry. The major detectable fragments were then mapped to specific cleavage sites. Of the detected major digest fragments, the immunoproteasome had increased ratio of non-destructive / destructive cleavages in the ALY sequence (Fig. 1.13A), while the immunoproteasome maintained the intact ALY 10-mer. In addition, the immunoproteasome catalyzed a major cleavage site after Q296 and L298 (LQ/CLQ**ALYVDSLFFL**RGRLD and LQCL/Q**ALYVDSLFFL**RGRLD) 1 and 3 residues N-terminal to the ALY 10-mer (Fig. 1.13B). Such cleavage may prime the peptide for amino-peptidase trimming.

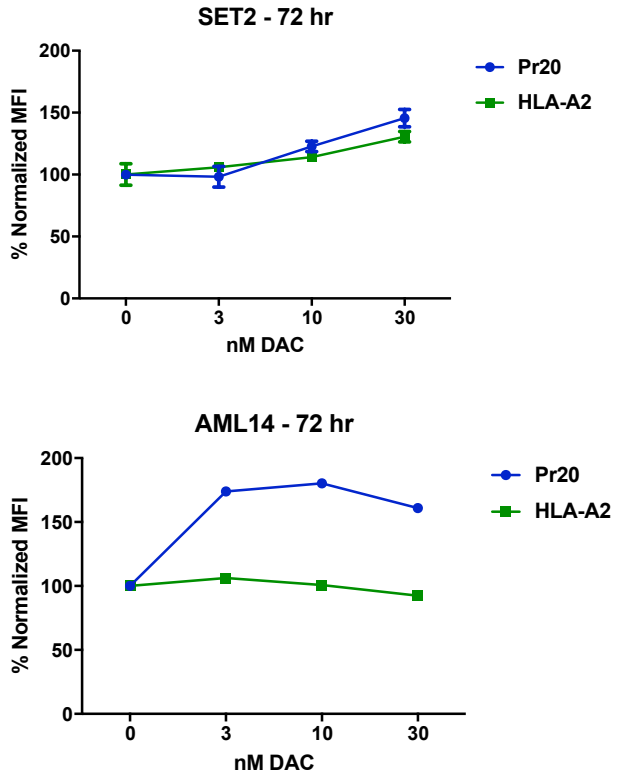

Figure 1.12. Decitabine increases Pr20 binding *in vitro.*
SET2 and AML14 cells were treated with the indicated dose of decitabine or DMSO vehicle for 72 hrs. Due to decitabine instability at 37° C, media with decitabine was replaced daily. Flow cytometry was used to determine MFI of Pr20 and HLA-A2 relative to DMSO vehicle control. Experiments were performed twice with SET2 and once with AML14.

In contrast, the constitutive proteasome mediated a major destructive cleavage site after A300 (LQCLQ**A/LYVDSLFFL**RGRLD) and after V303 (LQCLQ**ALYV/DSLFFL**RGRLD). Our analysis demonstrates that the relative cleavage after the C-terminal L309 (LQCLQ**ALYVDSLFFL**/RGRLD) was comparable between constitutive and immunoproteasome, suggesting that C-terminal cleavage of the ALY peptide was not a major mechanism of immunoproteasome restriction (Fig. 1.13B). An N-terminal cleavage after the Q299 (LQCLQ/**ALYVDSLFFL**RGRLD) was not a major cleavage site for either

proteasome form. The major differences in cleavage specificities between the constitutive and immunoproteasome on the precursor peptide is schematized (Fig. 1.13C). Taken together, the biochemical data show that the immunoproteasome enhances generation of the ALY 10-mer peptide through decreased internal destructive cleavage and increased N-terminal upstream cleavage, relative to the constitutive proteasome.

DISCUSSION

Immunotherapy has demonstrated potent clinical utility for several cancers. However, successful therapy would be improved by use of targets that are cancer-selective to minimize toxicity to essential healthy tissue. Although highly selective onco-fetal or cancer-testis tumor-associated antigens have been described, most are intracellular proteins that cannot be targeted by small molecule inhibitors or by using antibodies directed at cell-surface targets. Furthermore, most of these tumor antigens, such as PRAME, have context-dependent function and are not necessarily oncogenic. Thus, functional inhibition may not offer therapeutic benefit. Several groups have studied TCR-transgenic T cells specific against intracellular tumor-associated antigens, but this strategy has been limited due to challenges of large-sale manufacturing and safety concerns of the transgenic TCR recombining with the native TCR generating unknown specificity and possible auto-immune reactivity [53]. Recently described 'ImmTAC' molecules use a TCR-based recognition domain offering similar reactivity to TCRm antibodies, and also demonstrate high affinity [106]. TCRm antibodies such as Pr20 can target these 'undruggable' proteins with high affinity for redirected immune mediated cytolysis.

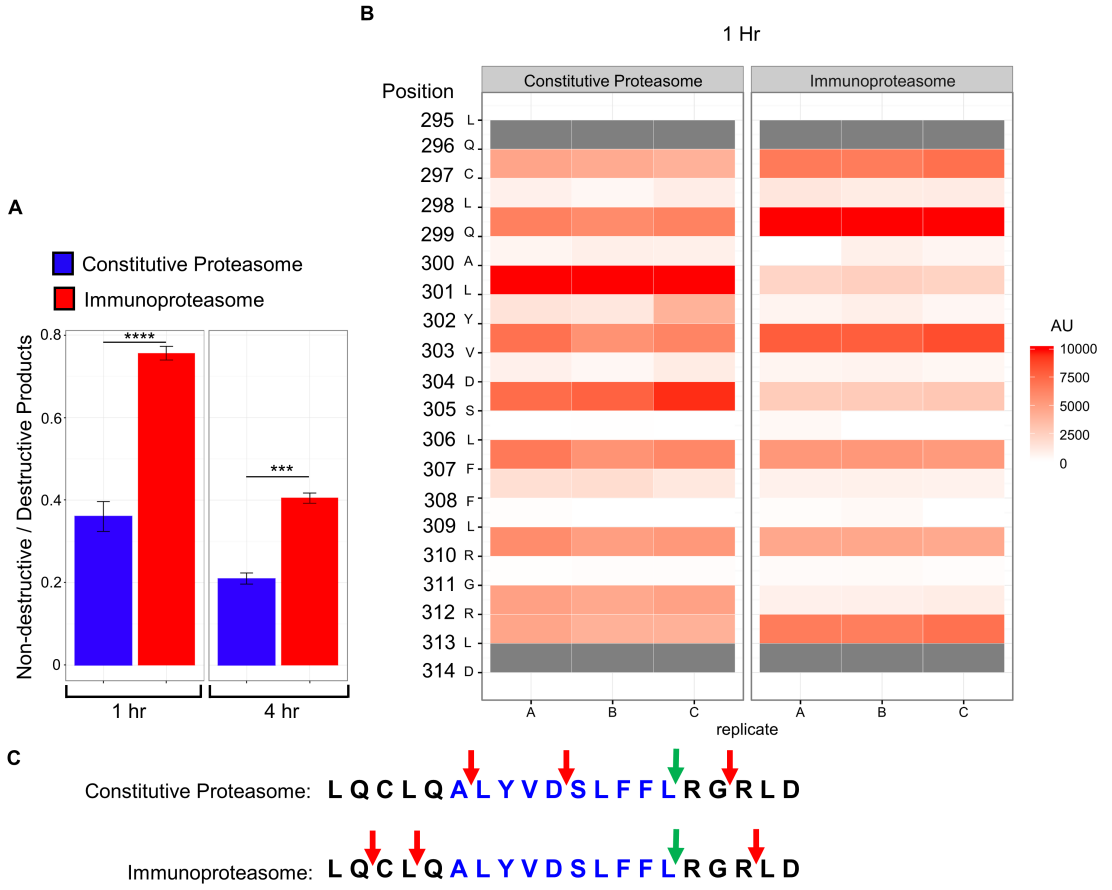

Figure 1.13. The Immunoproteasome catalyzes increased non-destructive cleavages on an ALY-precursor peptide.

A 20-mer ALY-elongated precursor peptide was incubated with purified constitutive proteasome or immunoproteasome for the indicated times. (A) All detectable fragments and their respective ion intensities were assigned to be "non-destructive" or "destructive" depending on if the N or C-terminal cleavages required to generate that fragment would have resulted in destruction of the ALY 10-mer. Ratios of ion intensity sums for "non-destructive/destructive products" are plotted. (B) Major cleavage sites along the precursor peptide after 1 hr were mapped by summing the ion intensities of each fragment resulting from a cleavage after the specific residue. Heat map with arbitrary units corresponding to ion intensities is shown, with 3 replicates illustrated in 3 bars for each proteasome preparation. Only fragments identified to be at least 2 residues or more could be mapped and thus cleavages before Q296 or after L313 were not accounted for. (C) Major differences in cleavage specificity between constitutive and immunoproteasome are schematized and mapped by red arrows. The green arrow denotes the canonical proteasomal cleavage to generate the C-terminal end of the ALY 10-mer. Data are from three technical replicates per experimental condition with mean ± SEM plotted. Groups compared using multiple T tests.

Pr20 specificity analyses were consistent with binding to the ALY peptide primarily on the C-terminal half amino acids at positions 5-9. However, because minimal contact residues were predicted in the N-terminus, we cannot exclude the possibility of cross-reactive peptide/HLA-A2 epitopes in the exome that share high C-terminal homology to ALY. Whether other theoretical peptide epitopes in the exome are expressed and processed appropriately in normal tissues is difficult to explore. The data shown here suggest that if potential cross-reactive peptides in the human exome are expressed, properly processed, and sufficiently presented, they are infrequent. Peptides have specific processing requirements including not only proteasomal degradation, but also aminopeptidase and oligopeptidase processing [107] which likely limit generation of cross-reactive epitopes. In addition, potential cross-reactive peptides may lack high affinity to HLA-A2 and thus will not form stable peptide/HLA-A2 complexes at the cell surface. Pr20 did not bind PRAME-negative/HLA-A2+ cells and did not bind more than a dozen other HLA-A2+ tumor lines, suggesting there were no broadly-presented cross-reactive peptides. In addition, Pr20 did not bind to or accumulate in any major organ in HLA-A2 transgenic mice, nor bind to normal human blood cell populations in healthy HLA-A2+ donors. Taken together, the data suggests that cross-reactive epitopes presented on HLA-A2 are non-abundant. Importantly, such off-targets are not increased in normal cells after IFNγ treatment.

The afucosylated Pr20M demonstrated therapeutic efficacy *in vivo*. Interestingly, at the experimental end-point, Pr20 binding to AML14 in Pr20M-treated mice was significantly higher than in AML14 in isotype-treated mice. This is intriguing because first, it shows that target down-regulation is not a mechanism of tumor escape in this model; and second, it also suggests that cellular interactions during Pr20M therapy

may increase epitope expression on target cells. This may be due to cytokines released by immune effectors during ADCC, as observed with other therapeutic antibodies [16,108]. It is important to note that the NSG mouse xenograft poorly models the human effector populations and the cytokine milieu that would be produced in a patient. In addition, because HLA-I is well characterized to be regulated by inflammatory cytokines and TCRm targets are presented in complex with HLA-I, it is possible that TCRm targets are regulated in a 'feed-forward' system where TCRm-mediated cytolysis leads to local cytokine release and increased target expression on neighboring tumor cells. Human IgG1 also has different affinities to mouse FcR and human FcR, and NSG mice lack functional NK cells and have defective macrophages and dendritic cells. Therefore, lack of and poorly functional effector cell populations in this model may limit efficacy of a TCRm which requires immune effectors for ADCC [104] which may in part explain the lack of tumor eradication and relapse within weeks. It is reasonable to hypothesize that TCRm therapy in an immunocompetent patient or model would demonstrate more potent therapy. To better understand the incomplete responses to the therapy *in vivo*, we tested whether combination of Pr20M antibody therapy with a second therapeutic TCRm antibody directed to an unrelated epitope also found on the target cells, would increase therapeutic effects (Fig. 1.14). This would yield more than double the target epitope numbers on each cell (based on radio-immunoassays to quantify TCRm epitope sites) and also rule out the issue of leukemia escape by down-regulation or loss of the PRAME epitopes from the leukemia cells. No significant improvement in leukemia control was demonstrated in these experiments, further bolstering the argument that lack of effector cell function and effector cell numbers were the critical deficiencies, not lack of (or loss of) target PRAME epitopes on the leukemia.

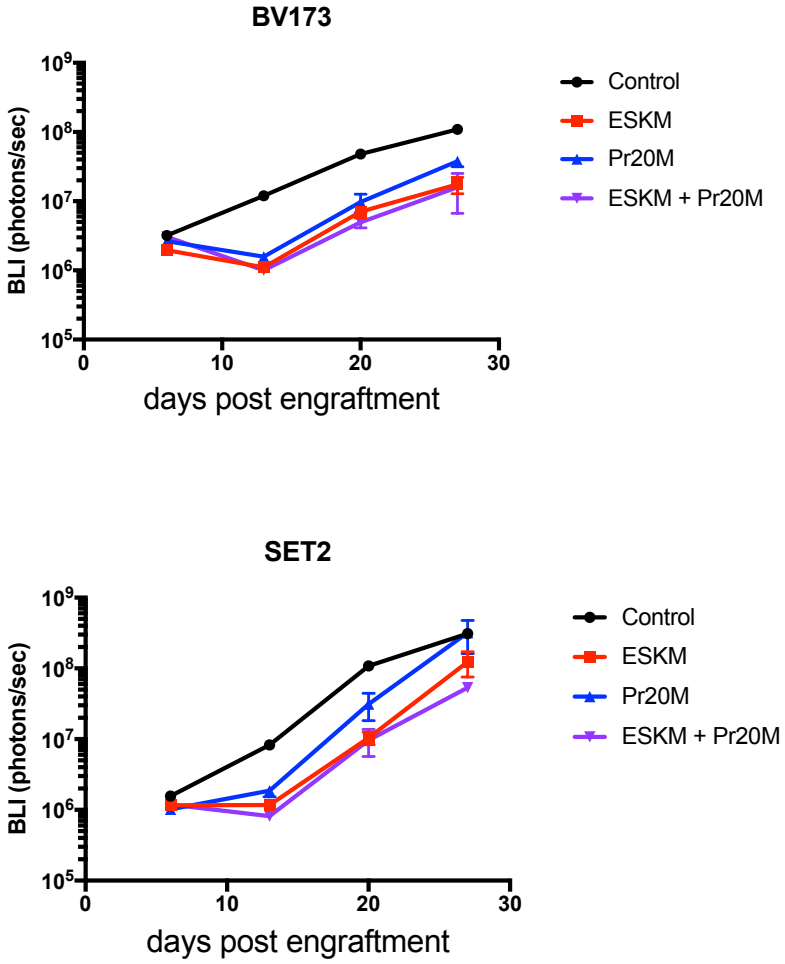

Figure 1.14. Pr20M and an additional TCRm (ESKM) are not additive in TCRm therapy *in vivo*.
NSG mice were engrafted with $0.5x10^6$ SET2 cells (AML) or $3x10^6$ BV173 cells (ALL) through tail vein injection. On day 6, mice were randomized into groups of 5. Mice were treated on day 6, 10, 13, and 17 after engraftment with 50 µg of Pr20M alone, 50 µg of ESKM (a TCRm against a peptide from WT1) alone, or Pr20M and ESKM in combination. Control mice were left untreated and tumor burden was assessed by bioluminescent imaging on the indicated days. Mean group BLI ± SEM is shown. BLI data was not significantly different on day 20 or 29 for either SET2 or BV173 models between the the ESKM + Pr20M combination group versus the ESKM alone or Pr20M alone (unpaired t-test). Experiment was performed once in the BV173 model and once in the SET2 model.

Generating an immunocompetent syngeneic mouse model in which to test these agents is difficult because murine PRAME does not comprise the human ALY peptide, which would have to be introduced genetically along with use of mice with transgenic human HLA-A2. It is also unknown if the ALY peptide can be properly cleaved and processed by the murine antigen presentation machinery and presented on transgenic HLA-A2 molecules. Co-infusion of human immune cell populations into NSG mice may provide an alternative model for effector cells and cytokines in these mice, but also leads rapidly to graft-versus-host disease and graft versus leukemia activity complicating the analysis, as seen in previous studies [43].

Binding studies demonstrated that Pr20 robustly bound to several PRAME+/HLA-A2+ leukemias and lymphomas cell lines, but did not bind well to a small sample size (n=9) of previously frozen PRAME+/HLA-A2+ primary AML. This is consistent with the lack of binding to several PRAME+/HLA-A2+ cancer cell lines. Our data demonstrates that PRAME and HLA-A2 expression alone is necessary, but insufficient for Pr20 binding. It is also important to note that the number of ALY peptide epitopes presented on HLA-A2 is highly limited (estimated at less than 0.1% of the HLA molecules on the surface based on Scatchard analyses) and may be below the detection limit of the flow cytometry assay with Pr20 in some cells. It is also possible that low epitope presentation is undetectable with our assays yet sufficient to initiate redirected lysis, however this could not be reliably studied with frozen primary AML samples.

Pr20 did not initially bind several PRAME+/HLA-A2+ melanomas and other solid tumors despite high levels of PRAME expression, but Pr20 binding dramatically

increased upon treatment with IFNγ, which was partially mediated by increases in the immunoproteasome β5i expression. β5i is well-characterized to have chymotrypsin-like enzymatic activity, cleaving after hydrophobic amino acids [56]. However, the specificity is complex and not fully understood. For instance, β5i cleavage can be inhibited by the presence of an additional hydrophobic residue directly C-terminal of a site as demonstrated *in vitro* using the enolase-1 protein as a model substrate [109]. IFNγ decreased PRAME protein expression, which may be caused by decreased mRNA expression but may also be due to differing kinetics of the immunoproteasome. Using a biochemical digestion assay in vitro, we demonstrated that the immunoproteasome cleaves and yields a presentable ALY-precursor peptide more efficiently then the constitutive proteasome. ALY peptide precursors generated through proteasomal digestion in vitro have been described [84], however direct comparison between constitutive proteasome and immunoproteasome on digestion of the ALY peptide has not been studied. The constitutive proteasome catalyzed a major destructive cleavage site after the first A300 of ALY (LQCLQ**A/LYVDSLFFL**RGRLD), whereas the immunoproteasome did not, possibly due to inhibition by the adjacent hydrophobic leucine. In addition, the immunoproteasome better catalyzed cleavages slightly N-terminal to the ALY peptide. Minor N-terminal elongated intermediate peptide may prime the peptide for amino-peptidase trimming into the ALY 10-mer; however, this was not studied. The knowledge of target presentation has broad implications when designing peptide vaccines, TCR, and TCRm antibodies for determining which tumors may respond best to these therapies. In addition, checkpoint blockade therapy, which has demonstrated effective clinical utility, relies on tumor-antigen presentation and CTL recognition to direct tumor cell lysis. Therefore, understanding the biochemical mechanisms of immunogenic peptide generation and presentation is critical for designing checkpoint blockade strategies and determining ideal tumor targets. Our

data suggest that tumors expressing the immunoproteasome such as leukemia and lymphomas would better respond to immunotherapies against ALY/HLA-A2 and that other cancer types may need pharmacologic up-regulation of the immunoproteasome in conjunction to make the immunotherapy effective.

Pr20 binding requires peptide presentation in the context of HLA-A2, and thus strategies to enhance HLA-A2 expression may also augment Pr20M-mediated therapy. It will be important to discover pharmacological modulators of HLA-I that can be used for combination therapy with TCRm antibodies or other HLA-I-based immunotherapies. For example, recent reports demonstrate that inhibition of MEK can increase cell-surface HLA-I which may enhance TCRm antibody therapy [110]. Additionally, several pharmacological agents that target histone-modifying enzymes such as methytransferase inhibitors and histone deacetylase inhibitors can induce expression of tumor-associated antigens including PRAME, and lead to enhanced cytolysis by effector T cells [111–113]. It would be important to understand if these agents could enhance antigen expression and synergize with TCRm therapy. However, these epigenetic drugs can also have context-dependent effects on immune cell function and therefore must be evaluated carefully to ensure they do not also inhibit the effector cells required for TCRm-mediated cytotoxicity [112,114].

Our data demonstrate the ability to target PRAME with a TCRm antibody. This approach enables us to target intracellular proteins to which the generation of small molecule inhibitors is not possible. TCRm allow access to a new universe of antibody protein targets, far larger and more tumor-specific than the currently available cell-surface protein targets. They also bypass the patient-specific limitations of CTL-based therapies. Only a few TCRm have been studied in pre-clinical models as agents for

cancer therapy [43,50,97,102,115–117]. Therefore, the present study on Pr20 adds additional proof-of-concept that TCRm can be potent and selective therapeutic agents. Finally, due to the well-characterized mAb format of TCRm, they can be readily engineered into alternative formats such as Fc-enhanced forms, as shown in this study, bispecific T cell engager [89,118] forms (BiTE), as done with a TCRm to WT1, or transduced as a chimeric antigen constructs (CARs) in T cells [91,92]. These additional formats may be required for effective targeting of these ultra-low density targets. Radioimmunoconjugates [119] and antibody-drug conjugates may also be explored in the context of TCRm in an effort to enhance potency against cancer cells.

AKNOWLEDGEMENTS

This study was supported by the Leukemia and Lymphoma Society, NIH P30CA 008748, NIH R01 CA55349, P01 CA23766, the Lymphoma Foundation, Tudor Funds, the MSKCC Technology Development Fund, and the Experimental Therapeutics Center. AYC and part of this work are supported by the Office of Assistant Secretary of Defense for Health Affairs through the Peer Reviewed Cancer Research Program under award no. W81XWH-16-1-0242. Opinions, interpretations, conclusions, and recommendations are those of the author and are not necessarily endorsed by the Department of Defense. We thank Elliott J Brea and Dmitry Pankov for productive discussion.

CHAPTER II: ENHANCING THERAPEUTIC EFFICACY OF TCRm THROUGH CD47/SIRPα BLOCKADE AND ENGINEERED BiTE AND CAR T CONSTRUCTS[*,†]

INTRODUCTION

CD47/SIRPα Signal Axis in Phagocytes and the SIRPα-variant CV1

Our data prove the concept that an antibody-based construct can therapeutically target the ALY/HLA-A2 complex on cancers. However, a major limitation of TCRm antibodies is that the epitope density is far lower than traditional antibody targets and have been estimated to be as low as approximately 200-1000 sites per cell[43,50]. This may limit therapeutic efficacy especially when immune effector mechanisms are critical for activity. Indeed, our data demonstrates that although Pr20M has therapeutic activity (Fig 1.7), leukemia-bearing mice treated with Pr20M do not have deep regressions and ultimately have progressive disease. Therefore, we hypothesized that therapy could be augmented using strategies to enhance immune effector activity such as CD47 axis blockade. CD47 is a transmembrane protein found on all cells and serves as a 'do not eat me' signal for phagocytes such as macrophages and dendritic cells. CD47 binds to SIRPα on phagocytes which signals through intracellular immunoreceptor tyrosine-based inhibitory motifs (ITIMs) to recruit and activate phosphatases SHP-1 and SHP-2[120]. This leads to inhibition of macrophage activation

---

* Modified from Mathias M, Sockolosky J, Chang AY, Tan K, Liu C, Garcia KC, Scheinberg D. CD47 Blockade enhances therapeutic activity of TCR mimic antibodies to ultra low density cancer epitopes. Leukemia. 2017 DOI:10.1038/leu.2017.223

† Some experiments were designed and conducted by or in collaboration with Jonathan Sockolosky at Stanford University (Fig. 2.1) and Melissa Mathias (Fig. 2.3). The Pr20-BiTE and Pr20-CAR constructs were made by Eureka Therapeutics.

in addition to inhibition of myosin elements and therefore prevention of phagocytic engulfment[121]. Several studies have demonstrated that CD47 blockade can be effective as cancer therapy especially when used in combination with antibodies that promote ADCP[88,122]. Based on these and other preclinical data, anti-CD47 mAbs have entered early stage clinical trails[123]. However, CD47 blockade using mAb or Fc-fusion protein approaches has also demonstrated substantial toxicity to healthy red blood cells leading to anemia, hypothesized to be caused by Fc engagement of the antibody despite an IgG4 isotype[124]. Instead, the Garcia group at Stanford University developed a high-affinity soluble SIRPα-variant called CV1 which lacks an Fc portion and does not cause anemia in mouse models[125]. CV1 has also demonstrated potent synergy with traditional mAb therapy such as Rituximab[124]. We therefore hypothesized that combination therapy of Pr20M with CV1 would lead to enhanced Pr20M-mediated ADCP and therefore substantially enhanced therapy.

It is also important to note that CD47 has additional functionality and is not just a 'do not eat me' signal for phagocytes. CD47 also binds the ligand thrombospondin-1 (TSP-1). Although context and cell type dependent, CD47 engagement can trigger apoptosis in some cell types through an interaction of the cytoplasmic tail of CD47 with BNIP3 pro-apoptotic BH3 domain protein[126]. In fact, CD47 knockout cells have demonstrated remarkable advantages in self-renewal[126]. In addition, CD47 had implicated roles in regulating mitochondria-dependent death pathways and autophagy[126,127]. These cell-intrinsic functions are important to understand and consider when utilizing CD47 blockade immunotherapy to ensure that strategies promote tumor cell death and not tumor-protective effects.

Bispecific Antibodies

Whereas naturally produced antibodies are canonically multivalent but clonally mono-specific, mAbs can be generated or engineered with multiple specificities. The most common and well studied for cancer therapy is the bispecific antibody. These consist of several formats but are broadly grouped into bispecific IgG (BsIgG) or bispecific antibody fragments (BsAb fragments)[1,128]. The major benefit of bispecific antibodies is that each molecule can engage two unique targets at once allowing for novel antibody functionality. This can include dual blockade of two receptors, fine-tuning of targeting only cells expressing dual epitopes, and redirected immune engagement not possible with natural antibodies[129]. The concept of bispecific antibodies has been demonstrated since 1961[128], however technologies to generate bispecific antibodies on a commercially feasible scale were not available till more recently. A major challenge of generate BsIgG is chain mispairing during co-expression of 2 light chains and 2 heavy chains in the same cell, leading to low yield of desired BsIgG and challenges to purifying the BsIgG from the mis-paired contaminants. Undesired heavy chain homodimers and light chain mispairing with non-cognate heavy chains can generate 9 theoretical undesired IgG products in addition to the desired BsIgG[128]. Innovative engineering approaches have allowed more efficient generation of BsIgG using strategies such as 'knob-in-hole' where a 'knob' mutation disfavors homodimerization and favors heterodimerization of a corresponding 'hole' mutation[128,130]. Other strategies include rationale electrostatic mutations as well as Fab arm exchange through processes such as the biochemical phenomenon of split inteins[128,131].

BsAb fragments are a class of bispecific antibodies that lack full antibody constant regions. Although several iterations of BsAb fragments have been generated, the most common consist of heavy and light chains connected through a short peptide linker.

The linker promotes inter-chain pairing and prevents intra-chain pairing of V_H and V_L domains such that 2 scFv chains can be co-expressed in a cell to produce a bispecific fragment called a diabody. Another common BsAb fragment design is a tandem scFv. Two scFv's are linked through a linker region allowing dual specificity to be encoded on one polypeptide chain. This construct is the basis of the bispecific T cell engager (BiTE) designed to redirect T cells as discussed following.

Bispecific T cell Engager (BiTE) Molecules

An additional method to improve potency of Pr20 is through adaptive the targeting moiety of the Pr20 mAb scFv to more potent biologic formats. The Bispecific T cell engager (BiTE)[90,132] construct is a powerful biologic agent that has recently reached clinical approval with the anti-CD19xanti-CD3 Blinatumomab (Amgen) which demonstrated significant responses and complete remission in 43% of adult patients with relapsed refractory cell acute lymphocytic leukemia disease[3,132]. BiTEs are antibody-based single-chain protein constructs composed of a tumor-antigen targeting scFv moiety linked to an anti-CD3 scFv moiety. The molecular weight of a BiTE molecule is approximately 55 kDa. The BiTE design allows engagement of a target tumor cell with the CD3 molecule of T cells. Upon engagement, BiTEs force target cell and T cells into extremely close proximity resulting in an immune synapsing, downstream CD3 signaling, and ultimately T cell activation, target cell lysis, and T cell proliferation[90,133]. This is unique to the natural T cell response because BiTEs bypass the need for peptide/MHC-specific priming through antigen presenting cells and therefore can redirect a polyclonal T cell response irrelevant of a T cell's endogenous specificity for peptide/MHC. In xenograft studies, BiTEs could potently redirect human T cells for tumor lysis without the need for additional co-stimulation[134], a required process of the natural T cell response. Additionally, whereas

mAbs typically harness innate immune effectors such as NK cells and macrophages, BiTEs can engage any T cell (the most abundant lymphocyte population) against the tumor, providing a much larger pool of immune effector cells. In addition, BiTEs can induce a phenomenon of epitope spreading whereby the activation of the polyclonal pool of T cells through the BiTE has been reported to induce a response to independent tumor antigen peptide/MHC targets[89]. This response may be through reactivation of inhibited or exhausted T cell after BiTE reactivity.

Although BiTEs have demonstrated functional potency and therapeutic benefit, they have challenges for their clinical use. These fusion proteins typically have a very short half-life of only a few hours in the serum[133]. This is owed to the lack of a Fc region and therefore BiTEs cannot undergo the process of neonatal Fc receptor (FcR_n)-mediated recycling[133]. The extremely short half-life makes dosing BiTEs a cumbersome process and currently BiTEs are administered through continuous intravenous infusion pumps[133]. In addition, cytokine release associated with T cell engagement presents a concern for side effects. As a precaution, BiTEs are currently administered along with dexamethasone, a glucocorticoid that can mitigate inflammation-related side effects[133].

Similar to BiTEs, bispecific killer cell engagers (BiKEs) are also a single-chain protein construct that uses an scFv against a tumor antigen linked to a scFv against CD16, the activating FcR found on NK cells[135]. Instead of engaging T cells, BiKEs engage NK cells with higher affinity than an antibody allowing BiKEs to function even when NK cells express low levels of CD16 as in myelodysplastic syndrome patients[135]. They can also be engineered into a novel trispecific killer cell engager (TriKE) construct consisting of the BiKE with an added arm to stimulate the IL15

receptor on NK cells promoting NK cell activation, proliferation, and serial killing[136,137].

Chimeric Antigen Receptor T cells (CAR T)

Chimeric antigen receptor T cell (CAR T)[138] constructs are powerful biologic agents that have recently reached clinical approval and have demonstrated significant responses in patients[138,139]. Current CAR T cells are a form of cellular therapy where an artificial receptor is transduced into T cells containing an extracellular targeting moiety composed of a scFv and an intracellular signaling moiety typically composed of the CD3ζ chain and either CD28 or 41BB co-stimulatory domains[139]. Upon target cell engagement, the CAR mediates activation and phosphorylation of CD3ζ, recruitment of ZAP70, and subsequence T cell activation and ultimate cytotoxicity[139]. CAR T cells have only recently gained FDA approval status but has already demonstrated robust and meaningful clinical outcomes in hematological malignancies. Clinically approved CAR T cells include the anti-CD19 CAR Tisagenlecleucel[140] (Novartis) for the treatment of refractory B cell lymphoblastic leukemia in pediatric and young adult patients and another anti-CD19 CAR Axicabtagene ciloleucel[141] (Kite Pharma) for treatment of adults with a specific type of B cell non-Hodgkin's lymphoma.

It is important to appreciate the history of CAR T cell technological development because it represents a paradigm-shift in cellular therapy and what is considered a 'drug'. Indeed in 2017, CAR T cells made history as the first FDA-approved gene therapy but the technology to make CAR T cells required decades of work and the cumulative advances in basic understanding and engineering in several fields – virology, immunology, molecular biology. First generation CAR T cells were reported

in 1989 as a construct consisting of an scFv targeting domain, a transmembrane domain, and the CD3ζ signaling domain (signal 1)[142]. Although these constructs proved the concept that T cells could be endowed with a novel specificity, they had limited efficacy in clinical trials, believed to be due to activation-induced cell death and limited expansion[143,144]. Second generation CAR T cells mitigated this through the addition of a co-stimulatory domain (signal 2) to the CAR cytoplasmic tail such as CD3ζ-CD28 or CD3ζ-41BB. Third generation CAR T cells combine multiple co-stimulatory domains on the CAR cytoplasmic tail such as CD3ζ-CD28-41BB or CD3ζ-CD28-OX40, to augment potency[139]. Excitingly, new generations of 'armored' CAR T cells are further engineered to secrete cytokines or express functionally active ligands[145]. For example, The Brentjens group at Memorial Sloan Kettering has developed an armored CAR constitutively secreting the cytokine IL-12. The IL-12 secretion dramatically improved anti-tumor efficacy and could overcome the tumor microenvironment in mouse models[146].

Like mAbs, current FDA-approved BiTEs and CARs only target cell-surface receptors namely CD19 in B cell leukemias and lymphomas[147]. However, because BiTEs and CARs utilize scFv as the targeting moieties, the scFv of a TCRm antibody could be grafted into a BiTE or CAR vector to generate these T cell-redirecting biologic agents against peptide/MHC-I targets. Indeed this has been studied pre-clinically for a select few TCRm constructs[91,92,148–150]. Although a TCRm-CAR may have similar specificity for peptide/MHC-I as a TCR-transduced T cell, the engineered intracellular signaling moieties in a CAR T cell provide them with biochemically unique activation abilities due to coupled activation and co-stimulatory signals. This is thought to benefit the CAR activation, function, and persistence[139] compared to TCR transduced T cells.

We hypothesize that rational combination therapy of Pr20M with CV1 to enhance macrophage-mediated ADCP would augment therapeutic efficacy compared to either agent alone in animal models of leukemia. We also hypothesize that engineered Pr20-BiTE and Pr20-CAR constructs would lead to enhanced redirected cytotoxicity and robust therapeutic efficacy.

MATERIALS AND METHODS

Antibody Dependent Cellular Phagocytosis (ADCP) Assays

Human and mouse macrophage-mediated antibody-dependent cellular phagocytosis (ADCP) assays were performed as follows. Human blood was obtained from the Stanford Blood Center using IRB approved protocols and monocytes were isolated via CD14 positive selection (Miltenyi) and magnetic isolation. Recovered CD14+ monocytes were plated at a density of 10,000,000 monocytes per 150 mm TC treated dishes in IMDM + GlutaMAX media (Gibco) supplemented with 10% human serum and 1% P/S and cultured for 7 days at 37 °C to yield human monocyte derived macrophages (MDMØ). Phagocytosis assays were repeated in duplicate.

Mouse macrophages were derived from bone marrow (BMDMs). Mouse bone marrow cells were flushed with a syringe from the tibia and femurs of NSG mice into IMDM + GlutaMAX supplemented with 10% FBS and 1% P/S. Cells were collected by centrifugation followed by RBC lysis with ACK buffer for 3 – 5 mins (Gibco), quenched with complete media, and filtered through a 70 μM cell strainer. Cells were pelleted by centrifugation, re-suspended in media containing 10 ng/mL M-CSF (Peprotech) and plated on 3 x 10 cm untreated petri dishes per mouse in 10 mL media and cultured for 7 days without replenishing or changing media to derive BMDMs.

To quantify macrophage-mediated ADCP, tumor cells were harvested, labeled with carboxyfluorescein succinimidyl ester (CFSE), washed with serum free IMDM + GlutaMAX, and plated at a density of 100,000 cells/well in 25 µL in a 96-well ultra low attachment round bottom plate (Costar, Cat. 7007) on ice. Tumor cells were opsonized by addition of 25 µL of various antitumor antibodies, CD47 blocking reagents, and/or controls for 30 min on ice. Macrophages were harvested by enzymatic dissociation and cell scraping, pelleted, washed in serum free IMDM, and added to opsonized tumor cells at a density of 50,000 cells/well in 50 µL media for a final assay volume of 100 µL and an effector to tumor cell ratio of 1:2. ADCP was measured after incubation for 2 hr at 37 °C with the following test groups: MØ + cancer cells alone, MØ + cancer cells opsonized with TCRm or control antibody alone (10 µg/mL mAb final), MØ + cancer cells opsonized with CV1 alone (100 nM final), and MØ + cancer cells opsonized with the combination (10 µg/mL mAb + 100 nM CV1). Cells were then pelleted and washed with autoMACS running buffer (Miltenyi), and stained with a 1:100 dilution of anti-mouse F4/80-APC (Biolegend) for mouse BMDMs or a 1:100 dilution of anti-human CD206–Alexa647 (Biolegend) for human MDMØ in autoMACS buffer for 1 hr at 4 °C. Cells were pelleted, washed, and re-suspended in a 1:10000 dilution of DAPI and analyzed by FACS using the CytoFLEX equipped with a high throughput sampler. Phagocytosis was quantified gating based on SSC-A and FSC-A, singlets, live/dead (DAPI negative/low), and phagocytosis quantified as the percentage of F4/80-APC or CD206-Alexa647 positive macrophages that are also CFSE positive.

Flow Cytometry

For cell surface staining, cells were blocked using FcR blocking reagent (Miltenyi 130-059-901) at the manufactures recommended dilution for 15 minutes on ice, then

incubated with appropriate fluorophore -conjugated mAbs for 30 min on ice and washed twice before resuspension in a viability dye (either DAPI or propidium iodide at 1 μg/mL). Antibodies used include anti-HLA-A2 clone BB7.2-APC (ebioscience 17-9876-42), BB7.2-FITC (MBL K0186-4). Pr20 or its human IgG1 isotype control (Eureka Therapeutics ET901) was conjugated to APC using the lightning-link kit (Innova Bioscience 705-0010) and staining was performed at 3 μg/mL, which was determined to be a saturating concentration. Flow cytometry data were collected on a LSRfortessa (Beckton Dickinson) or an Accuri C6 (Beckton Dickinson) and analyzed with FlowJo V10 software.

CAR T Cell Transduction

Healthy donor PBMC were isolated through ficoll density centrifugation. Quantities described as follows were scaled up when more cells were required. $5x10^6$ PBMC were washed and resuspended in 2 mL of RPMI media with 10% FBS. 125uL of anti-CD3/CD28 Dynabeads (Invitrogen) were washed once before resuspension 125 uL and added to the PBMCs. Recombinant human IL-2 was added to a concentration of 100 IU/mL. 6-well non-tissue culture treated plates were coated with RetroNectin (Clontech) by diluting Retronectin to 20 ug/mL with PBS and coating plates with 2 mL of diluted Retronectin for 1 hours at 37° C. Retronectin was removed and the plate was blocked with 2% BSA in PBS for 30 mins at room temp. Plates were washed once with PBS before transduction. Transduction was performed 48 hours after CD3/CD28 Dynabead activation. 2 mL of activated T cells at $0.5x10^6$ cells/mL was added to each well of RetroNectin-coated plate. 100 uL of concentrated lentivirus was added per well (MOI 5). Spinoculation was performed at 2000xg for 1 hr at 30° C. Cells were then rested at 37° C overnight. 2 mL of fresh media was then added with 100 IU/mL IL-2. Two days later, virus and Dynabeads were removed from cells by pipetting to

disaggregate beads from cells and using a magnet to remove the beads. Cells were then assayed for transduction efficiency using ALY/HLA-A2 tetramer staining and used for experiments.

T Cell Activation and Cytotoxicity Assays

Jurkat T cells transduced with Pr20-CAR or incubated with Pr20-BiTE, were labeled with CFSE and incubated overnight at the indicated E:T ratios with the indicated target cell lines. Flow cytometry was used to gate for CD3+ T cells (Clone OKT3 eBioscinece11-0037-41) and median fluorescence intensity (MFI) for the early activation marker CD69-APC (eBioscience 17-0691-80) was quantified. For primary healthy donor T cell assays, after successful Pr20-CAR transductions, Pr20-CAR T cells or mock-transduced were incubated with CFSE-labeled AML14 cells at an E:T of 3:1. AML14 cells were labled with CFSE by washing cells twice with PBS, incubating them with 100 nM CFSE for 10 minutes, then quenching the reaction with complete media and washing with media 3 times. 16 hours later, flow cytometry for CFSE+ AML14 cells was used to determine depletion of AML14 cells. For Pr20-BiTE experiments, Healthy donor PBMCs and AML14-GFP target cells were co-cultured in the presence of 0.01 ug/mL Pr20-BiTE or control BiTE for 16 hours at an E:T of 30:1. Flow cytometry was used to determine proportion of GFP+ AML14 cells to measure depletion.

Statistical Analysis

Due to sample size and anticipated non-linearity of the time effect, we analyzed the data as area under the curve (AUC) for leukemic burden per mouse. Tumor burden expressed as AUCs were compared between groups using the Kruskal-Wallis test. When the Kruskal-Wallis test indicated significant differences among the groups

($p<0.05$), subsequent pairwise comparison were conducted. Survival studies were done using bilateral hind leg paralysis as surrogate for death or using predetermined morbidity characteristics. Overall survival was estimated by the Kaplan-Meier approach and compared among groups using the log-rank test. ns is defined as $p > 0.05$. * is defined as $p< 0.05$. ** is defined as $p<0.01$. *** is defined as $p < 0.001$. All statistical tests were conducted using a permutation test procedure.43 Statistical testing were performed using R 3.3.1 (R Core Team, Vienna Austria),

Trials of Pr20M with CV1 in Mice

Mouse research was conducted under protocols approved by the MSK institutional animal care and use committee. Therapeutic trials were conducted in human xenograft models in 6-week-old male non-obese/diabetic severe combined immunodeficient (NOD/SCID) with IL2γ receptor negative (NSG) mice from Jackson laboratory. Mice were engrafted via tail vein injection with 3 million BV173 and AML14 cells transduced with the firefly luciferase gene. Disseminated engraftment of leukemia was confirmed via bioluminescent imaging (BLI) in all mice before beginning treatment. Mice were randomly assorted into the following five treatment groups with equal mean BLI flux (photons/second): 1) control without treatment, 2) TCRm antibody alone, 3) CV1 alone, 4) CV1 and an afucosylated isotype control antibody, and 5) CV1 and TCRm antibody. TCRm antibodies were administered retro-orbitally biweekly at doses of 50 μg. For combination therapy studies CV1 was administered daily via intraperitoneal injection at doses of 100 μg. Leukemic burden was assessed by bioluminescence imaging, recorded as flux of protons per second and repeatedly measured at days 6, 13, 20, and 27, post engraftment. Mice were treated twice a week beginning on day 6 through 27 for a total of six doses of TCRm and/or 21 daily doses of CV1. Additional mouse or human PBMC's were not administered.

RESULTS

Pr20M can mediate ADCP and combination of Pr20M with CD47/SIRPα axis blockade leads to superior therapy against leukemia models *in vivo*

Although therapeutic activity was observed in Pr20M mono-therapy *in vivo*, tumor growth was only reduced and animals all ultimately progressed with disease. NSG mice are deficient in T, B and NK cells, and have poorly functional macrophages[103]. However, we hypothesize that NSG macrophages are a major immune effector population that could mediate ADCP in our models. In addition, cancer cells often upregulate CD47, the 'do not eat me' signal that interacts with SIRPα on macrophages. This functionally inhibits macrophages phagocytosis of tumor cells and is believed to be a resistance mechanism developed by cancers to evade immune elimination. We hypothesized that the addition of CV1, a high-affinity soluble SIRPα-variant[125] could block CD47 and enhance Pr20M-mediated ADCP. To evaluate whether Pr20M could mediate ADCP, we incubated human monocyte-derived macrophages and NSG splenic macrophages with CFSE-labeled AML14 cells *in vitro*. Using flow cytometry, we determined proportion of CFSE+ macrophages indicating phagocytosis. We evaluated the ability of CV1 to enhance Pr20M-dependent macrophage phagocytosis of leukemia cells *in vitro* in AML14 and BV173 cells – both of which express PRAME, HLA-A2, and CD47. The HLA-A2-negative cell line HL60 was used as a negative control. Blockade of leukemia cell CD47 with CV1 alone did not promote macrophage phagocytosis of AML14, BV173 or HL60 (Fig. 2.1A). Pr20M alone did not promote ADCP of HL60 or BV173, but significantly increased phagocytosis of AML14 (Fig. 2.1A). The combination of TCRm mAb and CV1 significantly increased macrophage phagocytosis of AML14 and BV173, but not

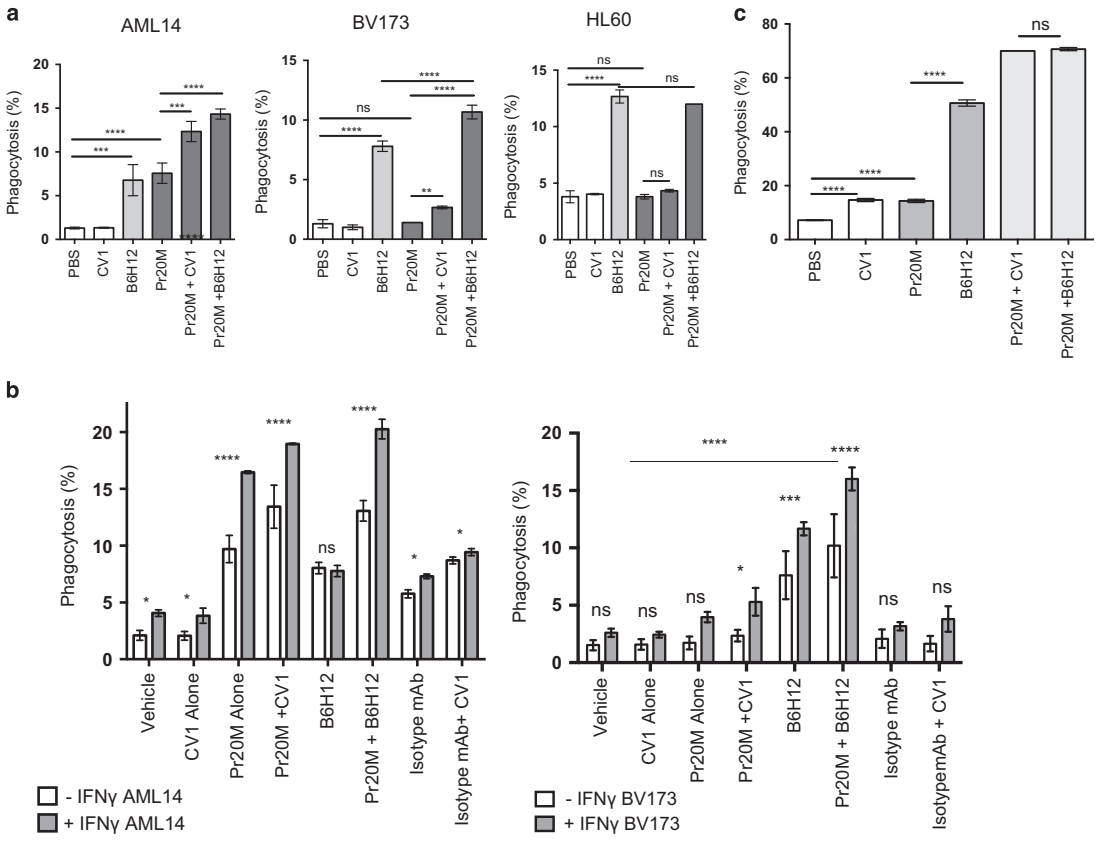

Figure 2.1. CD47 blockade using CV1 enhances Pr20M-mediated ADCP of leukemia cells *in vitro*.

(a) Human macrophage phagocytosis of AML14, BV173, and HL60 treated with various combinations of TCRm and CV1 quantified by flow cytometry. Experiments were completed in duplicate with various human donors. (b) Left panel: AML14 cells were pretreated with 100 ng/µl of IFNγ for 72 h. Isolated human macrophages were incubated with pretreated AML14 cells in the presence of (1) PBS, (2) CV1 alone, (3) Pr20M alone, (4) combination therapy with Pr20M and CV1, (5) positive control B6H12 (previously described), (6) B6H12 with Pr20M (7) irrelevant control mAb and (8) irrelevant control mAb with CV1. All groups showed an increase in ADCP with IFNγ pretreatment. Increase was most significant in Pr20M alone, combination therapy, and B6H12 with Pr20M. Right panel: BV173 cell line was pretreated with 100 ng/µl of IFNγ for 72 hours. Isolated Human macrophages were incubated with pretreated BV173 cell line as above. All groups show an increase in ADCP with IFNγ pretreatment. Increase is significant in combination therapy, positive control, and positive control with Pr20. (c) NSG-derived mouse macrophage ADCP of CSFE labeled AML14 cells quantified by flow cytometry. These experiments were performed in duplicate with consistent results.

the control HL60, indicating the effect was TCRm antigen-specific. As expected, the positive control anti-CD47 blocking IgG1 antibody, B6H12, induced a significant increase in ADCP of all three leukemia cell lines, and potentiated TCRm-mediated phagocytosis of AML14 and BV173. ADCP with NSG mouse macrophages showed improved phagocytosis with CV1 alone and significantly increased phagocytosis with CV1 and TCRm Pr20M in combination (Fig. 2.1C). Collectively, these results indicate that CD47 blockade is effective at improving ADCP *in vitro* of antibodies that target ultra-low density tumor antigens, such as TCRm mAbs. IFNγ is a potent immunocytokine with pleiotropic effects, including induction of MHC class I and II expression and increased antigen processing and presentation[151]. Anti-CD47 mAb therapy triggers a phagocyte type I and II interferon (IFN) response in the tumor microenvironment that presumably increases tumor cell surface peptide-MHC (pMHC) density[88]. As the epitope target of TCRm mAbs is presented by pMHC, we hypothesized that promoting IFNγ signaling may boost TCRm mAb effector functions by increasing target antigen density on the tumor cell surface. IFNγ treatment of AML14 increased HLA-I expression, resulting in increased binding of Pr20M (Fig. 2.2). IFNγ significantly increased expression of TCRm mAb epitopes of interest and increased macrophage-mediated ADCP of both AML14 and BV173 *in vitro* (Fig. 2.1B). CV1 treatment alone did not increase HLA-I expression on either cell line. We next asked if combination CV1 and Pr20M therapy would improve potency *in vivo*. Although Pr20M mAb or CV1 monotherapy significantly reduced leukemia burden in the AML14 model (Fig. 2.3A), combination therapy had an markedly increased effect compared to either agent alone, with a 3 log reduction in leukemia burden relative to control untreated mice, a 10-fold reduction relative to the single agent groups (Fig. 2.3A), and significantly improved survival for the combination therapy (Fig. 2.3B). After therapy was stopped on the final day of bioluminescent imaging, leukemia

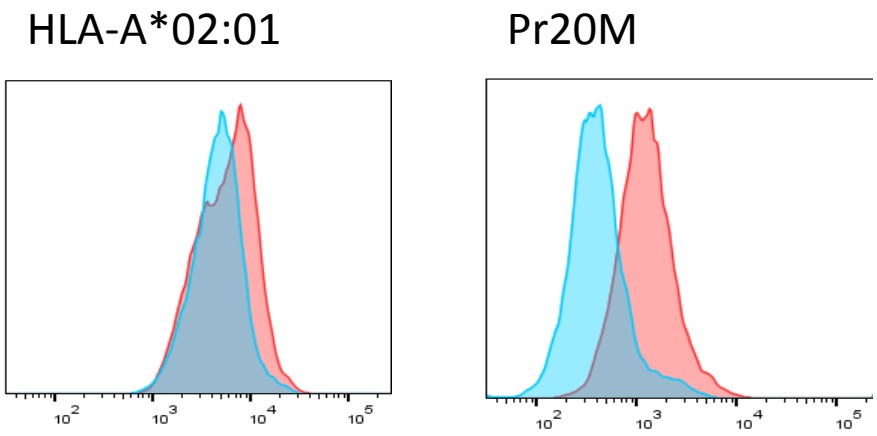

Figure 2.2. Effects of IFNγ on PRAME antigen expression.
A) AML14 cell line was pretreated with 100 ng/mL IFNγ for 72 hours. Treated (red) displayed a doubling of HLA expression compared to untreated controls (blue). B) Treated (red) showed a 10-fold increase in Pr20 binding compared to untreated controls (blue).

relapsed not at the initial sites (bone marrow and spleen), but in lymphomatous nodules. Our data demonstrate that combination therapy of CD47 blockade with a TCRm can lead to dramatic therapeutic efficacy despite an extremely low mAb epitope density.

Pr20-BiTE and Pr20-CAR Formats Potently Direct Tumor Lysis However Also Lead to Off-target Activities

To determine whether the BiTE or CAR formats could be used to enhance therapeutic potential of Pr20, we tested these constructs in an *in vitro* depletion assay. Pr20-CAR was successful transduced into primary T cells using lentiviral infection leading to approximately 70% transduction efficiency overall with successful transduction in both the CD4 and CD8 T cell compartments as measured by ALY/HLA-A2 tetramer analysis. (Fig. 2.4). The transduction efficiency is comparable to the CARs used in

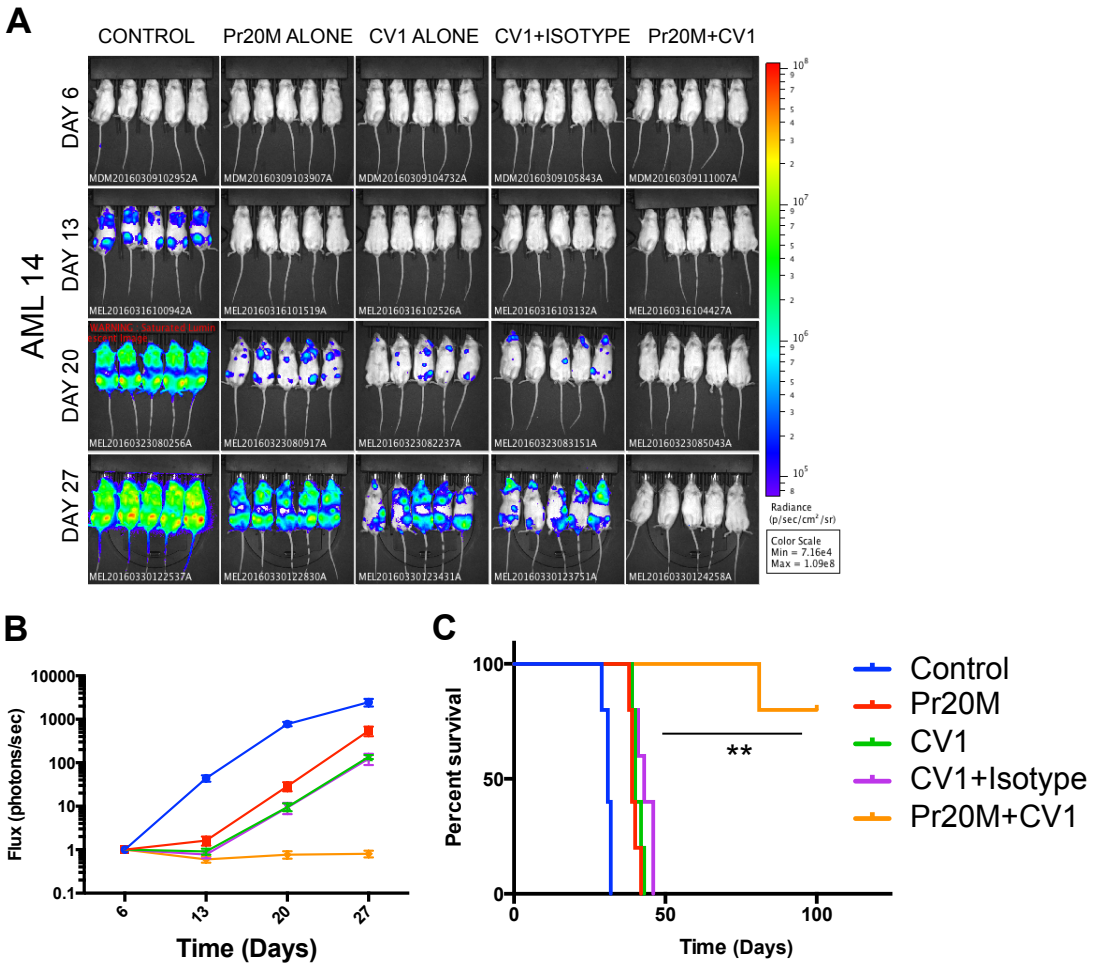

Figure 2.3. Combination Therapy with CV1 and Pr20 leads to leukemia suppression and prolonged survival in AML14 cell line *in vivo*.

(A) NSG Mice were engrafted via tail vein injection with $3x10^6$ cells/mouse of AML14 transfected with Luciferase gene. Mice were imaged via BLI on day 6. Mice were randomized to have equal group mean engraftment. Treatment started on day 6. Pr20M was administered retro-orbitally biweekly at 50ug. CV1 was administered intraperitoneally daily at 100ug. Mice were imaged once a week for 3 weeks. B) Graph showing normalized mean flux in photons/second of mice at days 6, 13, and 20, and 27. C) Kaplan Meir Survival curve showing survival data. Control and Single treated groups had 100% death within 50 days. Experiment was truncated at 100 days at which time 4 of 5 mice were alive. $P<0.0001$. D) At 67 days, 1 mouse in combination group had lymphomatous growth requiring sacrifice. The 4 remaining animals had lower tumor burden via BLI than on day of engraftment.

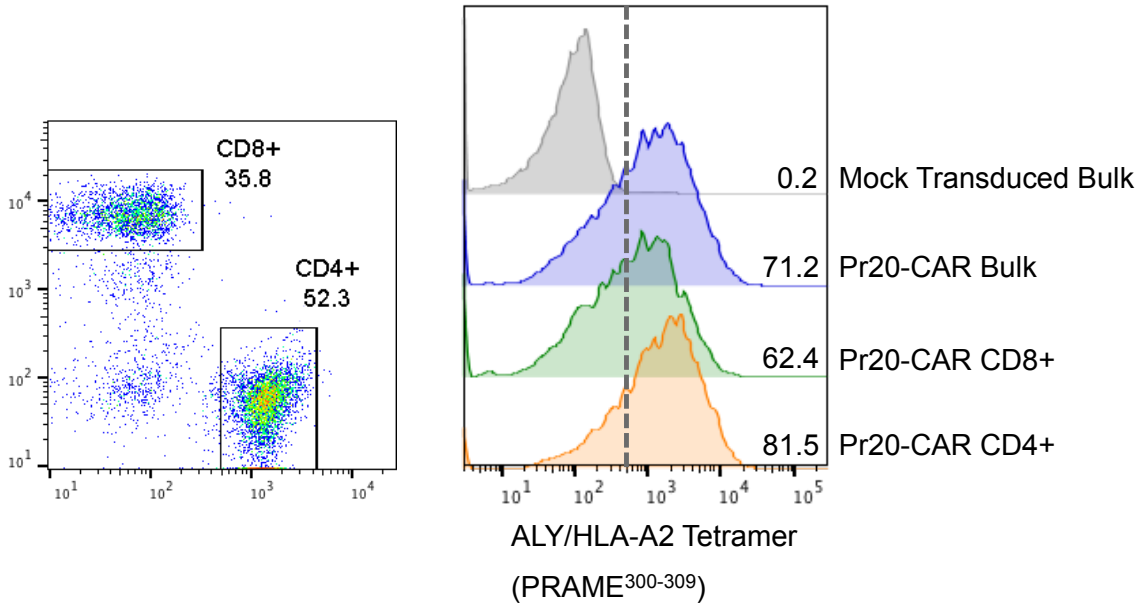

Figure 2.4. Pr20-CAR can be transduced into primary human healthy-donor T cells with high efficiency.

Healthy-donor primary T cells were activated using anti-CD3/CD28 beads and recombinant human IL-2. Lentiviral particles were transduced into T cells and 24 hours later CAR transduction was assessed by ALY/HLA-A2 tetramer analysis using flow cytometry. Total bulk cells, CD8+ T cells, and CD4+ T cells were analyzed for ALY/HLA-A2 tetramer positive cells.

clinical practice and reactivity to the ALY/HLA-A2 tetramer demonstrates that the CAR protein is appropriately expressed, a potential issue when engineering scFv onto transmembrane scaffolds. Both Pr20-BiTE and Pr20-CAR mediated lysis against approximately 90% of PRAME+/HLA-A2+ AML14 cells *in vitro* within 16-18 hours demonstrating superb potency of the constructs (Fig. 2.5). We next evaluated whether potency of Pr20-BiTE or Pr20-CAR would lead to off-target toxicities. Using a panel of cell lines, Jurkat T cells were co-cultured with tumor cell lines in the presence of Pr20-BiTE or a Control-BiTE. Using the early activation marker CD69, we observed that Pr20-BiTE mediated CD69 activation of Jurkat T cells when co-cultured with the

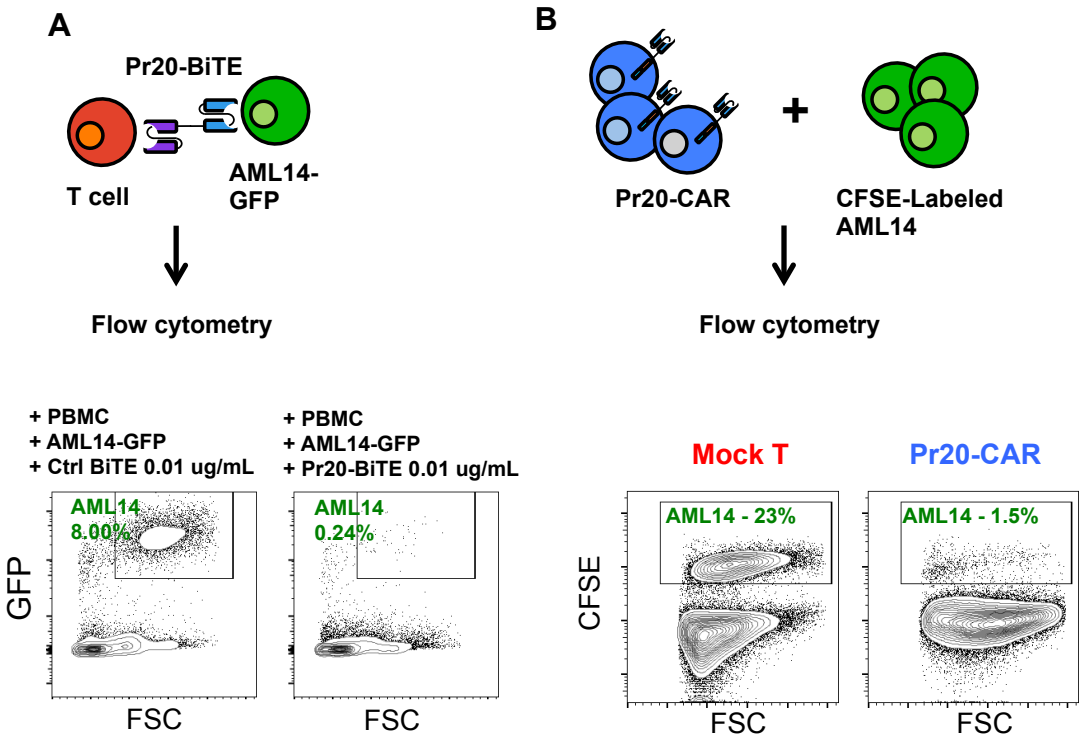

Figure 2.5. Pr20-BiTE and Pr20-CAR mediate cytotoxicity against a PRAME+/HLA-A2+ AML *in vitro.*

(A) Healthy donor PBMCs and AML14-GFP target cells were co-cultured in the presence of 0.01 ug/mL Pr20-BiTE or control BiTE for 16 hours at an E:T of 30:1. Flow cytometry was used to determine proportion of GFP+ AML14 cells to measure depletion. (B) Healthy donor T cells were transduced with Pr20-CAR and incubated with CFSE-labeled AML14 cells at an E:T of 3:1. 16 hours later, flow cytometry for CFSE+ AML14 cells was used to determine depletion.

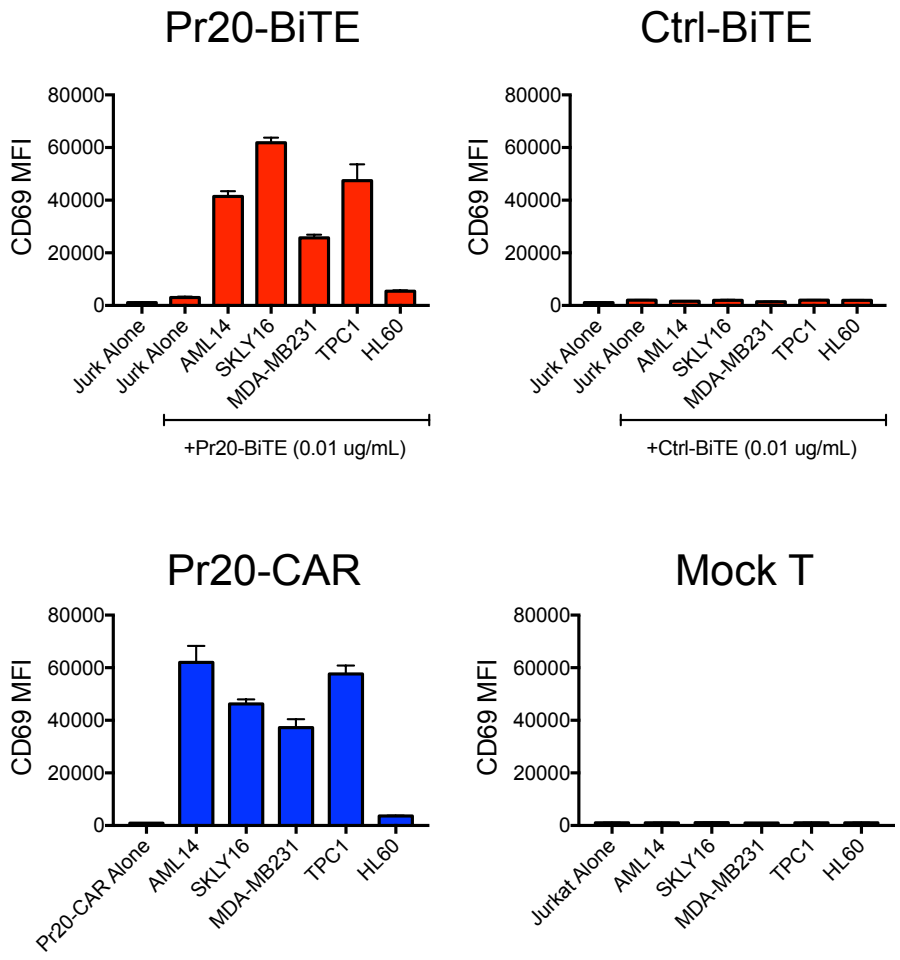

AML14	(PRAME+ / HLA-A2+)
SKLY16	(PRAME- / HLA-A2+)
MDA-MB231	(PRAME- / HLA-A2+)
TPC1	(PRAME- / HLA-A2+)
HL60	(PRAME+ / HLA-A2-)

Figure 2.6. Pr20-BiTE and Pr20-CAR activate T cells in co-cultures with PRAME+/HLA-A2+ cancer cells, but induce non-specific activation.

Jurkat effector T cells were labeled with CFSE before cells were co-cultured with indicated cell lines overnight at an E:T of 2:1 in the presence or absence of 0.01 ug/mL Pr20-BiTE or a control-BiTE. For Pr20-CAR experiments, Pr20-CAR was transduced into Jurkat T cells and >98% ALY/HLA-A2 tetramer+ purity was determined before assays. Pr20-CAT Jurkat cells or mock-transduced Jurkat cells (Mock T) were co-cultured with indicated target cells overnight. Flow cytometry using an anti-CD69 antibody was used to measure early T cell activation on the jurkat cells for both Pr20-BiTE and Pr20-CAR experiments and MFI is graphed.

PRAME+ / HLA-A2+ positive control AML14 (Fig. 2.6). However, we also observed substantial CD69 activation after co-culture with several PRAME-negative / HLA-A2+ cell lines such as SKLY16, MDA-MB231, and TPC1. We detected minimal CD69 activation after co-culture with the PRAME+/HLA-A2-negative leukemia HL60, suggesting off-target activation was dependent on HLA-A2 expression. We performed similar experiments for the Pr20-CAR construct co-culturing tumor cells with Pr20-CAR transduced Jurkat T cells or mock transduced Jurkats. Similar to the Pr20-BiTE data, although Pr20-CAR Jurkats demonstrated CD69 activation against PRAME+/HLA-A2+ AML14, they also activated against PRAME-negative / HLA-A2+ cell lines demonstrating off-target activation (Fig. 2.6). To determine whether the Pr20-BiTE off-target activation was intrinsic to cancer cell lines, we performed Pr20-BiTE culture experiments with healthy donor PBMC. When HLA-A2+ PBMC was cultured for 16 hours with Pr20-BiTE, we observed no depletion in T or B cell lineages. However, we observed significant depletion of the CD14+ monocyte population (Fig. 2.7 Left Panels). No substantial depletion of T cell, B cell, or monocyte populations was detected in a HLA-A2-Neg healthy PBMC control (Fig. 2.7 Right Panels) again suggesting off-target cytotoxicity was dependent on HLA-A2 expression. This observation was unexpected because Pr20 did not demonstrate substantial binding in flow cytometry assays to CD14+ populations in HLA-A2+ healthy donor whole blood (Fig 1.3E). Together, our data suggests engineering TCRm scFv into extremely potent biologic agents such as BiTEs and CARs should be approached with caution due to the possibilities of cross-reactive peptide epitopes or low-affinity interactions with HLA-A2; both of which can potentially lead to off-target toxicities.

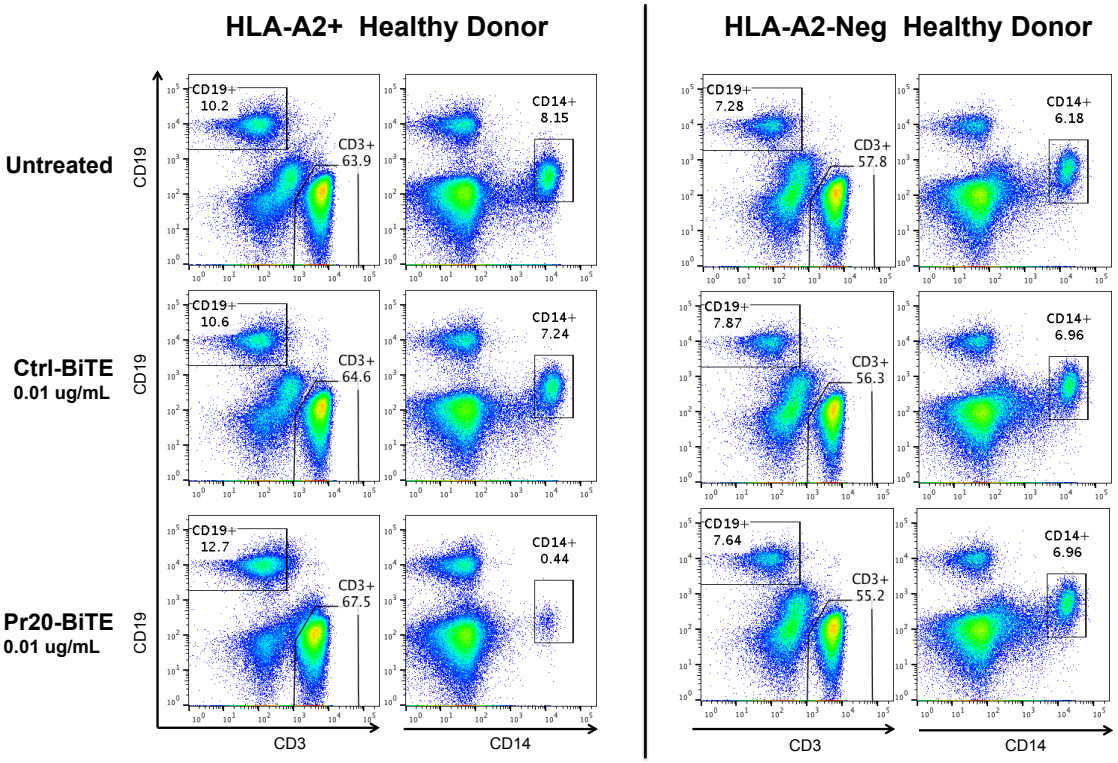

Figure 2.7. Pr20-BiTE mediates depletion of healthy donor PBMC monocyte population.
Healthy donor PBMC were isolated and cultured for 16 hours with either untreated, in the presence of 0.01 ug/mL of control-BiTE (ET901 see materials and methods), or Pr20-BiTE. Flow cytometry was used to determine T cell (CD3+), B cell (CD19+), and monocyte (CD14+) populations to assay for depletion. HLA-A2+ CD14+ depletion data is representative of three independent experiments with n=3 healthy donors. The experiment with HLA-A2-Negative healthy donor was performed once.

DISCUSSION

The dramatic therapeutic effect when combining Pr20M and CV1 *in vivo* was an exciting observation. Several factors may explain the potent therapy. First, the *in vivo* microenvironment may positively alter macrophage effector function. Second, neutrophils express both SIRPα and Fc receptors and have been implicated in responses to anti-CD47 antibody treatment. Blocking SIRPα signaling may alter neutrophil transmigration, trafficking and therapeutic activity[127]. Third, the leukemias

we evaluated preferentially engrafted in organs with high intrinsic numbers of phagocytic cells. Fourth, cross-species differences in Fc receptor biology, as well as alternative xenogeneic ligand-receptor interactions between human tumor cells and mouse immune effectors may alter antibody and immune cell function[152]. NSG mice are B cell-, T cell-, and NK cell-deficient, and although they have intact IFNγ-dependent signaling, they have defective innate immunity and cytokine signaling pathways[153]. While it is difficult to draw parallels between human and mouse systems, in the human, a greater variety of more potent effectors and an immunocompetent host that responds to pro-inflammatory signaling could allow even greater efficacy of this drug combination in the human patient. In addition, NSG mice have low circulating IgG levels that could compete with TCRm for Fc receptor interactions[153]. Not surprisingly, we found that IFNγ-dependent signaling enhanced TCRm mAb-dependent, macrophage-mediated phagocytosis *in vitro*. This enhancement of phagocytosis was likely mediated through multiple mechanisms including direct IFNγ-dependent macrophage activation, as well as indirectly via TCRm-specific mechanisms involving increases in tumor cell in HLA expression and antigen presentation. Thus, strategies that promote an IFNγ response, could uniquely potentiate the activity of TCRm. Therefore, the combination of CV1 and TCRm in this specific milieu leads to remarkable tumor kill. It will be important to determine if this effect is specific to leukemia, or also other cancers. In conclusion, the greater than additive effect of these agents together *in vivo* is particularly unexpected given the extremely low epitope density of the PRAME-derived peptide epitopes. The synergy between CV1 and antitumor antibodies may be especially pronounced with TCRm compared to traditional mAbs since the targets of TCRm mAbs are presented by HLA and are thus regulated by cytokine signaling. Although we demonstrated the unusual therapeutic utility of antagonizing CD47 to potentiate the antitumor activity of TCRm,

we anticipate this approach may be applicable to other mAbs that target a low cell surface density tumor antigen. This strategy could turn poorly efficacious antibodies into powerful antitumor therapeutics and significantly expand the possible cancer antigen targets of monoclonal antibodies.

In addition, it is important to highlight that several studies have demonstrated that effective CD47 blockade therapy in syngeneic mouse models requires stimulation of the adaptive immune system, for example through cytosolic DNA sensing via the STING pathway in dendritic cells[88] and subsequence cross-priming of tumor antigens or through immune checkpoint blockade of PD-L1[154]. Though the biochemical and cellular mechanisms of CD47 blockade may be different in syngeneic models and xenografts, it is reasonable to hypothesize that in an immunocompetent model, a TCRm and CD47 blockade may also synergize to augment cross-presentation engage the adaptive immunity for multi-modal immune attack.

The off-target cytotoxicity and T cell activation of the Pr20-BiTE and CAR constructs were initially surprising given that using the same panel of PRAME-negative cell lines and healthy PBMC populations, our flow cytometry data demonstrated that Pr20 did not bind to detectable levels. We hypothesize either that there are cross-reactive targets below the limit of detect using flow cytometry-based assays or that the antibody 'footprint' and contact with the HLA-A2 protein provided enough interaction to trigger a T cell response. Recent data has proven that T cell activation can occur with as few as 3-10 ligands[155,156] and therefore it is reasonable to hypothesize that low-affinity interactions that were not detected by flow cytometry could be enough to mediate T cell activation and cytotoxicity. In addition, Pr20 was designed to have an

epitope footprint over the composite structure of ALY and HLA-A2, however, it is unknown where and to what extent Pr20 contacts HLA-A2. This is difficult to discern without data from a crystal structure. Therefore, it is reasonable to hypothesize that enough contact and affinity to HLA-A2 can mediate activation of a potent BiTE or CAR T cell. Indeed, upon review of the literature, The Sadelain group at Memorial Sloan Kettering recently reported another TCRm CAR targeting a NY-ESO1 tumor antigen peptide/HLA-A2 demonstrated reactivity and cytotoxicity against HLA-A2+ cells tested irrespective of NY-ESO1 expression[148]. However, rational mutagenesis to minimize contact with HLA-A2 was successful in fine-tuning the NY-ESO1 peptide/HLA-A2 CAR for specificity to NY-ESO1, and therefore it is reasonable to believe that a similar strategy can be applied to Pr20-CAR. Together, our data suggests that the engineered Pr20-BiTE and Pr20-CAR constructs have off-target activities against peptide/HLA-A2 and are not PRAME-antigen-specific. Our data also suggests that caution must be taken when engineering high-affinity scFv fragments against peptide/HLA-I into highly potent therapeutic formats such as BiTEs and CARs and each construct must be evaluated empirically.

AKNOWLEDGEMENTS

We thank Dr. Jonathan Sockolosky and Dr. K. Christopher Garcia at Stanford University for performing *in vitro* ADCP assays and providing CV1. *In vivo* experiments were performed in collaboration with Dr. Melissa Mathias.

CHAPTER III: IDENTIFICATION OF STRATEGIES AND SMALL MOLECULES THAT REGULATE HLA-I†

INTRODUCTION

Checkpoint Blockade Immunotherapy Through CTLA4 and PD-1/PD-L1

Immune checkpoint blockade therapy has recently become a powerful tool to treat specific solid tumors and has demonstrated astounding clinical results. Checkpoint blockade therapy relies on the concept that anti-tumor T cells are dysfunctional, but can be re-activated through blockade of inhibitory signals – 'releasing the brakes' from the immune system[157]. It is now well established that cancer patients can develop an immune response against their tumor but the tumor-specific T cells are either not well-activated or the tumor infiltrating lymphocytes are challenged with a hostile tumor microenvironment that suppresses their function. CTLA4 is an inhibitory receptor protein found on T cells that competes with the co-stimulatory receptor protein CD28 (also found on T cells) for binding to their shared ligand CD80/86 on antigen presenting cells[157,158]. Whereas the interaction of CD28 with CD80/86 is necessary for appropriate co-stimulation and T cell priming against an antigen, the interaction of CTLA4 with CD80/86 leads to T cell functional inhibition[157,158]. Therefore, checkpoint blockade with mAbs against CTLA4 such as Ipilimumab (Bristol-Myers Squibb) can help to prime and activate anti-tumor T cells[159]. Approved by the FDA in 2011 for metastatic melanoma, Ipilimumab demonstrated that immune

† Some experiments were designed and conducted by or in collaboration with Myles Fennell from the MSK Gene Editing and Screening Core facility (Fig. 3.1, 3.2, and Table 3.1), Christina Bebernitz and Mitchell Wang (Fig. 3.3, 3.4, 3.7), and Lauren Dong (Fig. 3.8 and 3.9)

checkpoint blockade was indeed a powerful strategy against cancer and a subset of patients see long-term durable responses[160]. Tumors also often upregulate expression of another immune checkpoint protein celled PD-L1. PD-L1 binds to PD-1 on T cells to inhibit T cell function and can even promote T cell apoptosis[161]. Therefore, it is commonly believed that tumors increase expression of PD-L1 as a mechanism of immune evasion. On the basis of this biology, several mAbs against both PD-I and PD-L1 were developed. Gratifyingly, several of these mAbs demonstrated superb efficacy and gained FDA approval for several solid tumor indications such as the anti-PD-1 Nivolumab[160] (Bristol-Myers Squibb) for metastatic melanoma, non-small cell lung cancer, and renal cell carcinoma; and Pembrolizumab[162] (Merck and Co.) for metastatic melanoma and cancers with microsatellite instability or DNA repair deficiencies. Anti-PD-L1 mAbs have also gained approval such as Atezolizumab[163] (Genentech / Roche) for urothelial carcinoma and non-small cell lung cancer; Durvalumab[164] (MedImmune / Astrazeneca) for urothelial carcinoma, and Avelumab[165] (Pfizer / Merck KGaA) for Merkel cell carcinoma and urothelial carcinoma.

Immunological Activity in Tumor Microenvironment is Important for Successful Immune Checkpoint Blockade Therapy

Although immune checkpoint blockade therapy has been clinically successful, not all patients respond and not all tumors respond. We are only beginning to understand the prognostic signs that may predict whether a particular tumor would respond to checkpoint blockade, and the mechanisms of resistance[166]. In broad terms, a solid tumor can be immunologically ‘hot’ or ‘cold’. Immunologically ‘hot’ tumors are inflamed and heavily infiltrated with lymphocytes while immunologically ‘cold’ tumors are non-inflamed and exclude T cells. It is now recognized that ‘hot’ tumors

respond better to checkpoint blockade therapy[167]. What makes a tumor microenvironment 'hot' is less clear. It is commonly accepted that higher tumor mutational burden correlates with increased T cell infiltrates and with higher rate of response to anti-PD-1 at least in melanoma.[168] However, mutational burden is not the only prognostic factors, because some tumor types such as clear cell renal cell carcinoma do not necessarily have high mutational burden yet are 'hot', have a high amount of T cell infiltrates, and respond to checkpoint blockade[169]. It is becoming increasingly clear that a major factor that generates a 'hot' tumor is appropriate MHC antigen presentation machinery expression and an interferon gene signature in the tumor[168,169]. A major focus now in immuno-oncology is developing combinatorial strategies to convert a 'cold' tumor into a 'hot' tumor thereby augmenting endogenous anti-tumor T cell responses as well as providing a pool of anti-tumor T cells for additional checkpoint blockade to bolster. It is increasingly clear that the innate immune system plays a pivotal role in initiating an anti-tumor response. Antigen presenting cells such as dendritic cells must sense pathogen associated molecular patterns through TLRs[170] or damage associated molecular patterns on tumor cells in order to prime an effective T cell response[171]. Several exciting studies demonstrate promising strategies to augment innate sensing of tumors through STING agonists[171–173] and enhanced antigen-presenting cell priming of T cells through combination of TLR9 agonists and OX40 agonists[174].

HLA-I Expression is Essential for a Broad Range of Immunotherapies, Down-regulation is a Mechanism of Checkpoint Blockade Resistance, and HLA-I can be Modulated Pharmacologically

HLA-I is a central immune recognition molecule that is essential for activity of immune checkpoint blockade, TCRm or any TCR-based agent, and cancer vaccines.

Immune checkpoint blockade still ultimately relies on recognition of tumor cells through peptide/HLA-I and TCR interactions. In fact, a major mechanism of resistance to anti-CTLA4, anti-PD1, and anti-PD-L1 checkpoint blockade is down-regulation or loss of cell-surface HLA-I expression[175–178] demonstrating the importance of HLA-I expression for success of drug class. Therefore, strategies to increase tumor-cell surface HLA-I would be applicable to augment a broad range of immunotherapies including TCRm, TCR-transgenic T cells, cancer vaccines, and check point inhibitors. Pro-inflammatory cytokines such as IFNγ can increase HLA-I expression and antigen presentation dramatically, but are difficult to use as drugs due to major toxic side effects[179]. Our lab has previously reported a shRNA kinome screen in which we determined that MAPK activation decreased HLA-I and pharmacological inhibition of the MAPK pathway with the MEK inhibitor Trametinib could increase HLA-I[110] . It would be useful to understand what pharmacological inhibitors could be used in combination with immunotherapy to boost HLA-I expression and tumor-antigen presentation. Conversely it is important to know what pharmacological inhibitors would decrease HLA-I to determine combinations to avoid.

Cellular Engineering Approaches Risk Introduction of Immunogenic Foreign Genes

Although for cancer immunotherapy it may be most logical to identify strategies to increase MHC-I and HLA-I expression, there are also several scenarios where the ability to decrease MHC-I expression may be beneficial. For example, modern lentiviral and CRISPR/Cas9 technology has allowed genetic engineering of cells *ex vivo* and introduction of functional foreign genes before reinfusion. Indeed, the possibilities to introduce bacterial enzymes or synthetic proteins into cells for novel functionalities are tantalizing. For example, the herpes simplex virus thymidine kinase

gene (HSV-TK) is being explored as a suicide gene in induced neural stem cells. These engineered cells can home into a glioblastoma to deliver a localized pro-drug activating enzyme system[180]. Upon systemic administration of the pro-drug Ganciclovir, the engineered neural stem cells catalyze formation of a localized cytotoxic agent. In addition, CAR T cells have been engineered to express several foreign proteins such as immuno-modulating BiTE molecules and flagellin adjuvant[181], and even a custom-gated synthetic notch receptor coupled with the yeast Gal4 transcription factor[181,182]. However, a concern is that these foreign proteins can by processed and presented on MHC-I leading to an endogenous immune response that may ultimately kill the required engineered cells. One strategy to prevent host T cell responses against transgenic proteins is through ablation of β2M. Because β2M is an essential structural component of MHC-I, deletion of β2M functionally prevents cell-surface expression of all MHC-I alleles making it an attractive target for gene editing strategies such as CRISPR/Cas9[183]. This strategy is being explored to generate universal CAR T cells that circumvent the logistically challenging requirement of autologous transductions of current FDA-approved CAR T[184]. However, MHC-I also has a role as an NK cell inhibitory signal and NK cells can lyse cells lacking MHC-I[185,186]. This NK cell functionality is thought to have evolved to counter viral mechanisms to inhibit MHC-I expression[186] to evade adaptive immunity. Instead, we hypothesized that inhibition of TAP function could prevent a response against an immunogenic transgene. A fraction of MHC-I peptides are TAP-independent and therefore cell-surface MHC-I expression would be partially maintained[187]. Indeed, past studies have shown that although murine NK cells detectably lyse TAP-deficient splenocytes, they are not as prone to NK cell attack as β2M-deficient splenocytes[185].

Viral Immunoevasins have Evolved to Modulate Host Cell Antigen Presentation Machinery

Viral immunoevasins are a class of proteins that function to interfere specifically with the MHC class I pathway of antigen processing and presentation. They are well studied in human cytomegaloviruses and help the virus to minimize immune detection by human CD8+ T cells[188]. They can inhibit several key components of the antigen presentation pathway. For example, US11 and US2 induce degradation of MHC-I molecules while UL82 delays egress of MHC-I complexes from the ER to the Golgi. Multiple viral immunoevasins also target TAP to prevent efficient peptide loading onto HLA-I. For example, ICP47 prevents peptide transport through physically obstructing the peptide-binding site[189]. Meanwhile, US6 specifically inhibits TAP by inducing conformational changes resulting in abrogated ATP binding to TAP1 thereby preventing TAP-mediated peptide transport and shuttling onto MHC-I molecules[189189,190]. In fact, T-Vec (Amgen), the only FDA-approved oncolytic virus for cancer (melanoma), was engineered from HSV-1 through the removal of ICP47 to increase immunogenicity, and the addition of the GM-CSF gene, a potent immune stimulator cytokine that promoters differentiation of progenitor cells into dendritic cells[191]. Together, the goal was to make T-Vec ultimately more immunostimulatory to cytotoxic T cells. However, ICP47 has been shown to have minimal activity on murine TAP[192] and therefore cannot be tested in murine models. Fortunately, US6 inhibits murine TAP (although to a lesser degree)[193] and therefore is a prime candidate immunoevasin to study in an immunocompetent murine model. We hypothesize that overexpression of US6 could inhibit TAP to prevent an immune response against a transgene product, but still allow for sufficient cell-surface MHC-I to prevent NK cell attack.

HLA-I is a key immune receptor essential for recognition of viral or tumor-associated antigens by cytotoxic T cells. It is commonly believed and documented that cancers can down-regulate HLA-I cell-surface expression as a means of immune escape[177,194,195]. In fact, reports show that even the hypoxic tumor microenvironment can down-regulate HLA-I[196]. Appropriate expression of HLA-I is required for success of a broad range of cancer immunotherapy strategies including cancer vaccines, adoptive T cells, transgenic TCRs, checkpoint blockade therapy, and the experimental TCRm antibodies. Therefore, pharmacological strategies to increase expression of HLA-I could have strong utility in combination immunotherapy. In contrast, the ability to down-regulate HLA-I and antigen processing machinery may allow the use of immunogenic transgenes in genetically engineered cells without the concern of an endogenous CD8 T cell response.

MATERIALS AND METHODS

High Throughput Screen for Small Molecule Inhibitors that Regulate HLA-I

Several smaller commercially available compound libraries were concatenated to generate a library of approximately 6,700 unique compounds. All libraries consisted of only FDA-approved drugs or known bioactive compounds. All pipetting and aspiration was performed using robotics. JMN mesothelioma cells were plated at 500 cells per well in 50 uL in 384-well high-throughput screen grade clear-bottom plates. Cells were allowed to settle for 10 minutes at room temperature before placing plates into 37°C incubator to prevent temperature-influence on fluid dynamics of the media and uneven cell seeding. Plates were incubated overnight at 37°C. Compounds were then added from 100 uM stock wells (solubilized in 10% DMSO and 90% PBS) by adding 2.5 uL of each compound per well. This leads to a final concentration of 5 uM

and 0.5% DMSO. 2.5 uL of 10% DMSO/90% PBS or 100 ng/mL IFNγ were added to one column per plate as a negative and positive control respectively. These controls could also assist in detecting assay irregularities and trends during robotic pipetting. Cells were then incubated for 72 hours at 37°C. Cells were then fixed by adding 10 uL of 20% paraformaldehyde, along with an incubation at room temperature for 15 minutes, followed by 4 washes of 100 uL PBS per wash and aspirating down to 15 uL (minimum residual volume allowable through the robotic pipetting without aspirating cells off the plate as determined during optimization experiments). Cells were next blocked with 15 uL of 6% BSA leading to a final in-well concentration of 3% BSA for 20 minutes before 3 more washes. 15 uL of primary anti-HLA-A2 antibody (clone BB7.2) was then added to each well at a dilution of 2.5 ug/mL in 1% BSA in PBS and incubated for 1 hr at room temp. Cells were washed 3 times with PBS before secondary antibody: anti-mouse A488 (A-11001 Thermo Fisher Scientific) was added at 1:500 in 6% BSA (leading to a final in-well concentration of 3% BSA) and 2.5 ug/mL of Hoechst dye for nucleus staining. Secondary antibody was incubated at room temperature for 1 hr and washed 3 times before high-throughput imagining. After acquisition, images were analyzed using high-throughput image analysis software to determine average cell florescence intensity (I) and area (A). By multiplying (I)x(A) = average signal per cell, we quantified signal per well versus DMSO control as a 'percent of control' (POC). We also used a reverse 'normalized percent inhibition' analysis where DMSO controls were set at 0% and IFNγ positive controls were set at 100%, and each well was given a NPI quantification along that scale. Both POC and NPI analyses were normalized per plate to reduce plate-to-plate effects and variation of staining and assay artifacts introduced by plate changes and robotics.

Flow Cytometry

For cell surface staining, cells were washed once before being trypsinized from the plates using Trypsin-EDTA (0.25%) (Thermo Fischer Scientific 25200056), then incubated with appropriate fluorophore-conjugated mAbs for 30 min on ice and washed twice before resuspension in a viability dye (either DAPI or propidium iodide at 1 μg/mL). Antibodies used include anti-HLA-A2 clone BB7.2-APC (ebioscience 17-9876-42), BB7.2-FITC (MBL K0186-4), and anti-HLA-A,B,C clone W6/32-APC (biolegend 311409). Flow cytometry data were collected on a LSRfortessa (Beckton Dickinson) or an Accuri C6 (Beckton Dickinson) and analyzed with FlowJo V10 software.

Western Blot and qPCR Analysis

Total cell lysate was extracted using RIPA buffer and quantified using the DC protein assay (Biorad). 15-30 μg of protein was loaded and run on 4-12% SDS PAGE gels. After 1 hr block with 5% milk at room temperature, immunoblotting was performed using antibodies against HLA-A (Santa Cruz A-18), 5-Lipoxygenase (Cell Signaling Technology 3289), STAT1 (Cell Signaling 9175), phospho-STAT1^{Tyr701} (Cell Signaling 9167), and IRF1 (Cell Signaling 8478s). Antibodies were probed at manufacturers recommended dilution overnight at 4°C before a secondary antibody conjugated to HRP was used for imaging. Replicate samples were probed using the indicated antibodies when noted, or blots were stripped with Restore™ Western Blot Stripping Buffer (ThermoFisher Scientific 21063), re-blocked with 5% milk, and re-probed with an anti-GAPDH-HRP direct conjugated antibody (Cell Signaling Technology 3683) as a loading control. qPCR was performed using the Taqman real-time PCR system. RNA was extracted using the Qaigen RNeasy, 1 μg of RNA was reverse transcribed into cDNA using qScript cDNA SuperMix (Quanta Biosciences)

TaqMan probes and primers were designed from 'assay-on-demand' gene expression products (Applied Biosystems). Primer and probes were HLA-A (assay ID number: Hs01058806_g1) and the endogenous reference gene control was TATA-box binding protein (TBP) (assay ID number: HS99999910). Reactions were carried out in triplicates using standard thermocycling conditions (2 minutes at 50°C, 10 minutes at 95°C, 40 cycles of 15 seconds at 95°C, and 1 minute at 60°C. The results are presented as relative differences in expression vs the endogenous reference control gene ($2^{-\Delta Ct}$), or fold changes based on the differences of normalized Ct values compared to control samples, assuming optimal primer efficiency ($2^{-\Delta\Delta Ct}$). Samples that did not amplify after 40 cycles or amplified at an equal or later Ct value compared to a water sample were considered negative and are not plotted with a value. For RT-PCR reactions, RNA was extracted using the Qaigen RNeasy, and 1 μg of RNA was reverse transcribed into cDNA using qScript cDNA SuperMix (Quanta Biosciences) standard PCR cycling was used using the DreamTaq master mix system (ThermoFischer Scientific) with standard thermocycling conditions as recommended by the manufacturer. Primers used to amplify cDNA were as follows: US6-For: GAGGACTTTGCGCACCAATGUS6 US6-Rev: ACAGGTCAGCCTACCCTCAA and murine GAPDH-For: TGATGGGTGTGAACCACGAG murine GAPDH-Rev: TCTTGCTCAGTGTCCTTGCT. RT-PCR products were run on a 2% agarose gel with syber safe gel stain before imaging.

Antibody-dependent Cellular Cytotoxicity

JMN cells used as ADCC target cells were first pre-treated for 72 hours with 1.5uM BW-B70c. They were then trypsinized, washed, and incubated with 50 μCi of ^{51}Cr for 1 hour at 37 °C and washed 3 time to remove free ^{51}Cr. Indicated concentrations of

ESKM were incubated with target cells and fresh PBMCs at effector:target ratios of 50:1 for 6 hours at 37 °C. The assay was performed in 96-well format with 5000 target cells per well and 250,000 PBMC. The supernatant was harvested, and the cytotoxicity was measured by scintillation counting.

Transduction of US6

US6 overexpression vector was a gift from the Tortorella lab at Mount Sinai School of Medicine. US6 vector was sequenced to confirm composition of the standard Uniprot sequence of CMV US6 (P14334_US06_HCMVA). US6 was cloned into a retroviral overexpression vector pLgPW[197], which uses a CMV promoter to drive expression of US6 along with eGFP driven off of the LTR promoter. US6-pLgPW was packaged into retrovirus through transfection of 293T cells expressing retroviral glycoprotein along with a VSV-G pseudotyping plasmid. Viral supernatant was collected before Spinoculation for 2 hours into EL4-Ova cells. Transduced cells were purified through fluorescence activated cell sorting for eGFP+ cells.

CRISPR Knock-out Studies

LentiCRISPRv2 (Addgene plasmid #52961) [96] was a gift from Feng Zhang (Broad Institute, Cambridge, MA). Small guide RNA sequences targeting murine TAP1 and β2M were as follows: (TAP1: CCTAGGACTAGGGGTCCGCG β2M: AGTCGTCAGCATGGCTCGCT). sgRNA were cloned into the LentiCRISPRv2 and lentivirus was produced after transfection with packaging plasmids into HEK293T cells. MCA205 were transduced with LentiCRISPRv2 and transduced cells were selected using 5 μg/mL puromycin for 48 hours. Successful knockout was detected using an indirect method of flow cytometry for H2Kb because TAP1 and β2M both control H2Kb expression. Initially, puromycin-resistant cells from MCA205 Cas9-

β2M were bimodal for H2Kb expression suggesting that the sgRNA did not mediate CRISPR/Cas-9 destruction in a subset of cells. Fluorescence activated cell sorting was used to sort out the H2Kb-low cells presumed to be the successful homozygous β2M knockouts.

RESULTS

High Throughput Screen for Small Molecule Inhibitors that Regulate HLA-I

To discover small molecule inhibitors that can be used to regulate HLA-I expression, a library of approximately 6,700 FDA-approved or known bioactive compounds were used in a high throughput screen. Briefly, the HLA-A2+ JMN mesotheliomas cells were plated onto 384-well plates overnight before compounds were added at a final concentration of 5 uM using robotics. Cells were incubated for 72 hours before washing, fixing with paraformaldehyde, and immunofluorescence staining with an anti-HLA-A2. Images were captured through high-throughput plate imaging and analyzed for fluorescent signal per cell using software that can distinguish cell boarders. Each plate contained 1 column of cells treated with 100 ng/mL IFNγ as a positive staining control as well as an assay control to distinguish inter- and intra-plate variability that may be introduced during processing and robotic manipulations. The screen was performed twice and all data was pooled together. To identify lead compound hits, we quantified total HLA-A2 fluorescent signal per cell by the formula IxA where I = average cell fluorescence intensity and A = cell area. Average cell fluorescence intensity was used because images are collected in two dimensions and fluorescence intensity is not homogenous over a given cell due to microscope focus and image capture. We used a reverse normalized percent inhibition (NPI) approach where DMSO controls were set at 0%, IFNγ positive controls were set at 100%, and

values were normalized per plate to account for inter-plate variability. We identified lead compounds as those that caused >60% NPI for IxA and had reproducibility of at least 2 hits (either between the two independent experiments or within the same experiment because several sub-libraries used contained redundant compounds). (Fig. 3.1A) A column of IFNγ positive controls can be easily visualized on a heat map of hits (Fig. 3.1A). Graphical representation demonstrates no obvious patterning of experimental hits suggesting there was no major cofounding assay effects such as plate effects or obvious errors resulting from faulty robotic pipetting patterns. Immunofluorescence signal increases substantially after IFNγ-treatment compared to DMSO-treated cells (Fig. 3.1B). We then excluded hits that cell counts of <5% compared to DMSO control based on DAPI counting because the cytotoxicity of these compounds may confound the data. Finally, we examined hit images manually and excluded compounds that were inherently florescent into the A488 detector (used for fluorescence microscopy) or if staining had artifacts such as poor-focus and debris. From this analysis, we generate a list of 23 lead compounds (Table 3.1). Based on the NPI analysis, we examined the known targets for our list of lead compounds. We identify 19 hits with known biological targets out of the 23 lead compounds (Table 3.1). To validate these targets, we repeated the assay with the 23 lead compounds, which allows us to perform the experiment in a much smaller scale and preventing artifacts that may be introduced from cumbersome handling. We observe that in the identical assay using a range of lower doses, most compounds validated and demonstrate dose-dependent regulation of HLA-I (Fig. 3.2) as measured by immunofluorescence, indicating a level of reproducibility in our initial screen. We also included the MEK inhibitor Trametinib, a known regulator of HLA-I in the JMN cell line as a positive control. Interestingly, although Trametinib potently increased HLA-I in the validation assay (Fig. 3.2), it did not appear as a candidate lead compound in our

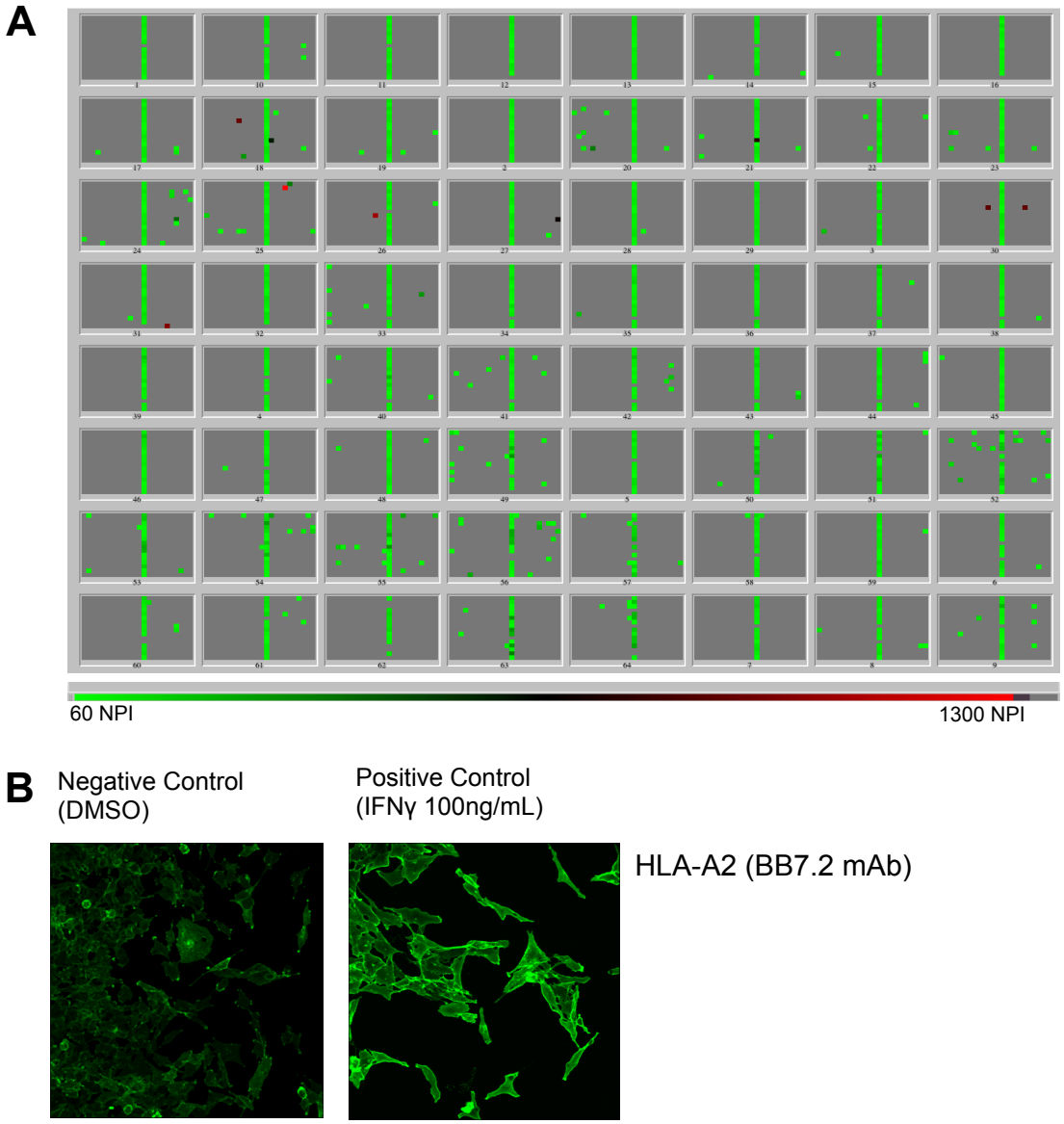

Figure 3.1. High throughput immunofluorescence screen to identify bioactive small molecule regulators of HLA-I.

(A) High throughput immunofluorescence screen was performed with ~6,700 unique compounds in an arrayed 384-well format. JMN Cells were treated for 72 hours at 37 degrees C with 5 uM of compound before washing, fixation, and staining with anti-HLA-A2. See chapter III material and methods for detailed methods. Heat map of >60% NPI for IxA setting the DMSO control to 0% and 100ng/mL IFNγ positive control to 100% and normalized per plate to demonstrate distribution of hits on the plates. Green denotes an >60% NPI hit while red denotes highest fluorescence. (B) Representative anti-HLA-A2 immunofluorescence staining of DMSO control and IFNγ-treated JMN cells from optimization experiments performed as in (A).

initial screen indicating a level of assay noise or inconsistencies in the stock libraries. This is not uncommon in arrayed compound high-throughput screening approaches.

Table 3.1. Lead compound hits, targets, HLA-A2 expression, and cell count.

List of lead compound hits from high-throughput screen that increase HLA-A2 expression. Inhibitor target, (average fluorescence intensity x area) NPI, (average fluorescence intensity x area) percent of control (POC), and cell count (POC) by DAPI staining is presented. NPI was calculated setting the DMSO control to 0% and 100ng/mL IFNγ positive control to 100% and normalized per plate

Compound name	Inhibitor Target	(IxA) NPI	(IxA) POC	Cell Count POC
As703026	MEK1/2	103.8	353.2	37.7
Azd4547	FGFR	95.4	233.2	45.0
Azd8330	MEK1/2	103.3	260.5	25.7
Bw-B 70c	5-lipoxygenase	122.3	351.3	33.5
Cediranib (Azd2171)	VEGFR	124.9	364.4	21.8
Crizotinib (Pf-02341066)	ALK, MET, ROS1	134.9	384.5	9.8
Everolimus (Rad001)	mTOR	69.4	253.1	48.1
Gf 109203x	Protein Kinase C	63.1	228.3	81.8
GSK1383281A	no data	66.2	207.8	5.5
GSK1389063A	no data	106.2	311.1	7.2
GW275568A	no data	60.9	199.3	74.6
GW684941X	no data	155.4	352.2	8.4
Indatraline Hydrochloride	Monoamine uptake Ib	65.1	188.4	81.2
Pd0325901	MEK1/2	172.2	421.2	24.0
Pha-665752	c-MET	148.7	379.1	54.4
Pkc412 >99%	Multi-Target Kinase Ib	149.6	327.5	10.5
Pyrromycin	anthracycline antibiotic	79.3	245.7	73.6
Sertraline Hydrochloride	Serotonin Reuptake Ib	105.4	292.0	65.1
Su 5416	VEGFR	76.5	254.7	76.1
T 98475	gonadotropin-releasing hormone Receptor	72.2	251.0	69.9
Tae684 (Nvp-Tae684)	ALK	390.4	897.3	8.7
Tak-285	EGFR	90.7	275.4	69.6
Tak-733	MEK1/2	78.8	257.3	27.1

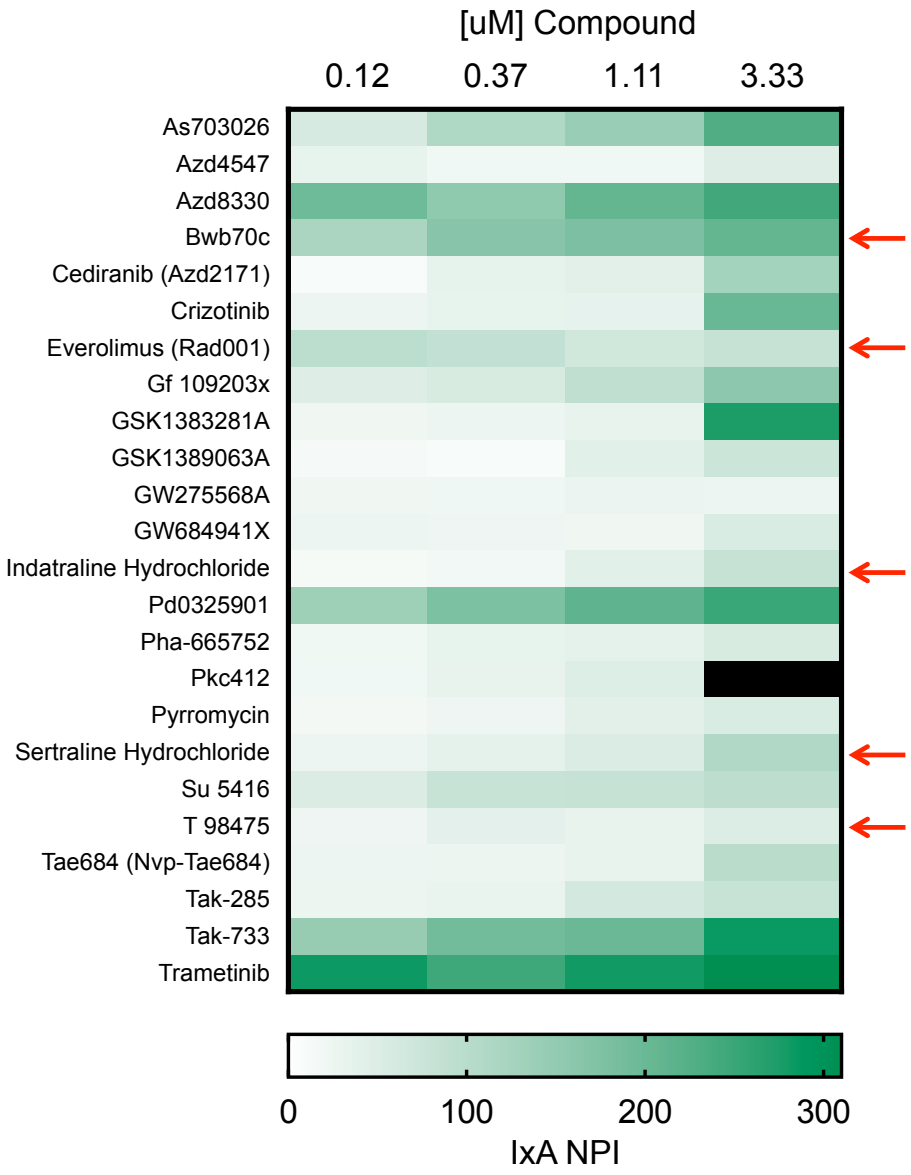

Figure 3.2. Lead compound hits validate in a dose titration assay.

Lead compound hits from the high-throughput screen were evaluated in a validation experiment repeated using similar assay set-up but performed in on small-scale to reduce the risk of assay artifacts. Cells were plated at 500 cells per well overnight before addition of compounds at a range of lower doses. After 72 hours of incubation at 37 degrees C, cells were washed, fixed, stained, and analyzed as in Figure 3.1. Heat map of IxA NPI performed in triplicate is plotted for each compound. Black box over Pkc412 denotes excluded sample because this dose led to below 5% cell count versus DMSO controls. Red arrows denote non-MAPK inhibitor compounds taken forward for further evaluation.

Validation of Hits Through Flow Cytometry

The identification of several MAPK pathway kinase inhibitors confirmed our past studies that MEK pharmacological inhibition could enhance cell-surface HLA-I[110]. However, we were curious to validate hits that were not directly linked to the MAPK pathway. Therefore, we utilized an orthogonal flow-cytometry based assay with the goal of validating novel hit compounds that were commercially available. Unexpectedly, some compounds (Sertraline, T98475, Indatraline) did not substantially increase cell-surface HLA-I at reasonable doses as detected by flow cytometry (Fig. 3.3). The discrepancy between the flow cytometry data and the immunofluorescence data from the screen may be intrinsic to the assay readouts as deliberated further in the discussion section. However, treatment with BW-B70c (iron chelating 5-Lipoxygenase (5-LO) inhibitor[198]) markedly increased HLA-I on JMN cell surface at pharmacologically relevant doses (Fig. 3.3). The mTOR inhibitor Everolimus also increased HLA-I to some extant. Because thorough mechanistic studies of 5-LO inhibitors on HLA-I expression have not been done, we pursued mechanistic evaluation of this novel strategy to enhance HLA-I expression.

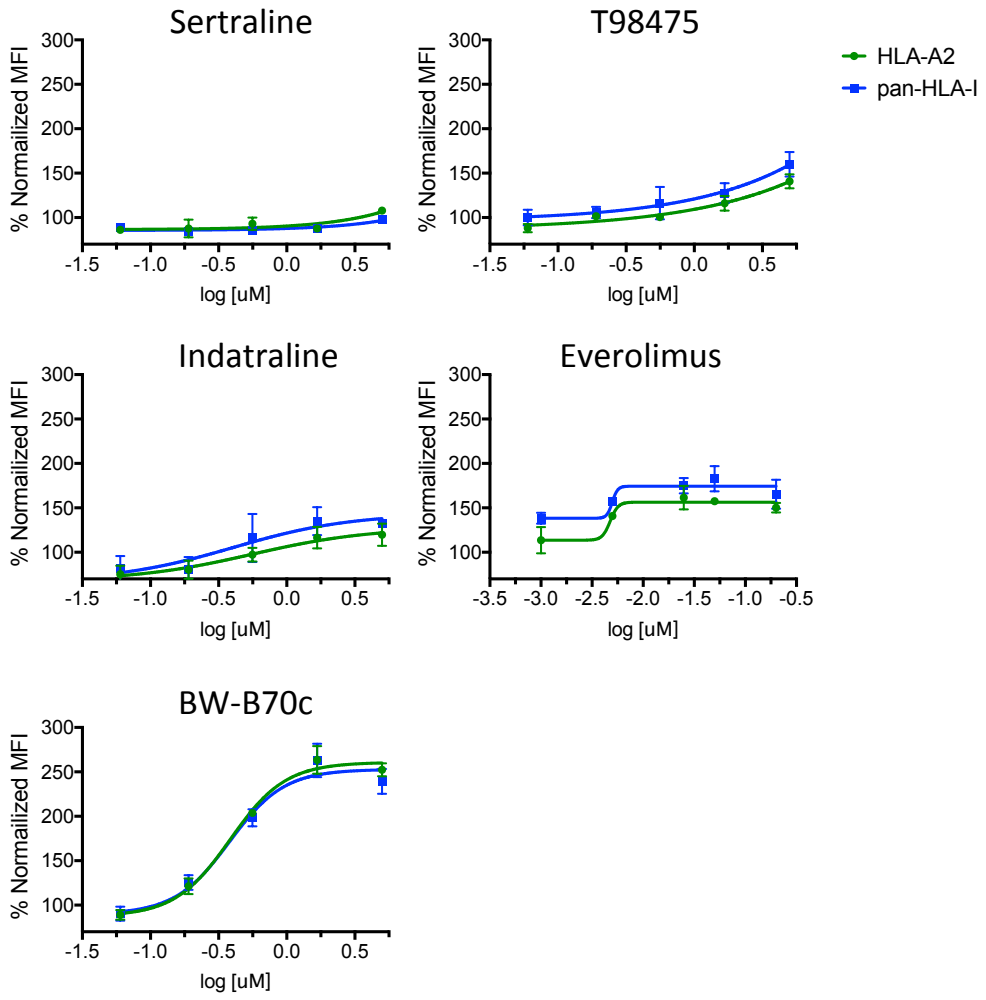

Figure 3.3. BW-B70c and Everolimus increase cell-surface HLA-A2 in orthogonal validation assay.

JMN cells were treated for 72 hours with the indicated compound over a range of concentrations from 5 uM – 0.06 uM (data shown for Everolimus was at lower doses of 200 nM – 1 nM due to cellular toxicity at higher doses). Cells were washed, trypsinized, and stained with anti-HLA-A2 for flow cytometric analysis using a HLA-A2-specific antibody (clone BB7.2), or a pan-HLA-I antibody (clone W6/32). Data is representative of 3 independent experiments.

BW-B70c Increases HLA-A2 Protein Expression Through Transcriptional Regulation

Cell-surface HLA-I is regulated through several mechanisms including transcriptional and translational regulation, stability through β2M expression, and enhanced peptide loading complex formation. To determine how BW-B70c regulated HLA-I, we treated JMN cells for 72 hrs and assayed for HLA-A mRNA transcript levels by qPCR and whole-cell protein expression by western blot. We determined that BW-B70c enhanced both HLA-A mRNA (Fig. 3.4A) and protein expression (Fig. 3.4B) in a dose-dependent manner. Next, we asked if this transcriptional regulation was mediated through STAT1 and IRF1, canonical transcription factors that regulates HLA-I expression. We demonstrate that upon BW-B70c treatment, there was a dose-dependent increase in STAT1, activated phospho-STAT1, and IRF1 protein expression by western blot analysis (Fig. 3.4B).

BW-B70c Increases Tumor-antigen Presentation and Sensitizes JMN Cells to TCRm-mediated ADCC

It is reasonable to hypothesize that the increased HLA-I after BW-B70c treatment would also enhance tumor-associated peptide/HLA-I complex presentation and TCRm-mediated ADCC. JMN does not express consistently detectable PRAME protein, but does express the oncofetal protein WT1 and binds another TCRm we developed called ESK1, targeting WT1-derived RMFPNAPYL (RMF) peptides in complex with HLA-A2. We therefore treated JMN cells with increasing concentrations of BW-B70c and determined amount of a ESK1 binding to measure

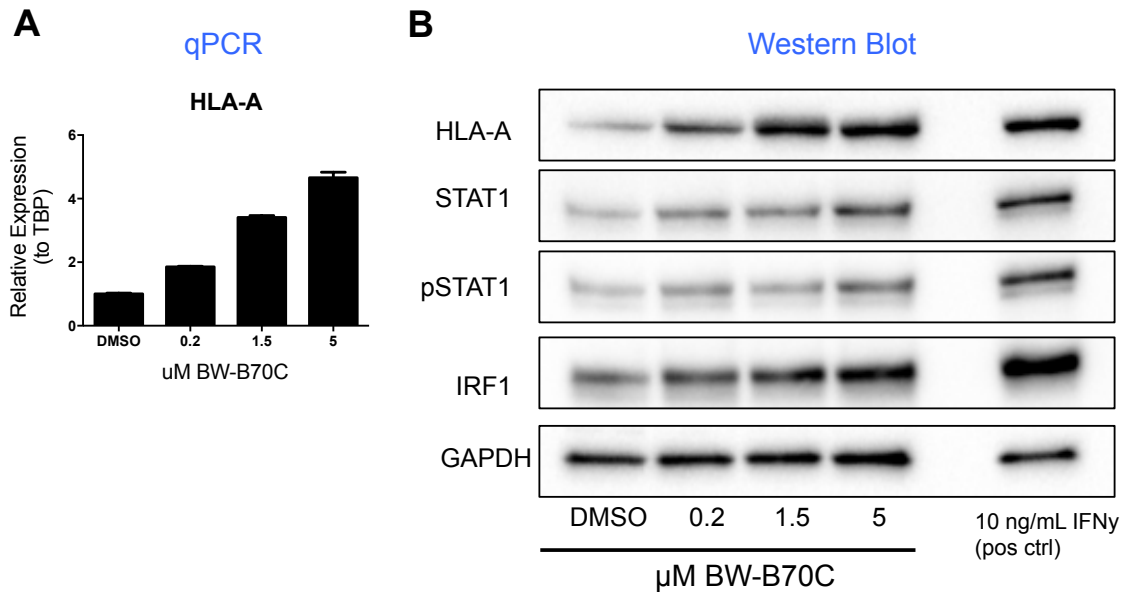

Figure 3.4. BW-B70c transcriptionally regulates HLA-I through IRF1.
JMN mesothelioma cells were treated with BW-B70c at the indicated concentrations for 72 hours. Cells were harvested and HLA-A transcript levels were measured by qPCR (A). Relative expression was normalized to TBP. (B) Protein expression of HLA-A was determined by western blot analysis. STAT1, phospho-STAT1^{701}, and IRF1 protein levels were also determined. Cells treated for 72 hours with IFNγ were also included as a positive control.

RMF/HLA-A2 presentation. BW-B70c treatment increased ESK1 binding in dose-dependent manner (Fig. 3.5A). In addition, pre-treatment of JMN cells with BW-B70c for 72 hours slightly sensitized JMN to ESKM-mediated (afucosylated form of ESK1^{99}) ADCC at lower concentrations of TCRm (Fig. 3.5B). Interestingly, the maximum ADCC was not enhanced suggesting that there is a maximum antigen-density threshold—at least for the JMN cell line in the assay—where enhancing TCRm-target epitopes does not enhance ADCC.

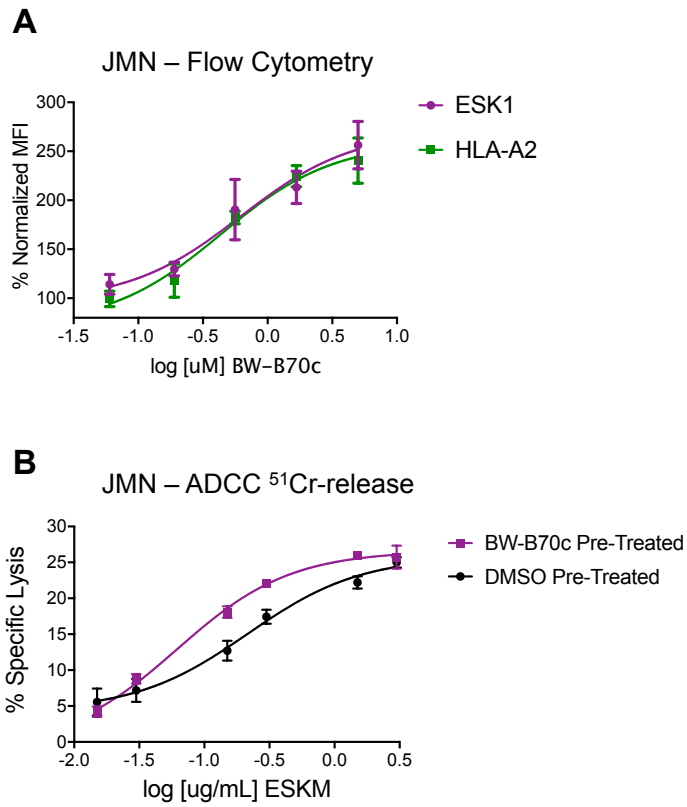

Figure 3.5. BW-B70c increases WT1 tumor antigen presentation on HLA-A2 and sensitizes JMN cells to TCRm-mediated ADCC.
(A) JMN cells were treated with the indicated dose of BW-B70c (ranging from 5uM - 0.06 uM) for 72 hours before flow cytometry using ESK1, an anti-WT1$^{126\text{-}134}$/HLA-A2 TCRm antibody was used to determine WT1 tumor antigen presentation. HLA-A2 cell-surface expression was also measured. (B) JMN cells were pre-treated with 1.5 uM BW-B70c for 72hours before being washed an used as targets in a ^{51}Cr-release ADCC assay with an human PBMC effectors at an E:T of 50:1.

Everolimus and BW-B70c are Additive with MEK Inhibitor Trametinib in Increasing Cell-surface HLA-I

Our previous work had demonstrated that MEK inhibition using Trametinib increases cancer cell-surface HLA-I *in vitro* and MHC-I *in vivo*[110]. In addition, other studies have established interesting yet complex communication between the MAPK and mTOR pathways that can cross-inhibit or cross-activate depending on the context[199,200]. Because the mTOR inhibitor Everolimus seemed to subtly increase

HLA-I, we next asked whether there was synergy or antagonism between Everolimus (mTOR ib) and Trametinib (MEK ib) for regulation of HLA-I. Both Trametinib and Everolimus increased cell-surface HLA-I on the JMN mesothelioma to levels that we expected (Fig. 3.6A). However, combination treatment with both Trametinib and Everolimus was more than additive for up-regulation of HLA-I (Fig. 3.6A). This suggests that in the context of HLA-I regulation, these inhibitors are not antagonistic. We were also interested in whether Trametinib was additive with BW-B70c. It is unknown if BW-B70c leads to MAPK signaling inhibition which could be a plausible mechanism of HLA-I regulation. Instead, we observed an additive effect of Trametinib and BW-B70c *in vitro* (Fig. 3.6B), suggesting that the major mechanism of BW-B70c-mediated HLA-I regulation was not through the MAPK pathway. All inhibitors decreased tumor viable cell count, which is ultimately a desired effect of therapy (Fig. 3.6A, B – Bottom Panels). Together, the data presented also suggest that multiple signaling pathways can be manipulated to further augment HLA-I expression. This has several implications in combination immunotherapy because it will be important to identify combination drugs that not only deplete tumor cells, but also sensitize remaining cells to immunotherapy.

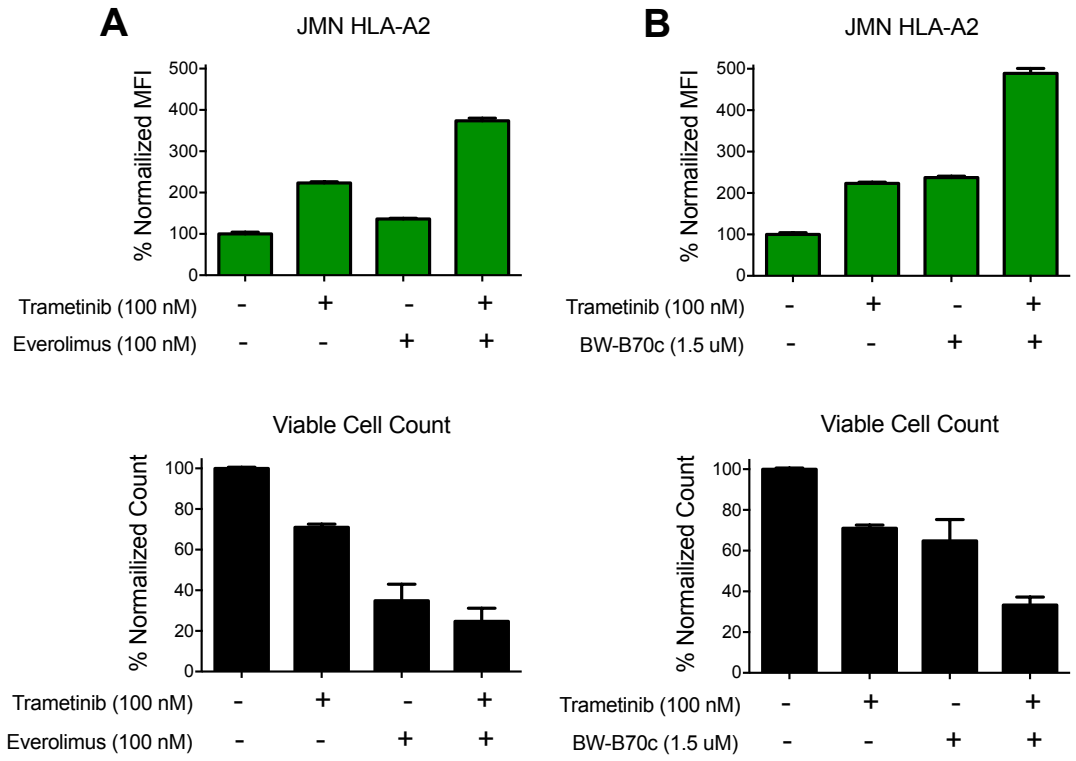

Figure 3.6. Everolimus and BW-B70c are additive with Trametinib in regulating HLA-I.

JMN mesothelioma cells were either left untreated or treated with 100 nM Trametinib in combination with either 100 nM Everolimus (A) or 1.5 uM BW-B70c (B) for 72 hours. Flow cytometry was used to determine cell-surface HLA-A2 expression. Viable cell counts (bottom panels) were measured by propidium iodide exclusion and raw counts from time-matched flow cytometry. All conditions were performed in triplicate.

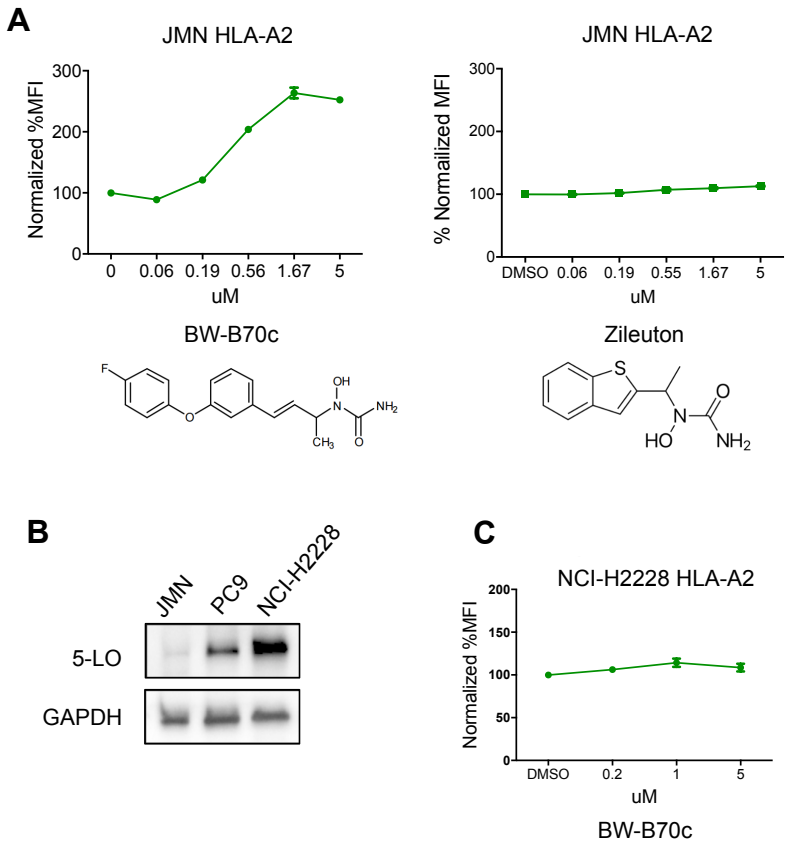

Figure 3.7. 5-LO inhibitor Zileuton does not affect JMN HLA-I expression and BW-B70c does not affect HLA-I expression in a 5-LO-high expressing lung cancer.
(A) JMN cells were treated with either BW-B70c or Zileuton at indicated doses for 72 hours before flow cytometry was used to determine cell-surface HLA-A2 expression. Molecular structures of both compounds are illustrated. Graphs include data from Figure 3.2 for comparison purposes. (B) JMN, PC9, and NCI-H2228 cell lysates were analyzed by western blot for 5-LO protein expression. GAPDH was used as a protein loading control. (C) The 5-LO-high expressing NCI-H2228 lung cancer line was treated with the indicated doses of BW-B70c for 72 hours before flow cytometric analysis for cell-surface HLA-I.

HLA-I regulation by BW-B70c is not dependent on 5-LO

BW-B70c is not an FDA-approved 5-LO inhibitor. Therefore, we were interested in determining if inhibition of 5-LO enzymatic activity with the FDA-approved 5-LO inhibitor Zileuton could increase HLA-I. Zileuton is used in the management of asthma and is though to inhibit 5-LO enzymatic activity as a iron chelator much like as

BW-B70c[198]. Disappointingly, Zileuton did not affect HLA-I in the JMN mesothelioma cells at any concentration tested suggesting that enzymatic inhibition of 5-LO may not account for the increased HLA-I after BW-B70c treatment (Fig. 3.7A Right Panel). In fact, protein expression of 5-LO in JMN cells was nearly undetectable by western blot analysis (Fig. 3.7B). In contrast, the non-small cell lung cancer cell lines PC9 and NCI-H2228 expressed high levels of 5-LO, yet NCI-H2228 did not up-regulate cell-surface HLA-I in response to BW-B70c treatment (Fig. 3.7B,C). Taken together, the data suggests that BW-B70c does not upregulate HLA-I on JMN cells through enzymatic inhibition of 5-LO.

US6 Immunoevasin Inhibits MHC-I Antigen Presentation

To determine utility of the CMV US6 immunoevasin protein for protecting engineered cells from host CD8+ T cell attack, we utilized a commonly used immunogenic cell line EL4-Ova (also known as EG.7)[201]. EL4-Ova is a derivative of the mouse T cell thymoma EL4 that has been engineered to express a copy of the highly immunogenic chicken ovalbumin protein[202]. We overexpressed US6 or vector control (pLgPW with GFP) in EL4-Ova through retroviral transduction and demonstrate stable expression as measured by RT-PCR for US6 (Fig. 3.8A). US6 inhibits TAP function to chaperone MHC-I peptides and as expected, overexpression of US6 led to reduced MHC-I cell-surface expression (Fig. 3.8B) confirming previous studies[193,203]. In addition, US6 overexpression decreased presentation of the highly immunogenic $Ova^{257-264}$ peptide (SIINFEKL) as measured using an antibody specific for SIINFEKL/H2Kb (Fig. 3.8C). To ensure that vector or US6 overexpression did not intrinsically hinder important biological processes that may inhibit viability or cell growth, we measured cell growth *in vitro*. We did not observe any significant difference between parental EL4, EL4-Ova, EL4-Ova vector control, or EL4-Ova US6 (Fig. 3.8D). To determine whether the

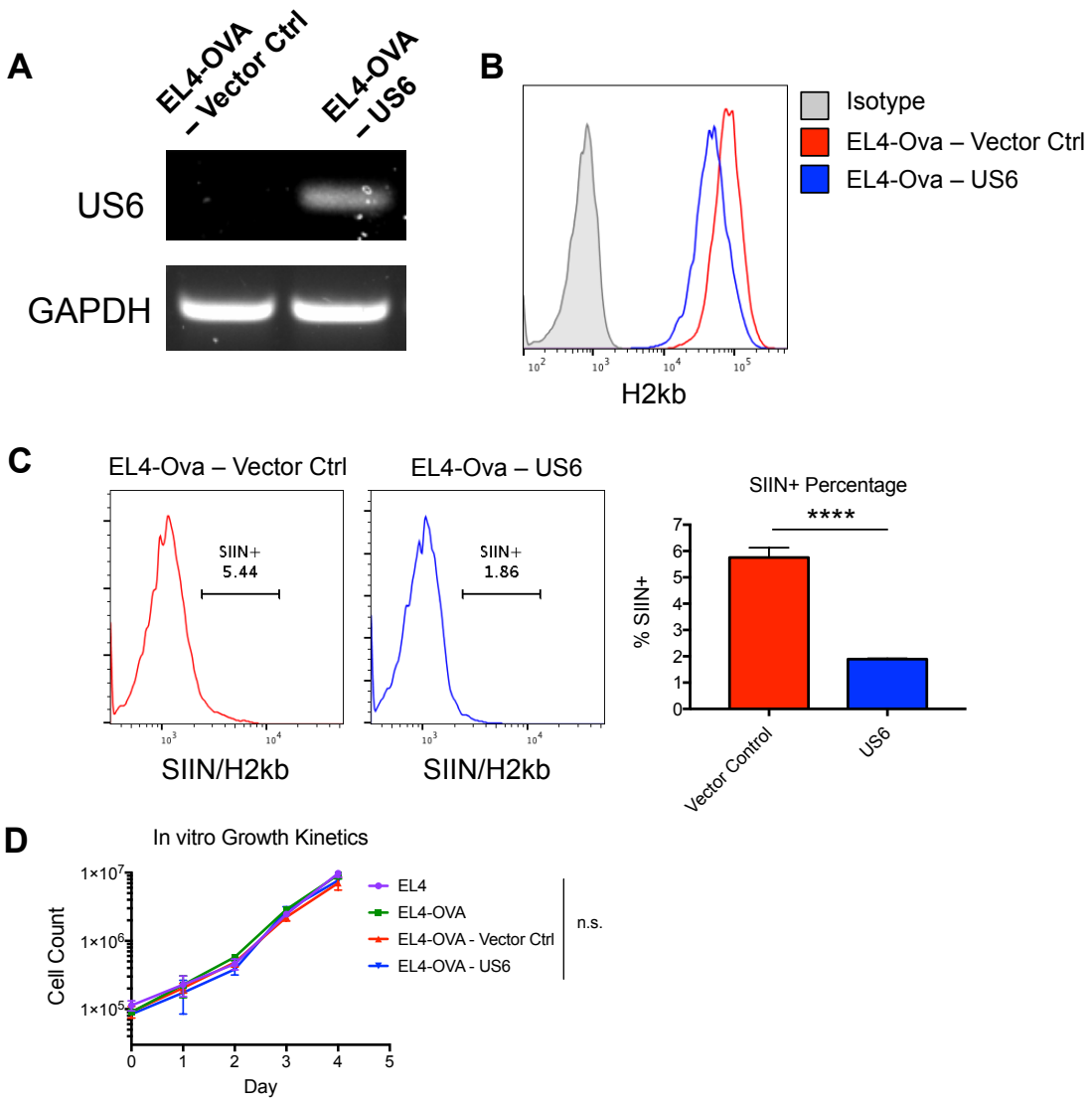

Figure 3.8. US6 immunoevasin decreases cell-surface MHC-I, antigen presentation, and does not affect cell growth.

(A) US6 was overexpressed in the EL4-Ova cell line through retro-viral transduction of a CMV promoter-based mammalian overexpression vector pLgPW that expresses GFP as a selectable marker. RT-PCR was used to confirm expression of US6 transcript. GAPDH transcript was used as a loading control. (B) Flow cytometry was used to determine cell-surface expression of the murine MHC-I allele H2Kb in US6 overexpressing EL4-Ova versus vector control. (C) Flow cytometry was used to determine presentation of a model antigen from Ova: SIINFEKL/H2Kb. Quantification of %SIIN+ cells is represented graphically on the right panel. (D) Each cell line or construct indicated was cultured *in vitro* starting at $1x10^5$ cells and trypan blue exclusion counting was performed every day for 4 days.

reduced Ova-peptide presentation would reduce immunogenicity *in vivo*, we engrafted mice subcutaneously with the parental EL4, EL4-Ova vector control, or EL4-Ova US6. The experiment is currently underway and the results are pending.

Genetic Deletion of TAP and β2M Lead to Loss of Cell-surface MHC-I and TAP Deletion in a Cas9-expressing Fibrosarcoma Leads to Reduced Tumor Growth in Immunocompetent Mice

The streptococcus pyogenes-derived Cas9 is thought to be immunogenic in mammals leading many to believe this will be a major challenge in utilizing CRISPR/Cas9-based therapeutics in humans[204]. Recent preliminary reports have already hinted that humans have pre-existing humoral antibody responses and cytotoxic T cell responses against Cas9 and Cas9-expressing cells[205]. This is important to understand because Cas9 is increasingly utilized in mouse models and CD8 T cell responses against Cas9 could affect experimental outcome. In addition, this may provide a model to study strategies to modulate MHC-I to protect foreign Cas9-bearing cellular therapeutics. Our US6 studies may be confounded *in vivo* by the unknown variable of potentially immunogenic US6 peptides presented on MHC-I. Therefore, we aimed to generate a more robust model by complete TAP deletion and ask how this would affect potential immunogenicity of Cas9-expressing cells. Using a murine fibrosarcoma coupled to a CRISPR/Cas9 system, we generate MCA205-Cas9 that constitutively expresses Cas9, MCA205-Cas9 TAP KO that has TAP1 deleted, and MCA205-Cas9 β2M KO that has β2M deleted. These lines were generated through lentiviral transduction of a plasmid encoding constitutive expression of Cas9 along with an sgRNA either against an irrelevant target, or against the respective TAP1 and β2M targets. All constructs also express the puromycin resistance PAC gene. Deletion of TAP1 and β2M led to near complete abrogation of MHC-I as measured by flow cytometry against H2Kb (Figure

3.9A). As expected, β2M deletion reduced H2Kb more than TAP1 deletion. To simultaneously ask the question of whether Cas9 expression abrogates cell growth under immune pressure *in vivo* and if TAP or β2M deficiency can protect transgenic cells *in vivo*, we engrafted MCA205 WT, MCA205-Cas9, MCA205-Cas9 TAP KO, and MCA205-Cas9 β2M KO cells subcutaneously into syngeneic C57BL/6N mice (Figure 3.9B). We observe in this preliminary study that MCA205 WT cells grew into large tumors by day 22 whereas MCA205-Cas9 tumors grow slower, presumably from immune pressures against Cas9, however this was not formally tested. Comparing the growth kinetics, MCA205-Cas9 β2M KO cells seemed to have initial growth delay, but by day 22 seemed to grow in a typical exponential pattern. Interestingly, MCA205-Cas9 TAP KO cells had the slowest growth kinetics and seemed to have starting plateauing at the experimental endpoint. The observation that Cas9 expression

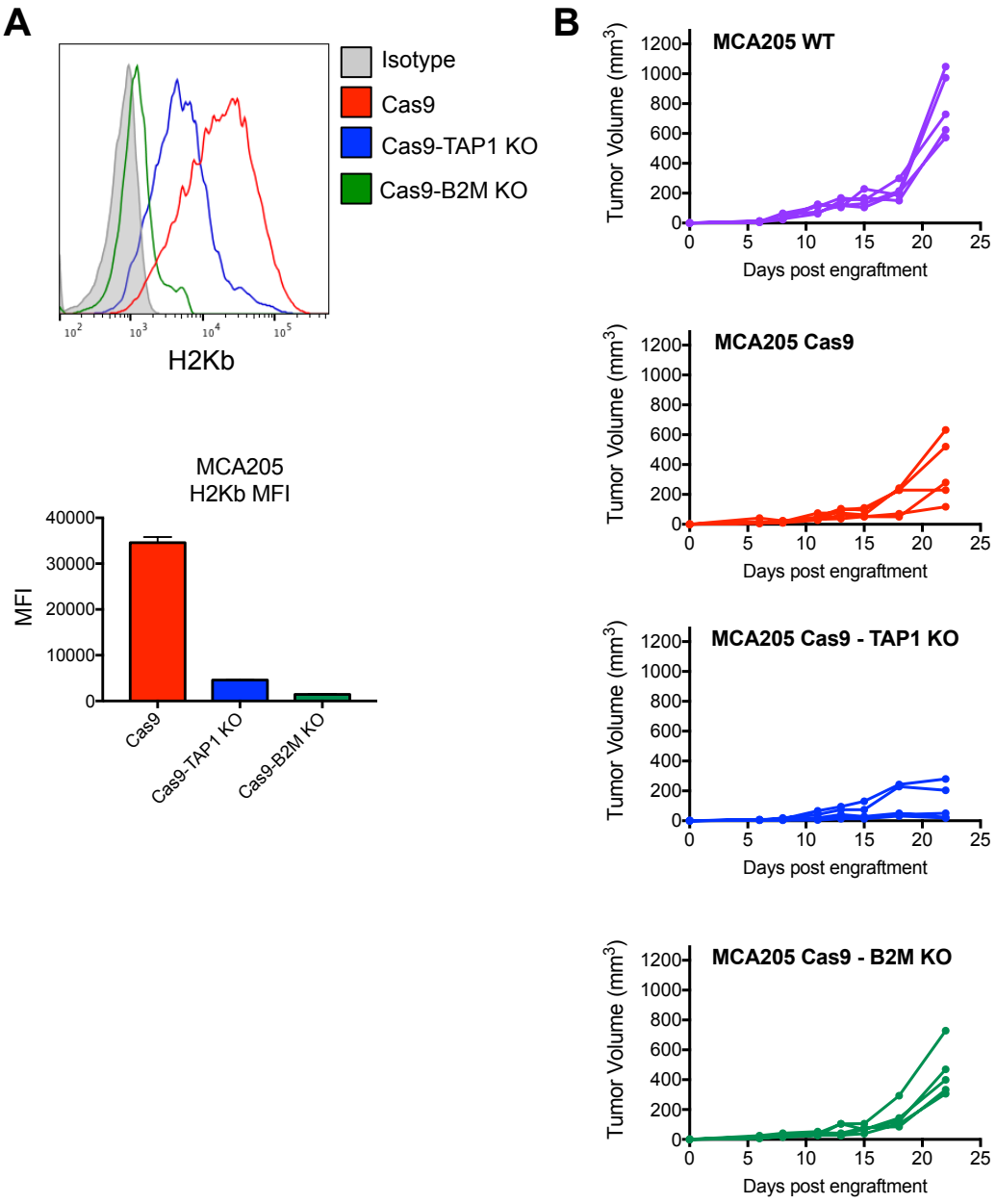

Figure 3.9. TAP and β2M deletion abrogate MHC-I expression and alters growth kinetics in a Cas9-expressing MCA205 tumor.

TAP1 and β2M were genetically ablated in the MCA205 fibrosarcoma line through CRISPR lentiviral transduction of stably expressed Cas9 and respective sgRNAs. (A) Flow cytometry to measure cell-surface MHC-I (H2Kb) expression. Overlaid plots are compared to an isotype control and MFI values are plotted (bottom panel). (B) $1.5x10^6$ MCA205 WT, MCA205 Cas9-expressing, MCA205 Cas9 – TAP Knock out, or MCA205 Cas9 – β2M knock out cells were engrafted subcutaneously on the hind flank of immunocompetent C57BL/6N mice. Tumors were measured over 22 days using caliper measurements. Experiment was performed once.

Alone slightly slows tumor growth compared to MCA205 WT (p=0.0121) suggests that Cas9 expressed in a cell may be immunogenic. The slightly delayed but still exponential growth kinetics of MCA205-Cas9 β2M KO suggests that complete loss of MHC-I does may not always lead to elimination by NK cells which is a highly regulated process and is context dependent. Finally, the delayed growth kinetics and day 17-22 plateau of MCA205-Cas9 TAP KO cells (Fig. 3.9B) suggests that complete deletion of TAP function would not be a useful strategy to protect cells harboring immunogenic proteins. We hypothesize that this may be mediated by immunity against non-TAP-dependent peptides either derived from self-proteins or transgenes Cas9 or PAC (puromycin resistance), or addition low-level NK-cell cytotoxicity as demonstrated against splenocytes from TAP-deficient mice[185].

DISCUSSION

HLA-I is a key immune recognition and modulatory molecule and therefore gaining a deeper understanding of how it can be modulated pharmacologically represents an attractive strategy to augment tumor immunotherapy. We demonstrate that a high-throughput immunofluorescence screen can be used to identify small molecule regulators of HLA-I. The methods for this approach are easily adaptable to discover modulators of other important immune receptor such as PD-L1, CD47, or HLA-II. Several inhibitors of the MAPK pathway were characterized as lead hit compounds, confirming and highlighting the importance of MAPK in regulation of HLA-I from our previous studies[110]. Two lead compounds validated in an orthogonal flow cytometry-based assay: the 5-LO inhibitor BW-B70c and the mTOR inhibitor Everolimus. Although we are confident in the reproducibility of the results, the discrepancy between the immunofluorescence results and the flow-cytometry results is likely due to assay artifacts such as how changes in cellular morphology affect the

automatic algorithm for determining boundaries on a cell in two-dimensional images. This is especially complex when cells are in contact with each other – a likely occurrence when cells are grown from a small number on a small area as was the case for our 384-well format plate screen starting with 500 cells per well. Although Everolimus only marginally increased HLA-I expression, we were interested in this compound because it is an FDA-approved drug used to prevent organ transplant rejection in addition to targeted therapy of advanced kidney cancer, progressive pancreatic neuroendocrine tumors, and advanced hormone-receptor positive but HER2-negative breast cancers. Everolimus had a greater than additive effect for increasing HLA-I in combination with the MEK inhibitor Trametinib suggesting that these pathways are linked in their regulation of HLA-I. Interestingly, Everolimus is known to inhibit T cell activation[206] allowing it to be useful for preventing transplant rejection. Unfortunately, this suggests it is unlikely that the marginal increase in HLA-I expression induced by mTOR inhibition would benefit T cell immunotherapy because Everolimus also severely inhibits T cell function. However, understanding the cross talk between MAPK and mTOR pathways in regulation of HLA-I would shed new light on biochemical mechanisms of HLA-I regulation.

Moreover, we were especially interested in the lead compound hit BW-B70c because it dramatically increase cell-surface HLA-I through a transcriptional mechanism correlated with increases in the canonical STAT1 and IRF1 transcription factors. BW-B70c increased HLA-I along with presentation of the RMF peptide derived from the tumor-associated antigen WT1. This led to increased sensitivity of JMN cells to TCRm-mediated ADCC targeting the RMF/HLA-A2 antigen, demonstrating functional relevance for regulation of HLA-I. Although BW-B70c was designed to be a 5-LO inhibitor, out data suggests that its effect on HLA-I expression was not through

inhibition of 5-LO enzymatic activity. 5-LO was nearly undetectable in JMN cells by western blot analysis and an additional iron chelator inhibitor of 5-LO Zileuton had no effect on HLA-I expression. Moreover, a lung cancer cell line NCI-H2228 that expressed abundant 5-LO did not increase HLA-I expression after treatment with BW-B70c. Determining the putative target of BW-B70c that regulates HLA-I will be shed light on how to manipulate HLA-I.

We were also interested in opting viral immunoevasins to protect engineered cellular therapeutics from immune recognition and attack. Cellular therapeutics such as stem cells and CAR T cells are now being experimentally engineered with synthetic and foreign genes, all of which may be immunogenic to host T cells. Therefore, we evaluated the use of the CMV immunoevasin US6 to inhibit TAP and functionally prevent immunogenic peptide/MHC-I presentation. We confirm that US6 expression inhibits cell-surface MHC-I expression and demonstrate that this leads to reduced presentation of SIINFEKL/H2Kb using the EL4-Ova mouse thymoma model. It will be exciting to see if the reduced antigen presentation would rescue growth under immune pressure *in vivo*. It is important to note that cells will contain vector components that may potentially be immunogenic (Neomycin resistance from original generation of EL4-Ova[202] and GFP from the pLgPW vector), however this is accounted for in the vector control experimental arm. Indeed, US6 is another foreign viral protein and through NetMHC prediction algorithms, we calculate several US6-derived peptides that are predicted to have ~100-300 nM affinity to C57BL/6N mouse MHC-I alleles H2Kb and H2Db (Table 3.2). This data is only a computational prediction and indeed the affinities are not as high as several other well-characterized MHC-I peptides such as Ova-derived SIINFEKL (which has a predicted affinity of 19.37 nM for H2Kb). In addition, the predictions do not account for processing steps

through proteasomal degradation or peptide-loading complex interactions that may be required to ultimately form stable peptide/MHC-I complexes. However, they still represent possible immunogenic peptides derived from US6 that can be tested experimentally.

Overexpression of Cas9 alone in the MCA205 fibrosarcoma decreased cell growth in an immunocompetent model suggesting that Cas9 has a level of immunogenicity. This is not surprising because Cas9 is a large bacterial protein (1368 residues long) and several Cas9-derived peptides may bind murine MHC-I and stimulate CD8+ T cell responses. Genetic deletion of β2M in the MCA205 fibrosarcoma slightly delayed growth *in vivo* and we hypothesize this to be the effect of NK cell cytotoxicity. Others have reported that β2M CRISPR knock out in other murine tumor cell lines prevents engraftment mediated by NK cells[207]. Although our data stands in contrast, the cellular mechanisms that govern NK cell activation and inhibition is extremely complex and context-specific so the data is not surprising[135,208,209]. More interestingly, deletion of TAP1 in MCA205 led to slower cell growth *in vivo*, which seemed to have plateaued between day 17 and 22. This is interesting because it was opposite of our hypothesis. The result could be explained through a combination of mechanisms. First, the lower MHC-I expression could promote a level of NK cell lysis. Second, deletion of TAP may allow the presentation of peptide epitopes that otherwise would have been outcompeted by the large pool of TAP-dependent epitopes. These epitopes are not presented on healthy cells and therefore represent T cell epitopes associated with impaired peptide processing (TEIPP)[210,211]. When presented after loss of TAP, these epitopes can generate CD8+ T cell responses and is believed to be a mechanism to prevent immune escape if there is deletion of TAP[210]. Although not formally tested, this represents a rationale mechanism to explain our results. Together, our data suggest

genetic TAP deletion to be a poor strategy in 'de-immunizing' genetically engineered cellular therapies.

Table 3.2. US6-derived Peptides have predicted affinities to murine MHC-I alleles.
The entire CMV US6 protein sequence was queried using NetMHC-Pan4.0 (http://www.cbs.dtu.dk/services/NetMHC/) to predict affinities of all possible 8, 9, 10, and 11-mer peptides to C57BL/6N MHC-I alleles (H2-Kb, H-2Db). The indicated peptides were predicted to have affinities of less than 500 nM. Peptide sequence, MHC-I allele, and predicted affinity (nM) are presented in the table.

Peptide	MHC-I Allele	Pred Affinity (nM)
GAVWNAFRL	H2Db	187.1
LGFLLMCAL	H2Kb	265.9
AVWNAFRLI	H2Kb	330
AVWNAFRL	H2Kb	128.5
HGFFAVTL	H2Kb	276.2
RLIERHGFF	H2Kb	239.3

AKNOLWEDGEMENTS

We would like to thank the MSK and Screening Core facility, namely Dr. Myles Fennell and Dr. Ralph Garippa, for their expertise and assistance in performing the high-throughput drug screen. We would also like to acknowledge students of the Weill

Cornell Pharmacology program Christina Beberbitz, Mitchell Wang, and Lauren Dong for their assistance with assays and experimental execution. Finally, we would like to thank Dr. Thomas J. Gardner and the Tortorella Group at Mount Sinai School of Medicine for the US6 and pLgPW overexpression vectors and helpful discussions about CMV immunoevasins.

THESIS SUMMARY

Pr20 mAb Binds PRAME+ and HLA-A2+ Cancer Cells and is Therapeutically Active *in vivo*

mAbs have proven to be a potent therapeutic modality for treating cancers however currently marketed mAbs exclusively target cell-surface antigens. TCRm antibodies such as Pr20 demonstrate that mAbs can also be used to target intracellular protein-derived peptides in the context of MHC-I. Pr20 bound to PRAME ALY peptide-pulsed T2 cells and PRAME+ / HLA-A2+ leukemias and lymphomas, but not healthy PBMC populations or PRAME-negative / HLA-A2+ cancer cell lines. We engineered the Fc afucosylated Pr20M that could direct ADCC against PRAME+ / HLA-A2+ cancer cells *in vitro*, but did not deplete healthy PBMC populations. Although Pr20M reacts against ALY/HLA-A2 much like a TCR-transduced T cell or peptide-stimulated T cell might, its mAb format allows for substantial ease of use as a drug. It could be directly infused rather than transduced ex vivo into patient-specific T cells and re-infused.

Pr20M also demonstrated therapeutic utility against xenograft models of AML and ALL. Unexpectedly, the AML cells extraction from the bone marrow of Pr20M-

treated mice did not lose target antigen expression and in fact bound Pr20 post-therapy better than AML cells from control mice. This suggests that there is some mechanism of increased antigen regulation that occurs during TCRm-therapy. We speculate that Pr20M recruitment of immune effectors such as macrophages in the NSG mouse may mediate local cytokine release modulating ALY/HLA-A2 antigen presentation.

The PRAME$^{300-309}$ ALY Epitope is Regulated by the Immunoproteasome

Initial studies testing Pr20 binding on a large panel of cell lines demonstrated that Pr20 did not bind several melanomas and other solid tumors despite high expression of both HLA-A2 and PRAME. This suggested that perhaps there were specific peptide-processing mechanisms that were important for generation of the ALY peptide. Because leukemias and lymphomas that express the immunoproteasome seemed to bind Pr20 better, we hypothesized and demonstrated that immunoproteasome expression and catalytic function was important for generation of the Pr20 epitope. Dramatic Pr20 binding was induced upon treatment with IFNγ, a pro-inflammatory cytokine well established to induce expression of the immunoproteasome. The IFNγ-induced Pr20 binding was partly dependent on β5i as demonstrated by reduced IFNγ-induced Pr20 binding after genetic ablation of β5i in melanoma cell lines. Biochemically, we define the mechanism to be that the immunoproteasome better maintains the ALY peptide because based on proteasome digestion assays *in vitro*. Incubation of an elongated pre-cursor peptide with the constitutive proteasome led to more internal destructive cleavages within the ALY 10-mer.

Pr20M and CD47 blockade with CV1 Leads to Dramatic Therapeutic Efficacy

Although we illustrate that Pr20M has some therapeutic efficacy alone, monotherapy did not lead to cures or long-term AML regression. Therefore we explored strategies to increase the therapeutic utility of Pr20M. We hypothesized that Pr20M could mediated ADCP from the NSG mouse macrophages and that by inhibiting the CD47 'do not eat me' signal, we could enhance ADCP and augment therapy. Indeed, we demonstrate that CD47 blockade using the CD47 antagonist SIRPα-variant peptide CV1 can enhance Pr20M-mediated ADCP by both human and NSG mouse macrophages *in vitro*. The phenotype translated well in animal models where combination therapy of Pr20M and CV1 led to dramatic therapeutic efficacy and long-term disease-free survival in AML xenograft studies.

Pr20-BiTE and Pr20-CAR can Potently Direct Lysis of PRAME+ /HLA-A2+ Leukemias but have Cross-reactivity to HLA-A2

We also explored engineering of the Pr20 scFv into the Pr20-BiTE and Pr20-CAR formats. BiTEs and CARs have recently gained FDA-approval for B-cell leukemia and lymphomas and there have been unprecedented clinical outcomes. Both BiTE and CAR formats can potently redirect T cells against a tumor antigen and can even lead to the phenomenon of antigen spreading[89], leading to further anti-tumor engagement by the endogenous immune response. Our data demonstrate that the Pr20 scFv can be engineered onto BiTE and second-generation 41BBζ CAR constructs and be expressed appropriately. Pr20-BiTE and Pr20-CAR both mediated rapid and robust depletion of a PRAME+ / HLA-A2+ AML cell line *in vitro* demonstrating potency of these biologics. However, Pr20-BiTE also mediated depletion of CD14+ monocytes from HLA-A2+ healthy donor PBMC suggesting that this population expressed a cross-reactive epitope at levels below the limit of detection of flow cytometry, but high enough for BiTE-mediated cytotoxicity. Pr20-CAR transduced into the Jurkat model T

cell line maintained reactivity to ALY/HLA-A2 by tetramer staining and activated when co-cultured with PRAME+/HLA-A2+ cells, demonstrating stable and functional expression of the construct. However, Pr20-CAR Jurkat cells also activated against a panel of PRAME-Negative but HLA-A2+ cell lines suggesting cross reactivity to other peptide/HLA-A2 molecules or that baseline reactivity to HLA-A2 alone with the CAR construct was sufficient to activate the T cell. Taken together, our data demonstrate the need for caution when engineering TCRm scFv into potent BiTE and CAR formats perhaps due to their typically higher affinity than natural TCRs.

A High-throughput Screen Validates that MAPK can Regulate HLA-I and Identifies BW-B70c as a Lead Experimental Compound that Increases HLA-I

We utilized an unbiased high-throughput arrayed screen to identify small molecule regulators of HLA-I. Several hit compounds were inhibitors for various kinases along the MAPK pathway; validating previous findings in the lab that MAPK pathway is important for regulation of HLA-I. We performed further studies on hit compounds that were not directly associated with inhibition of MAPK and confirmed that the mTOR inhibitor Everolimus and the 5-LO inhibitor BW-B70c could increase JMN mesothelioma HLA-I expression. Both of these compounds were additive with the MEK inhibitor Trametinib in increasing HLA-I and therefore we concluded that Everolimus and BW-B70c regulated HLA-I through pathways independent of MEK. We focused on the BW-B70c because it dramatically increased HLA-I. We determined the mechanism to be transcriptional through regulation of the STAT1 and IRF1 expression. BW-B70c not only increased HLA-I, but also increased cell-surface presentation of a WT1-tumor antigen-derived peptide RMF/HLA-A2. This increase in presentation sensitized JMN cells to ADCC mediated by ESKM, a TCRm against RMF/HLA-A2. However, we concluded that BW-B70c regulated HLA-I

independently of 5-LO because other 5-LO inhibitors did not affect HLA-I levels, JMN cells do not express appreciable levels of 5-LO, and an additional cell that that expressed high levels of 5-LO did not increase HLA-I after treatment of BW-B70c. The putative target of BW-B70c responsible for the HLA-I phenotype has yet to be determined.

US6 Inhibits Antigen Presentation and Deletion of TAP does not Promote Cell Growth *in vivo* Under Immune Pressure

We also explored the use of the viral immunoevasin TAP inhibitor US6 to inhibit antigen presentation on MHC-I in the ultimate hopes of utilizing US6 to protect engineered cells harboring foreign or synthetic genes from host T cells. US6 overexpression led to decreased MHC-I and Ova-derived SIINFEKL/H2Kb presentation. Genetic ablation of TAP also did not increase growth of a fibrosarcoma *in vivo*, and in fact inhibited its growth compared to controls suggesting that genetic deletion of TAP was not a effective strategy to 'de-immunize' genetically altered cells bearing foreign proteins.

FUTURE DIRECTIONS

TCRm mAbs change the paradigm for what targets are accessible to antibody-based biological agents. The data presented here provide demonstration that TCRm can be generated against the tumor-associated antigen PRAME, and have therapeutic utility in preclinical models. Indeed, TCRm have diverse potential in cancer therapy. However, there are also unique challenges that must be addressed before these agents move into clinical evaluations. Our on-going studies hope to address the challenges

and guide the direction of this developing technology.

A major hurdle in development of TCRm antibodies is antigen specificity. Whereas traditional anti-cancer mAbs typically recognize a three-dimensional conformational epitope allowing for precise specificity, TCRm are designed to recognize a composite epitope comprised of a small (8-10 residue) linear peptide sequence buried in a largely invariant MHC molecule found on all healthy cells. Some of these residues face in toward the binding pocket of MHC and thus do not directly form salt-bridges or other interactions with the TCRm. Furthermore, crystal structure analyses of TCRm have demonstrated that a substantial portion of binding energy may result from contacts with the MHC portion[148,212]. Therefore the variable and biochemically available epitope for TCRm to target is highly limited. Specificity and potential cross-reactivity of TCR-based agents is a major concern because a clinical trial using affinity-matured TCR-transduced T cells against the MAGE-A3 antigen let to rapid cardiac toxicities and death[213]. It was later discovered that the anti-MAGE-A3 TCR reacted with a peptide derived from the protein Titan highly expressed in cardiomyocytes[213]. Based on peptide sequence, the cross-reactivity could not be predicted with the available experimental or computational tools despite rigorous preclinical testing. Instead, we are developing a high-throughput pooled screen approach to identify possible cross-reactive targets experimentally. Using a vector constructed with a genetically barcoded peptide antigen, we have developed a system called "PresentER" that can encode MHC-I peptides. PresentER can be used in a pooled library screen where tens of thousands of peptides are transduced into cells and fluorescence activated cell sorting (FACS) using the TCRm and subsequence deep sequencing can identify the possible cross-reactive targets. The studies using PresentER to determine cross-reactive peptide/HLA-A2 targets of Pr20 are currently underway. Moreover, mass

spectrometry approaches to elute and identify MHC-bound peptides from cells have become increasingly sensitive. Such approaches are powerful because they can experimentally identify the MHC-I "peptidome" in contrast to methods that only computational predict cross-reactive peptide or even peptides that bind MHC-I. Our group is currently developing methods to immunoprecipitate bound ligands of Pr20 to determine what cross-reactive epitopes exist.

Another approach to limiting cross-reactive targets is through increased stringency when panning for TCRm clones during phage-display. Whereas Pr20 was developed using positive panning against the target ALY/HLA-A2 and negative panning against a completely irrelevant RHAMM-R3 peptide/HLA-A2, future approaches should investigate negative panning against a more biochemically similar peptide in the aims of increasing specificity. Additionally, Pr20 primarily bound the C-terminal half of the ALY peptide. Future strategies to select TCRm clones that bind with a larger 'foot-print' over the middle residues may increase specificity because the anchor residues at the peptide N- and C-termini are relatively conserved across MHC-I binding peptides and may therefore be less antigenically unique. Such strategies are currently being investigated.

In addition, it will be important to identify tumor-associated peptide/MHC antigens that are generated by both the constitutive and immunoproteasome because these represent ideal targets of TCRm and TCR-based agents. As demonstrated by the data presented here, specific peptides such as the $PRAME^{300-309}$ ALY peptide and the $WT1^{126-134}$ RMF peptide[62] are better generated by the immunoproteasome, and may be destroyed by the constitutive proteasome, ultimately limiting the cancers that would present ALY and be sensitive to Pr20. Targeting peptide/MHC antigens that are

generated by both major proteasome forms would broaden the tumor types that could be treated with such therapies and may also help prevent antigen escape relapse that down-regulate the proteasome components required to generate the peptide.

Lastly, it will be important to identify rational combination immunotherapies through enhancement of HLA-I. Increased antigen presentation may not only sensitize cancers to TCRm as shown here and in past work from our lab, but also potentiate other immunotherapy strategies such as TCR-transduced T cells, ImmTACs, and check-point blockade of CTLA-4, PD-1/PD-L1, and several others in current clinical investigation. We have yet to identify the pharmacologically important target of BW-B70c responsible for enhancement of HLA-I in the JMN mesothelioma cell line. We aim to approach this through the use of an analog compound of BW-B70c that is conjugated to a magnetic bead. The analog compound/magnetic bead can then be used to pull-down the putative target protein from cell lysates and be identified using mass spec. These exciting studies discussed have been initiated and will continue to elucidate unknown biochemical mechanisms of tumor-antigen presentation and refine the strategies used to develop TCRm antibodies, vaccines, and other TCR-based therapeutic agents and cells. These studies are meaningful and illuminate deep insights into cancer biology and immuno-oncology in our ultimate quest to understand, command, and conquer cancer.

REFERANCES

1. Weiner GJ. Building better monoclonal antibody-based therapeutics. *Nat Rev Cancer*. 2015;15(6):361-370. doi:10.1038/nrc3930
2. Lim SH, Levy R. Translational Medicine in Action: Anti-CD20 Therapy in Lymphoma. *J Immunol*. 2014;193(4):1519-1524. doi:10.4049/jimmunol.1490027
3. Carter PJ, Lazar GA. Next generation antibody drugs: pursuit of the "high-hanging fruit." *Nat Rev Drug Discov*. 2017;17(3):197-223. doi:10.1038/nrd.2017.227
4. Woof JM, Burton DR. Human antibody–Fc receptor interactions illuminated by crystal structures. *Nat Rev Immunol*. 2004;4(2):89-99. doi:10.1038/nri1266
5. Schrama D, Reisfeld R a, Becker JC. Antibody targeted drugs as cancer therapeutics. *Nat Rev Drug Discov*. 2006;5(2):147-159. doi:10.1038/nrd1957
6. Boller S, Li R, Grosschedl R. Defining B Cell Chromatin: Lessons from EBF1. *Trends Genet*. 2018:1-13. doi:10.1016/j.tig.2017.12.014
7. Mishra AK, Mariuzza RA. Insights into the Structural Basis of Antibody Affinity Maturation from Next-Generation Sequencing. *Front Immunol*. 2018;9(February):117. doi:10.3389/fimmu.2018.00117
8. Lipman NS, Jackson LR, Trudel LJ, Weis-Garcia F. Monoclonal Versus Polyclonal Antibodies: Distinguishing Characteristics, Applications, and Information Resources. *ILAR J*. 2005;46(3):258-268. doi:10.1093/ilar.46.3.258
9. Rossant CJ, Carroll D, Huang L, Elvin J, Neal F, Walker E, Benschop JJ, Kim EE, Barry ST, Vaughan TJ. Phage display and hybridoma generation of antibodies to human CXCR2 yields antibodies with distinct mechanisms and epitopes. *MAbs*. 2014;6(6):1425-1438. doi:10.4161/mabs.34376
10. Moran N. Mouse platforms jostle for slice of humanized antibody market. *Nat Biotechnol*. 2013;31(4):267-268. doi:10.1038/nbt0413-267
11. Jakobovits A, Amado RG, Yang X, Roskos L, Schwab G. From XenoMouse technology to panitumumab, the first fully human antibody product from transgenic mice. *Nat Biotechnol*. 2007;25(10):1134-1143. doi:10.1038/nbt1337
12. Bradbury ARM, Sidhu S, Dübel S, McCafferty J. Beyond natural antibodies: The power of in vitro display technologies. *Nat Biotechnol*. 2011;29(3):245-254. doi:10.1038/nbt.1791
13. Ahmad ZA, Yeap SK, Ali AM, Ho WY, Alitheen NBM, Hamid M. scFv antibody: principles and clinical application. *Clin Dev Immunol*. 2012;2012:980250. doi:10.1155/2012/980250
14. Hornig N, Färber-schwarz A. Antibody Engineering. Chames P, ed. 2012;907:713-727. doi:10.1007/978-1-61779-974-7
15. Zhang R, Shen W. *Antibody Engineering*.; 2012. doi:10.1007/978-1-61779-974-7
16. Agarwal A, Vieira CA, Benita K, Sidner RA, Fineberg NS, Pescovitz MD. Rituximab, Anti-CD20, Induces In Vivo Cytokine Release But Does Not Impair Ex Vivo T-Cell Responses. *Am J Transplant*. 2004;(1):1357-1360.

doi:10.1111/j.1600-6143.2004.00502.x
17. England TN. Use of chemotherapy plus a monoclonal antibody against Her2 for metastatic breast cancer that overexpresses Her2. *English J*. 2001;344(11):783-792. doi:10.1056/NEJM200103153441101
18. Gerratana L, Bonotto M, Bozza C, Ongaro E, Fanotto V, Pelizzari G, Puglisi F. Pertuzumab and breast cancer: another piece in the anti-HER2 puzzle. *Expert Opin Biol Ther*. 2017;17(3):365-374. doi:10.1080/14712598.2017.1282944
19. Falduto A, Cimino F, Speciale A, Musolino C, Gangemi S, Saija A, Allegra A. How gene polymorphisms can influence clinical response and toxicity following R-CHOP therapy in patients with diffuse large B cell lymphoma. *Blood Rev*. 2017;31(4):235-249. doi:10.1016/j.blre.2017.02.005
20. Vu T, Claret FX. Trastuzumab: Updated Mechanisms of Action and Resistance in Breast Cancer. *Front Oncol*. 2012;2(June):1-6. doi:10.3389/fonc.2012.00062
21. Weiner GJ. Rituximab: Mechanism of action. *Semin Hematol*. 2010;47(2):115-123. doi:10.1053/j.seminhematol.2010.01.011
22. Noguchi T, Kato T, Wang L, Maeda Y, Ikeda H, Sato E, Knuth A, Gnjatic S, Ritter G, Sakaguchi S, Old LJ, Shiku H, Nishikawa H. Intracellular tumor-associated antigens represent effective targets for passive immunotherapy. *Cancer Res*. 2012;72(7):1672-1682. doi:10.1158/0008-5472.CAN-11-3072
23. Muller S, Zhao Y, Brown TL, Morgan AC, Kohler H. TransMabs: cell-penetrating antibodies, the next generation. *Expert Opin Biol Ther*. 2005;5(2):237-241. doi:10.1517/14712598.5.2.237
24. Shin SM, Choi DK, Jung K, Bae J, Kim JS, Park SW, Song KH, Kim YS. Antibody targeting intracellular oncogenic Ras mutants exerts anti-tumour effects after systemic administration. *Nat Commun*. 2017;8(May):1-14. doi:10.1038/ncomms15090
25. Yewdell JW, Anton LC, Bennink JR. Defective ribosomal products (DRiPs): a major source of antigenic peptides for MHC class I molecules? *J Immunol*. 1996;157(5):1823-1826. doi:10.4049/jimmunol.0901907
26. Rock KL, Farfán-Arribas DJ, Colbert JD, Goldberg AL. Re-examining class-I presentation and the DRiP hypothesis. *Trends Immunol*. 2014;35(4):144-152. doi:10.1016/j.it.2014.01.002
27. Wieczorek M, Abualrous ET, Sticht J, Álvaro-Benito M, Stolzenberg S, Noé F, Freund C. Major histocompatibility complex (MHC) class I and MHC class II proteins: Conformational plasticity in antigen presentation. *Front Immunol*. 2017;8(MAR):1-16. doi:10.3389/fimmu.2017.00292
28. Lankat-Buttgereit B, Tampé R. The Transporter Associated With Antigen Processing: Function and Implications in Human Diseases. *Physiol Rev*. 2002;82(1):187-204. doi:10.1152/physrev.00025.2001
29. Grommé M, Uytdehaag FG, Janssen H, Calafat J, van Binnendijk RS, Kenter MJ, Tulp A, Verwoerd D, Neefjes J. Recycling MHC class I molecules and endosomal peptide loading. *Proc Natl Acad Sci U S A*. 1999;96(18):10326-10331. doi:10.1073/pnas.96.18.10326
30. Durgeau A, Virk Y, Corgnac S, Mami-Chouaib F. Recent Advances in Targeting CD8 T-Cell Immunity for More Effective Cancer Immunotherapy.

Front Immunol. 2018;9(January). doi:10.3389/fimmu.2018.00014
31. Morris GP, Allen PM. How the TCR balances sensitivity and specificity for the recognition of self and pathogens. *Nat Immunol*. 2012;13(2):121-128. doi:10.1038/ni.2190
32. Hanahan D, Weinberg RA. Hallmarks of cancer: The next generation. *Cell*. 2011;144(5):646-674. doi:10.1016/j.cell.2011.02.013
33. Ott PA, Hu Z, Keskin DB, Shukla SA, Sun J, Bozym DJ, Zhang W, Luoma A, Giobbie-Hurder A, Peter L, Chen C, Olive O, Carter TA, Li S, Lieb DJ, Eisenhaure T, Gjini E, Stevens J, Lane WJ, Javeri I, Nellaiappan K, Salazar AM, Daley H, Seaman M, Buchbinder EI, Yoon CH, Harden M, Lennon N, Gabriel S, Rodig SJ, Barouch DH, Aster JC, Getz G, Wucherpfennig K, Neuberg D, Ritz J, Lander ES, Fritsch EF, Hacohen N, Wu CJ. An immunogenic personal neoantigen vaccine for patients with melanoma. *Nature*. 2017;547(7662):217-221. doi:10.1038/nature22991
34. Cobbold M, De La Peña H, Norris A, Polefrone JM, Qian J, English AM, Cummings KL, Penny S, Turner JE, Cottine J, Abelin JG, Malaker SA, Zarling AL, Huang HW, Goodyear O, Freeman SD, Shabanowitz J, Pratt G, Craddock C, Williams ME, Hunt DF, Engelhard VH. MHC class I-associated phosphopeptides are the targets of memory-like immunity in leukemia. *Sci Transl Med*. 2013;5(203):1-11. doi:10.1126/scitranslmed.3006061
35. Apcher S, Daskalogianni C, Fåhraeus R. Pioneer translation products as an alternative source for MHC-I antigenic peptides. *Mol Immunol*. 2015;68(2):68-71. doi:10.1016/j.molimm.2015.04.019
36. Yewdell JW, David A. Nuclear translation for immunosurveillance. *Proc Natl Acad Sci*. 2013;110(44):17612-17613. doi:10.1073/pnas.1318259110
37. Vigneron N, Stroobant V, Chapiro J, Ooms A, Morel GDS, Bruggen P van der, Boon T, Eynde BJ Van den. An Antigenic Peptide Produced by Peptide Splicing in the Proteasome. *Science (80-)*. 2009;587(April). doi:10.1126/science.1095522
38. Abelin JG, Keskin DB, Sarkizova S, Hartigan CR, Zhang W, Sidney J, Stevens J, Lane W, Zhang GL, Eisenhaure TM, Clauser KR, Hacohen N, Rooney MS, Carr SA, Wu CJ. Mass Spectrometry Profiling of HLA-Associated Peptidomes in Mono-allelic Cells Enables More Accurate Epitope Prediction. *Immunity*. 2017;46(2):315-326. doi:10.1016/j.immuni.2017.02.007
39. Robinson J, Halliwell JA, Hayhurst JD, Flicek P, Parham P, Marsh SGE. The IPD and IMGT/HLA database: Allele variant databases. *Nucleic Acids Res*. 2015;43(D1):D423-D431. doi:10.1093/nar/gku1161
40. Trowsdale J, Knight JC. Major Histocompatibility Complex Genomics and Human Disease. *Annu Rev Genomics Hum Genet*. 2013;14(1):301-323. doi:10.1146/annurev-genom-091212-153455
41. Marsh SGE, Albert ED, Bodmer WF, Bontrop RE, Dupont B, Erlich HA, Geraghty DE, Hansen JA, Hurley CK, Mach B, Mayr WR, Parham P, Petersdorf EW, Sasazuki T, Schreuder GMT, Strominger JL, Svejgaard A, Terasaki PI, Trowsdale J. Nomenclature for factors of the HLA system, 2004. *Hum Immunol*. 2005;66(5):571-636. doi:10.1016/j.humimm.2005.02.002

42. Bassani-Sternberg M, Pletscher-Frankild S, Jensen LJ, Mann M. Mass spectrometry of human leukocyte antigen class I peptidomes reveals strong effects of protein abundance and turnover on antigen presentation. *Mol Cell Proteomics*. 2015;14(3):658-673. doi:10.1074/mcp.M114.042812
43. Dao T, Yan S, Veomett N, Pankov D, Zhou L, Korontsvit T, Scott A, Whitten J, Maslak P, Casey E, Tan T, Liu H, Zakhaleva V, Curcio M, Doubrovina E, O'Reilly RJ, Liu C, Scheinberg D a. Targeting the intracellular WT1 oncogene product with a therapeutic human antibody. *Sci Transl Med*. 2013;5(176):176ra33. doi:10.1126/scitranslmed.3005661
44. Gonzalez-Galarza FF, Christmas S, Middleton D, Jones AR. Allele frequency net: A database and online repository for immune gene frequencies in worldwide populations. *Nucleic Acids Res*. 2011;39(SUPPL. 1):913-919. doi:10.1093/nar/gkq1128
45. Straetemans T, Van Brakel M, Van Steenbergen S, Broertjes M, Drexhage J, Hegmans J, Lambrecht BN, Lamers C, Bruggen P Van Der, Coulie PG, Debets R. TCR gene transfer: MAGE-C2/HLA-A2 and MAGE-A3/HLA-DP4 epitopes as melanoma-specific immune targets. *Clin Dev Immunol*. 2012;2012. doi:10.1155/2012/586314
46. Hassan C, Chabrol E, Jahn L, Kester MGD, De Ru AH, Drijfhout JW, Rossjohn J, Falkenburg JHF, Heemskerk MHM, Gras S, Van Veelen PA. Naturally processed non-canonical HLA-A*02:01 presented peptides. *J Biol Chem*. 2015;290(5):2593-2603. doi:10.1074/jbc.M114.607028
47. Meydan C, Otu HH, Sezerman OU. Prediction of peptides binding to MHC class I and II alleles by temporal motif mining. *BMC Bioinformatics*. 2013;14(Suppl 2). doi:10.1186/1471-2105-14-S2-S13
48. Dunbar J, Knapp B, Fuchs A, Shi J, Deane CM. Examining variable domain orientations in antigen receptors gives insight into TCR-like antibody design. *PLoS Comput Biol*. 2014;10(9):e1003852. doi:10.1371/journal.pcbi.1003852
49. Singh NK, Riley TP, Baker SCB, Borrman T, Weng Z, Baker BM. Emerging Concepts in TCR Specificity: Rationalizing and (Maybe) Predicting Outcomes. *J Immunol*. 2017;199(7):2203-2213. doi:10.4049/jimmunol.1700744
50. Chang AY, Gejman RS, Brea EJ, Oh CY, Mathias MD, Pankov D, Casey E, Dao T, Scheinberg DA. Opportunities and challenges for TCR mimic antibodies in cancer therapy. *Expert Opin Biol Ther*. 2016;2598(May):1-9. doi:10.1080/14712598.2016.1176138
51. Maslak PG, Dao T, Bernal Y, Chanel SM, Zhang R, Frattini M, Rosenblat T, Jurcic JG, Brentjens RJ, Arcila ME, Rampal R, Park JH, Douer D, Katz L, Sarlis N, Tallman MS, Scheinberg DA. Phase 2 trial of a multivalent WT1 peptide vaccine (galinpepimut-S) in acute myeloid leukemia. *Blood Adv*. 2018;2(3):224-234. doi:10.1182/bloodadvances.2017014175
52. Chang AY, Gejman RS, Brea EJ, Oh CY, Mathias MD, Pankov D, Casey E, Dao T, Scheinberg DA. Opportunities and challenges for TCR mimic antibodies in cancer therapy. *Expert Opin Biol Ther*. 2016:1-9. doi:10.1080/14712598.2016.1176138
53. Stärck L, Popp K, Pircher H, Popp K, Pircher H, Uckert W. Immunotherapy

with TCR-Redirected T Cells: Comparison of TCR-Transduced and TCR-Engineered Hematopoietic Stem Cell − Derived T Cells. *J Immunol*. 2014;192(1). doi:10.4049/jimmunol.1202591

54. Yewdell JW. The seven dirty little secrets of major histocompatibility complex class I antigen processing. *Immunol Rev*. 2005;207:8-18. doi:10.1111/j.0105-2896.2005.00309.x
55. Geng F, Wenzel S, Tansey WP. Ubiquitin and proteasomes in transcription. *Annu Rev Biochem*. 2012;81:177-201. doi:10.1146/annurev-biochem-052110-120012
56. Ferrington D a, Gregerson DS. *Immunoproteasomes: Structure, Function, and Antigen Presentation.* Vol 109.; 2012. doi:10.1016/B978-0-12-397863-9.00003-1
57. Huber EM, Basler M, Schwab R, Heinemeyer W, Kirk CJ, Groettrup M, Groll M. Immuno- and constitutive proteasome crystal structures reveal differences in substrate and inhibitor specificity. *Cell*. 2012;148(4):727-738. doi:10.1016/j.cell.2011.12.030
58. Kincaid EZ, Che JW, York I, Escobar H, Reyes-vargas E, Delgado JC, Welsh RM, Karow ML, Murphy AJ, Valenzuela DM, Yancopoulos GD, Rock KL. Mice completely lacking immunoproteasomes show major changes in antigen presentation. *Nat Immunol*. 2012;13(2):129-135. doi:10.1038/ni.2203
59. Muchamuel T, Basler M, Aujay M a, Suzuki E, Kalim KW, Lauer C, Sylvain C, Ring ER, Shields J, Jiang J, Shwonek P, Parlati F, Demo SD, Bennett MK, Kirk CJ, Groettrup M. A selective inhibitor of the immunoproteasome subunit LMP7 blocks cytokine production and attenuates progression of experimental arthritis. *Nat Med*. 2009;15(7):781-787. doi:10.1038/nm.1978
60. Hallermalm K, Seki K, Wei C, Castelli C, Rivoltini L, Kiessling R, Levitskaya J. Tumor necrosis factor-α induces coordinated changes in major histocompatibility class I presentation pathway, resulting in increased stability of class I complexes at the cell surface. *Blood*. 2001;98(4):1108-1115. doi:10.1182/blood.V98.4.1108
61. Guillaume B, Stroobant V, Bousquet-Dubouch M-P, Colau D, Chapiro J, Parmentier N, Dalet A, Van den Eynde BJ. Analysis of the processing of seven human tumor antigens by intermediate proteasomes. *J Immunol*. 2012;189(7):3538-3547. doi:10.4049/jimmunol.1103213
62. Jaigirdar A, Rosenberg SA, Parkhurst M. A high-avidity WT1-reactive T-cell receptor mediates recognition of peptide and processed antigen but not naturally occurring WT1-positive tumor cells. *J Immunother*. 2016;39(3):105-116. doi:10.1097/CJI.0000000000000116
63. Ma W, Vigneron N, Chapiro J, Stroobant V, Germeau C, Boon T, Coulie PG, Van Den Eynde BJ. A MAGE-C2 antigenic peptide processed by the immunoproteasome is recognized by cytolytic T cells isolated from a melanoma patient after successful immunotherapy. *Int J Cancer*. 2011;129(10):2427-2434. doi:10.1002/ijc.25911
64. Murata S, Yashiroda H, Tanaka K. Molecular mechanisms of proteasome assembly. *Nat Rev Mol Cell Biol*. 2009;10(2):104-115. doi:10.1038/nrm2630

65. Sasaki K, Takada K, Ohte Y, Kondo H, Sorimachi H, Tanaka K, Takahama Y, Murata S. Thymoproteasomes produce unique peptide motifs for positive selection of $CD8^+$ T cells. *Nat Commun*. 2015;6(May):1-10. doi:10.1038/ncomms8484
66. Takada K, Van Laethem F, Xing Y, Akane K, Suzuki H, Murata S, Tanaka K, Jameson SC, Singer A, Takahama Y. TCR affinity for thymoproteasome-dependent positively selecting peptides conditions antigen responsiveness in CD8+ T cells. *Nat Immunol*. 2015;16(10):1069-1076. doi:10.1038/ni.3237
67. Wadelin F, Fulton J, McEwan P a, Spriggs K a, Emsley J, Heery DM. Leucine-rich repeat protein PRAME: expression, potential functions and clinical implications for leukaemia. *Mol Cancer*. 2010;9:226. doi:10.1186/1476-4598-9-226
68. Ikeda H, Lethe B, Lehmann F, van Baren N, Baurain J, de Smet C, Chambost H, Vitale M, Moretta a, Boon T, Coulie P. Characterization of an antigen that is recognized on a melanoma showing partial HLA loss by CTL expressing an NK inhibitory receptor. *Immunity*. 1997;6(2):199-208. doi:10.1016/S1074-7613(00)80426-4
69. Ikeda H, Lethé B, Lehmann F, Van Baren N, Baurain JF, De Smet C, Chambost H, Vitale M, Moretta A, Boon T, Coulie PG. Characterization of an antigen that is recognized on a melanoma showing partial HLA loss by CTL expressing an NK inhibitory receptor. *Immunity*. 1997;6(2):199-208. doi:10.1016/S1074-7613(00)80426-4
70. Epping MT, Bernards R. A causal role for the human tumor antigen preferentially expressed antigen of melanoma in cancer. *Cancer Res*. 2006;66(22):10639-10642. doi:10.1158/0008-5472.CAN-06-2522
71. Oberthuer A, Hero B, Spitz R, Berthold F, Fischer M. The Tumor-Associated Antigen PRAME Is Universally Expressed in High-Stage Neuroblastoma and Associated with Poor Outcome The Tumor-Associated Antigen PRAME Is Universally Expressed in High-Stage Neuroblastoma and Associated with Poor Outcome. *Clin Cancer Res*. 2004;10:4307-4313.
72. Greiner J, Ringhoffer M, Taniguchi M, Li L, Schmitt A, Shiku H, Döhner H, Schmitt M. mRNA expression of leukemia-associated antigens in patients with acute myeloid leukemia for the development of specific immunotherapies. *Int J Cancer*. 2004;108(5):704-711. doi:10.1002/ijc.11623
73. Ding K, Wang X-M, Fu R, Ruan E-B, Liu H, Shao Z-H. PRAME Gene Expression in Acute Leukemia and Its Clinical Significance. *Cancer Biol Med*. 2012;9(1):73-76. doi:10.3969/j.issn.2095-3941.2012.01.013
74. Radich JP, Dai H, Mao M, Oehler V, Schelter J, Druker B, Sawyers C, Shah N, Stock W, Willman CL, Friend S, Linsley PS. Gene expression changes associated with progression and response in chronic myeloid leukemia. *Proc Natl Acad Sci U S A*. 2006;103(8):2794-2799. doi:10.1073/pnas.0510423103
75. Doolan P, Clynes M, Kennedy S, Mehta JP, Crown J, O'Driscoll L. Prevalence and prognostic and predictive relevance of PRAME in breast cancer. *Breast Cancer Res Treat*. 2008;109(2):359-365. doi:10.1007/s10549-007-9643-3
76. Gerber JM, Qin L, Kowalski J, Ph D, Smith BD, Griffin C a, Vala MS,

Collector MI, Zahurak M, Matsui W, Gocke CD, Sharkis SJ, Levitsky HI, Jones RJ. Characterization of Chronic Myeloid Leukemia stem cells. *Am J Hematol*. 2011;86(1):31-37. doi:10.1002/ajh.21915.Characterization

77. Epping MT, Wang L, Edel MJ, Carlée L, Hernandez M, Bernards R. The Human Tumor Antigen PRAME Is a Dominant Repressor of Retinoic Acid Receptor Signaling. *Cell*. 2005;122(6):835-847. doi:10.1016/j.cell.2005.07.003
78. Tajeddine N, Gala J-L, Louis M, Van Schoor M, Tombal B, Gailly P. Tumor-Associated Antigen Preferentially Expressed Antigen of Melanoma (PRAME) Induces Caspase-Independent Cell Death In vitro and Reduces Tumorigenicity In vivo. *Cancer Res*. 2005;65(16):7348-7355. doi:10.1158/0008-5472.CAN-04-4011
79. Wadelin FR, Fulton J, Collins HM, Tertipis N, Bottley A, Spriggs KA, Falcone FH, Heery DM. PRAME Is a Golgi-Targeted Protein That Associates with the Elongin BC Complex and Is Upregulated by Interferon-Gamma and Bacterial PAMPs. *PLoS One*. 2013;8(2). doi:10.1371/journal.pone.0058052
80. Rezvani K, Yong ASM, Tawab A, Jafarpour B, Eniafe R, Mielke S, Savani BN, Keyvanfar K, Li Y, Kurlander R, Barrett a J. Ex vivo characterization of polyclonal memory CD8+ T-cell responses to PRAME-specific peptides in patients with acute lymphoblastic leukemia and acute and chronic myeloid leukemia. *Blood*. 2009;113(10):2245-2255. doi:10.1182/blood-2008-03-144071
81. Weber G, Caruana I, Rouce RH, Barrett AJ, Gerdemann U. Generation of Tumor Antigen-Specific T Cell Lines from Pediatric Patients with Acute Lymphoblastic Leukemia — Implications for Immunotherapy. *Clin Cancer Res*. 2013;19(18):5079-5091. doi:10.1158/1078-0432.CCR-13-0955
82. Quintarelli C, Dotti G, De Angelis B, Hoyos V, Mims M, Luciano L, Heslop HE, Rooney CM, Pane F, Savoldo B. Cytotoxic T lymphocytes directed to the preferentially expressed antigen of melanoma (PRAME) target chronic myeloid leukemia. *Blood*. 2008;112(5):1876-1885. doi:10.1182/blood-2008-04-150045
83. Griffioen M, Kessler JH, Borghi M, Van Soest R a., Van Der Minne CE, Nouta J, Van Der Burg SH, Medema JP, Schrier PI, Frederik Falkenburg JH, Osanto S, Melief CJM. Detection and functional analysis of CD8+ T cells specific for PRAME: A target for T-cell therapy. *Clin Cancer Res*. 2006;12(10):3130-3136. doi:10.1158/1078-0432.CCR-05-2578
84. Kessler JH, Beekman NJ, Bres-Vloemans S a, Verdijk P, van Veelen P a, Kloosterman-Joosten a M, Vissers DC, ten Bosch GJ, Kester MG, Sijts a, Wouter Drijfhout J, Ossendorp F, Offringa R, Melief CJ. Efficient identification of novel HLA-A(*)0201-presented cytotoxic T lymphocyte epitopes in the widely expressed tumor antigen PRAME by proteasome-mediated digestion analysis. *J Exp Med*. 2001;193(1):73-88. doi:10.1084/jem.193.1.73
85. Weber JS, Vogelzang NJ, Ernstoff MS, Goodman OB, Cranmer LD, Marshall JL, Miles S, Rosario D, Diamond DC, Qiu Z, Obrocea M, Bot A. A phase 1 study of a vaccine targeting preferentially expressed antigen in melanoma and prostate-specific membrane antigen in patients with advanced solid tumors. *J Immunother*. 2011;34(7):556-567. doi:10.1097/CJI.0b013e3182280db1
86. Gutzmer R, Rivoltini L, Levchenko E, Testori A, Utikal J, Ascierto PA,

Demidov L, Grob JJ, Ridolfi R, Schadendorf D, Queirolo P, Santoro A, Loquai C, Dreno B, Hauschild A, Schultz E, Lesimple TP, Vanhoutte N, Salaun B, Gillet M, Jarnjak S, De Sousa Alves PM, Louahed J, Brichard VG, Lehmann FF. Safety and immunogenicity of the PRAME cancer immunotherapeutic in metastatic melanoma: results of a phase I dose escalation study. *ESMO Open*. 2016;1(4).

87. Sakamoto S, Noguchi M, Yamada A, Itoh K. Prospect and progress of personalized peptide vaccinations for advanced cancers. *Expert Opin Biol Ther*. 2016;16(5):689-698. doi:10.1517/14712598.2016.1161752
88. Liu X, Pu Y, Cron K, Deng L, Kline J, Frazier WA, Xu H, Peng H, Fu YX, Xu MM. CD47 blockade triggers T cell-mediated destruction of immunogenic tumors. *Nat Med*. 2015;21(10):1209-1215. doi:10.1038/nm.3931
89. Dao T, Pankov D, Scott A, Korontsvit T, Zakhaleva V, Xu Y, Xiang J, Yan S, Direito M, Guerreiro DM, Veomett N, Dubrovsky L, Curcio M, Doubrovina E, Ponomarev V, Liu C, Reilly RJO, Scheinberg DA. Therapeutic bispecific T-cell engager antibody targeting the intracellular oncoprotein WT1. *Nat Biotechnol*. 2015;(September):1-10. doi:10.1038/nbt.3349
90. Baeuerle P a, Reinhardt C. Bispecific T-cell engaging antibodies for cancer therapy. *Cancer Res*. 2009;69(12):4941-4944. doi:10.1158/0008-5472.CAN-09-0547
91. Rafiq S, Purdon TJ, Daniyan AF, Koneru M, Dao T, Liu C, Scheinberg DA, Brentjens RJ. Optimized T-cell receptor-mimic (TCRm) chimeric antigen receptor T-cells directed towards the intracellular Wilms Tumor 1 antigen. *Leukemia*. 2016;(December 2016):1-10. doi:10.1038/
92. He W, Wang W, Zhao Y, Liu C, Sun M, Gao B. Anti-melanoma activity of T cells redirected with a TCR-like chimeric antigen receptor. *Sci Rep*. 2014:2-9. doi:10.1038/srep03571
93. Persic L, Roberts A, Wilton J, Cattaneo A, Bradbury A, Hoogenboom HR. An integrated vector system for the eukaryotic expression of antibodies or their fragments after selection from phage display libraries. *Gene*. 1997;187:9-18.
94. Caron BPC, Laird W, Co MS, Avdalovic NM, Queen C, Scheinberg DA. Engineered Humanized Dimeric Forms of IgG Are More Effective Antibodies. *J Exp Med*. 1992;176:1191-1195.
95. Liu C, Xiang J, Yan S, Wang P, Tai C. Modified Host Cells and Uses Thereof. 2010.
96. Sanjana NE, Shalem O, Zhang F. Improved vectors and genome-wide libraries for CRISPR screening. *Nat Methods*. 2014;11(8):783-784. doi:10.1038/nmeth.3047
97. Sergeeva A, Alatrash G, He H, Ruisaard K, Lu S, Wygant J, Bradley W, Ma Q, Li D, John LS, Clise-dwyer K, Molldrem JJ, Mcintyre BW. An anti – PR1 / HLA-A2 T-cell receptor – like antibody mediates complement-dependent cytotoxicity against acute myeloid leukemia progenitor cells. *Blood*. 2011;117(16):4262-4272. doi:10.1182/blood-2010-07-299248
98. Shinkawa T, Nakamura K, Yamane N, Shoji-hosaka E, Kanda Y, Sakurada M, Uchida K, Anazawa H, Satoh M, Yamasaki M, Hanai N. The Absence of

Fucose but Not the Presence of Galactose or Bisecting N -Acetylglucosamine of Human IgG1 Complex-type Oligosaccharides Shows the Critical Role of Enhancing Antibody-dependent Cellular Cytotoxicity * those produced by Chinese hamster ovary (. *J Biol Chem*. 2003;278(5):3466-3473. doi:10.1074/jbc.M210665200

99. Veomett N, Dao T, Liu H, Xiang J, Pankov D, Dubrovsky L, Whitten JA, Park S-M, Korontsvit T, Zakhaleva V, Casey E, Curcio M, Kharas MG, O'Reilly RJ, Liu C, Scheinberg DA. Therapeutic Efficacy of an Fc-Enhanced TCR-like Antibody to the Intracellular WT1 Oncoprotein. *Clin Cancer Res*. 2014;20(15):4036-4046. doi:10.1158/1078-0432.CCR-13-2756
100. Umaña P, Jean-mairet J, Moudry R, Amstutz H, Bailey JE. Engineered glycoforms of an antineuro- blastoma IgG1 with optimized antibody- dependent cellular cytotoxic activity. *Nat Biotechnol*. 1999;17(February).
101. Chan AC, Carter PJ. Therapeutic antibodies for autoimmunity and inflammation. *Nat Publ Gr*. 2010;10(5):301-316. doi:10.1038/nri2761
102. Verma B, Jain R, Caseltine S, Rennels A, Bhattacharya R, Markiewski MM, Rawat A, Neethling F, Bickel U, Weidanz JA. TCR Mimic Monoclonal Antibodies Induce Apoptosis of Tumor Cells via Immune Effector-Independent Mechanisms. *J Immunol*. 2011;186(5):3265-3276. doi:10.4049/jimmunol.1002376
103. Carreno BM, Garbow JR, Kolar GR, Jackson EN, Engelbach JA, Becker-hapak M, Carayannopoulos LN, Piwnica-worms D, Linette GP. Immunodeficient Mouse Strains Display Marked Variability in Growth of Human Melanoma Lung Metastases. *Clin Cancer Res*. 2009;15(10):3277-3286. doi:10.1158/1078-0432.CCR-08-2502
104. Dubrovsky L, Brea EJ, Pankov D, Casey E, Dao T, Liu C, Scheinberg DA. Mechanisms of leukemia resistance to antibody dependent cellular cytotoxicity. *Oncoimmunology*. 2016;5(9):e1211221. doi:10.1080/2162402X.2016.1211221
105. Lü S, Wang J. The resistance mechanisms of proteasome inhibitor bortezomib. *Biomark Res*. 2013;1(1):13. doi:10.1186/2050-7771-1-13
106. Oates J, Hassan NJ, Jakobsen BK. ImmTACs for targeted cancer therapy : Why , what , how , and which. *Mol Immunol*. 2015;67(2):67-74. doi:10.1016/j.molimm.2015.01.024
107. Kessler JH, Khan S, Seifert U, Gall S Le, Chow KM, Paschen A, Bres-vloemans SA, Ru A De, Montfoort N Van, Franken KLMC, Benckhuijsen WE, Brooks JM, Hall T Van, Ray K, Mulder A, Doxiadis IIN, Swieten PF Van, Overkleeft HS, Prat A, Tomkinson B, Neefjes J, Kloetzel PM, Rodgers DW, Hersh LB, Drijfhout JW. Antigen processing by nardilysin and thimet oligopeptidase generates cytotoxic T cell epitopes. *Nat Immunol*. 2010;12(1):45-53. doi:10.1038/ni.1974
108. Lee DW, Gardner R, Porter DL, Louis CU, Ahmed N, Jensen M, Grupp SA, Mackall CL. Current concepts in the diagnosis and management of cytokine release syndrome. *Blood*. 2014;124(2):188-196. doi:10.1182/blood-2014-05-552729.current
109. Toes REM, Nussbaum AK, Degermann S, Schirle M, Emmerich NPN, Kraft

M, Laplace C, Zwinderman A, Dick TP, Müller J, Schönfisch B, Schmid C, Fehling H, Stevanovic S, Rammensee HG, Schild H. Discrete Cleavage Motifs of Constitutive and Immunoproteasomes Revealed by Quantitative Analysis of Cleavage Products. *JEM*. 2001;194(1).

110. Brea EJ, Oh CY, Manchado E, Budhu S, Gejman RS, Mo G, Mondello P, Han JE, Jarvis CA, Ulmert D, Xiang Q, Chang AY, Garippa RJ, Merghoub T, Wolchok JD, Rosen N, Lowe SW, Scheinberg DA. Kinase Regulation of Human MHC Class I Molecule Expression on Cancer Cells. *Cancer Immunol Res*. 2016:1-12. doi:10.1158/2326-6066.CIR-16-0177
111. Schrump DS, Fischette MR, Nguyen DM, Zhao M, Li X, Kunst TF, Hancox A, Hong JA, Chen GA, Pishchik V, Figg WD, Murgo AJ, Steinberg SM. Phase I Study of Decitabine-Mediated Gene Expression in Patients with Cancers Involving the Lungs , Esophagus , or Pleura. *Clin Cancer Res*. 2006;12(19):5777-5785. doi:10.1158/1078-0432.CCR-06-0669
112. Gang AO, Frøsig TM, Brimnes MK, Lyngaa R, Treppendahl MB, Grønbæk K, Dufva IH, Straten P, Hadrup SR. 5-Azacytidine treatment sensitizes tumor cells to T-cell mediated cytotoxicity and modulates NK cells in patients with myeloid malignancies. *Blood Cancer J*. 2014;4(e197). doi:10.1038/bcj.2014.14
113. Yan M, Himoudi N, Basu BP, Wallace R, Poon E, Adams S, Hasan F, Xue S-A, Wilson N, Dalgleish A, Williams O, Anderson J. Increased PRAME antigen-specific killing of malignant cell lines by low avidity CTL clones, following treatment with 5-Aza-2′-Deoxycytidine. *Cancer Immunol Immunother*. 2011;60(9):1243-1255. doi:10.1007/s00262-011-1024-4
114. Cao Q, Wang X, Jia L, Mondal AK, Diallo A, Hawkins GA, Das SK, Parks JS, Yu L, Shi H, Shi H, Xue B. Inhibiting DNA methylation by 5-Aza-2'-deoxycytidine ameliorates atherosclerosis through suppressing macrophage inflammation. *Endocrinology*. 2014;155(12):4925-4938. doi:10.1210/en.2014-1595
115. Cohen M, Reiter Y. T-Cell Receptor-Like Antibodies: Targeting the Intracellular Proteome Therapeutic Potential and Clinical Applications. *Antibodies*. 2013;2(3):517-534. doi:10.3390/antib2030517
116. Dubrovsky L, Dao T, Gejman R, Brea E, Chang A, Oh C, Casey E, Pankov D, Scheinberg DA. T cell receptor mimic antibodies for cancer therapy. *Oncoimmunology*. 2015;(October):00-00. doi:10.1080/2162402X.2015.1049803
117. Dubrovsky L, Pankov D, Brea EJ, Dao T, Scott A, Yan S, Reilly RJO, Liu C, Scheinberg DA. A TCR-mimic antibody to WT1 bypasses tyrosine kinase inhibitor resistance in human BCR-ABL 1 leukemias. *Blood*. 2014;123(21):3296-3305. doi:10.1182/blood-2014-01-549022.Presented
118. Huehls AM, Coupet TA, Sentman CL. Bispecific T-cell engagers for cancer immunotherapy. *Immunol Cell Biol*. 2014;93(3):290-296. doi:10.1038/icb.2014.93
119. McDevitt MR, Ma D, Lai LT, Simon J, Borchardt P, Frank RK, Wu K, Pellegrini V, Curcio MJ, Miederer M, Bander NH, Scheinberg DA. Tumor therapy with targeted atomic nanogenerators. *Science*. 2001;294(2001):1537-

1540. doi:10.1126/science.1064126
120. Oldenborg PA. Role of CD47 and signal regulatory protein alpha (SIRPα) in regulating the clearance of viable or aged blood cells. *Transfus Med Hemotherapy*. 2012;39(5):315-320. doi:10.1159/000342537
121. Weiskopf K. Cancer immunotherapy targeting the CD47/SIRPα axis. *Eur J Cancer*. 2017;76:100-109. doi:10.1016/j.ejca.2017.02.013
122. Chao MP, Alizadeh AA, Tang C, Myklebust JH, Varghese B, Gill S, Jan M, Cha AC, Chan CK, Tan BT, Park CY, Zhao F, Kohrt HE, Malumbres R, Briones J, Gascoyne RD, Lossos IS, Levy R, Weissman IL, Majeti R. Anti-CD47 Antibody Synergizes with Rituximab to Promote Phagocytosis and Eradicate Non-Hodgkin Lymphoma. *Cell*. 2010;142(5):699-713. doi:10.1016/j.cell.2010.07.044
123. Huang Y, Ma Y, Gao P, Yao Z. Targeting CD47: The achievements and concerns of current studies on cancer immunotherapy. *J Thorac Dis*. 2017;9(2):E168-E174. doi:10.21037/jtd.2017.02.30
124. Weiskopf K, Ring AM, Ho CCM, Volkmer J, Rijn M Van De, Weissman IL, Garcia KC. Engineered SIRPa Variants as Immunotherapeutic Adjuvants to Anticancer Antibodies. 2014;88(2013). doi:10.1126/science.1238856
125. Weiskopf K, Ring AM, Ho CCM, Volkmer J, Rijn M Van De, Weissman IL, Garcia KC. Engineered SIRPα Variants as Immunotherapeutic Adjuvants to Anticancer Antibodies. *Science (80-)*. 2013;341(6141):88-91. doi:10.1126/science.1238856
126. Kaur S, Soto-Pantoja DR, Stein E V., Liu C, Elkahloun AG, Pendrak ML, Nicolae A, Singh SP, Nie Z, Levens D, Isenberg JS, Roberts DD. Thrombospondin-1 signaling through CD47 inhibits self-renewal by regulating c-Myc and other stem cell transcription factors. *Sci Rep*. 2013;3:1-12. doi:10.1038/srep01673
127. Liu Y, Bühring HJ, Zen K, Burst SL, Schnell FJ, Williams IR, Parkos CA. Signal regulatory protein (SIRPa), a cellular ligand for CD47, regulates neutrophil transmigration. *J Biol Chem*. 2002;277(12):10028-10036. doi:10.1074/jbc.M109720200
128. Spiess C, Zhai Q, Carter PJ. Alternative molecular formats and therapeutic applications for bispecific antibodies. *Mol Immunol*. 2015;67(2):95-106. doi:10.1016/j.molimm.2015.01.003
129. Khan FH. Antibodies and Their Applications. *Anim Biotechnol Model Discov Transl*. 2013:473-490. doi:10.1016/B978-0-12-416002-6.00025-0
130. Strop P, Ho W-H, Boustany LM, Abdiche YN, Lindquist KC, Farias SE, Rickert M, Appah CT, Pascua E, Radcliffe T, Sutton J, Chaparro-Riggers J, Chen W, Casas MG, Chin SM, Wong OK, Liu S-H, Vergara G, Shelton D, Rajpal A, Pons J. Generating bispecific human IgG1 and IgG2 antibodies from any antibody pair. *J Mol Biol*. 2012;420(3):204-219. doi:10.1016/j.jmb.2012.04.020
131. Han L, Chen J, DIng K, Zong H, Xie Y, Jiang H, Zhang B, Lu H, Yin W, Gilly J, Zhu J. Efficient generation of bispecific IgG antibodies by split intein mediated protein trans-splicing system. *Sci Rep*. 2017;7(1):1-11.

doi:10.1038/s41598-017-08641-3
132. Kantarjian H, Stein A, Gökbuget N, Fielding AK, Schuh AC, Ribera J-M, Wei A, Dombret H, Foà R, Bassan R, Arslan Ö, Sanz MA, Bergeron J, Demirkan F, Lech-Maranda E, Rambaldi A, Thomas X, Horst H-A, Brüggemann M, Klapper W, Wood BL, Fleishman A, Nagorsen D, Holland C, Zimmerman Z, Topp MS. Blinatumomab versus Chemotherapy for Advanced Acute Lymphoblastic Leukemia. *N Engl J Med*. 2017;376(9):836-847. doi:10.1056/NEJMoa1609783
133. Yuraszeck T, Kasichayanula S, Benjamin JE. Translation and Clinical Development of Bispecific T-cell Engaging Antibodies for Cancer Treatment. *Clin Pharmacol Ther*. 2017;101(5):634-645. doi:10.1002/cpt.651
134. Dreier T, Baeuerle PA, Fichtner I, Grun M, Schlereth B, Lorenczewski G, Kufer P, Lutterbuse R, Riethmuller G, Gjorstrup P, Bargou RC. T Cell Costimulus-Independent and Very Efficacious Inhibition of Tumor Growth in Mice Bearing Subcutaneous or Leukemic Human B Cell Lymphoma Xenografts by a CD19-/CD3- Bispecific Single-Chain Antibody Construct. *J Immunol*. 2003;170(8):4397-4402. doi:10.4049/jimmunol.170.8.4397
135. Gleason MK, Ross J a, Warlick ED, Lund TC, Verneris MR, Wiernik A, Spellman S, Haagenson MD, Lenvik AJ, Litzow MR, Epling-Burnette PK, Blazar BR, Weiner LM, Weisdorf DJ, Vallera D a, Miller JS. CD16xCD33 bispecific killer cell engager (BiKE) activates NK cells against primary MDS and MDSC CD33+ targets. *Blood*. 2014;123(19):3016-3026. doi:10.1182/blood-2013-10-533398
136. Felices M, Sarhan D, Brandt L, Guldevall K, McElmurry R, Lenvik A, Chu S, Tolar J, Taras E, Spellman SR, Warlick ED, Verneris MR, Cooley S, Weisdorf D, Blazar BR, Onfelt B, Vallera D, Miller JS. CD16-IL15-CD33 Trispecific Killer Engager (TriKE) Overcomes Cancer-Induced Immune Suppression and Induces Natural Killer Cell-Mediated Control of MDS and AML Via Enhanced Killing Kinetics. *Blood*. 2016;128(22):4291 LP-4291. http://www.bloodjournal.org/content/128/22/4291.abstract.
137. Vallera DA, Felices M, McElmurry R, McCullar V, Zhou X, Schmohl JU, Zhang B, Lenvik AJ, Panoskaltsis-Mortari A, Verneris MR, Tolar J, Cooley S, Weisdorf DJ, Blazar BR, Miller JS. IL15 Trispecific Killer Engagers (TriKE) Make Natural Killer Cells Specific to CD33+Targets while Also Inducing Persistence, in Vivo Expansion, and Enhanced Function. *Clin Cancer Res*. 2016;22(14):3440-3450. doi:10.1158/1078-0432.CCR-15-2710
138. Brentjens RJ, Davila ML, Riviere I, Park J, Wang X, Cowell LG, Bartido S, Stefanski J, Taylor C, Olszewska M, Borquez-Ojeda O, Qu J, Wasielewska T, He Q, Bernal Y, Rijo I V., Hedvat C, Kobos R, Curran K, Steinherz P, Jurcic J, Rosenblat T, Maslak P, Frattini M, Sadelain M. CD19-Targeted T Cells Rapidly Induce Molecular Remissions in Adults with Chemotherapy-Refractory Acute Lymphoblastic Leukemia. *Sci Transl Med*. 2013;5(177):177ra38-177ra38. doi:10.1126/scitranslmed.3005930
139. Jackson HJ, Rafiq S, Brentjens RJ. Driving CAR T-cells forward. *Nat Rev Clin Oncol*. 2016;13(6):370-383. doi:10.1038/nrclinonc.2016.36
140. Mueller KT, Maude SL, Porter DL, Frey N, Wood P, Han X, Waldron E,

Chakraborty A, Awasthi R, Levine BL, Melenhorst JJ, Grupp SA, June CH, Lacey SF. Cellular kinetics of CTL019 in relapsed/refractory B-cell acute lymphoblastic leukemia and chronic lymphocytic leukemia. *Blood*. 2017;130(21):2317-2325. doi:10.1182/blood-2017-06-786129

141. Ajina A, Maher J. Prospects for combined use of oncolytic viruses and CAR T-cells. *J Immunother Cancer*. 2017;5(1):1-27. doi:10.1186/s40425-017-0294-6
142. Gross G, Waks T, Eshhar Z. Expression of immunoglobulin-T-cell receptor chimeric molecules as functional receptors with antibody-type specificity. *Proc Natl Acad Sci*. 1989;86(24):10024-10028. doi:10.1073/pnas.86.24.10024
143. Jensen MC, Popplewell L, Cooper LJ, DiGiusto D, Kalos M, Ostberg JR, Forman SJ. Antitransgene rejection responses contribute to attenuated persistence of adoptively transferred CD20/CD19-specific chimeric antigen receptor redirected T cells in humans. *Biol Blood Marrow Transplant*. 2010;16(9):1245-1256. doi:10.1016/j.bbmt.2010.03.014
144. Lamers CHJ, Sleijfer S, Vulto AG, Kruit WHJ, Kliffen M, Debets R, Gratama JW, Stoter G, Oosterwijk E. Treatment of metastatic renal cell carcinoma with autologous T-lymphocytes genetically retargeted against carbonic anhydrase IX: first clinical experience. *J Clin Oncol*. 2006;24(13). doi:10.1200/JCO.2006.05.9964
145. Yeku OO, Brentjens RJ. Armored CAR T-cells: utilizing cytokines and pro-inflammatory ligands to enhance CAR T-cell anti-tumour efficacy. *Biochem Soc Trans*. 2016;44(2):412-418. doi:10.1042/BST20150291
146. Yeku OO, Purdon TJ, Koneru M, Spriggs D, Brentjens RJ. Armored CAR T cells enhance antitumor efficacy and overcome the tumor microenvironment. *Sci Rep*. 2017;7(1):1-14. doi:10.1038/s41598-017-10940-8
147. Lim WA, June CH. The Principles of Engineering Immune Cells to Treat Cancer. *Cell*. 2017;168(4):724-740. doi:10.1016/j.cell.2017.01.016
148. Maus M V., Plotkin J, Jakka G, Stewart-Jones G, Rivière I, Merghoub T, Wolchok J, Renner C, Sadelain M. An MHC-restricted antibody-based chimeric antigen receptor requires TCR-like affinity to maintain antigen specificity. *Mol Ther - Oncolytics*. 2016;3(August):1-9. doi:10.1038/mto.2016.23
149. Oren R, Hod-Marco M, Haus-Cohen M, Thomas S, Blat D, Duvshani N, Denkberg G, Elbaz Y, Benchetrit F, Eshhar Z, Stauss H, Reiter Y. Functional Comparison of Engineered T Cells Carrying a Native TCR versus TCR-like Antibody–Based Chimeric Antigen Receptors Indicates Affinity/Avidity Thresholds. *J Immunol*. 2014;193(11):5733-5743. doi:10.4049/jimmunol.1301769
150. Zhao Q, Ahmed M, Tassev D V., Hasan A, Kuo TY, Guo HF, O'Reilly RJ, Cheung NKV. Affinity maturation of T-cell receptor-like antibodies for Wilms tumor 1 peptide greatly enhances therapeutic potential. *Leukemia*. 2015;29(11):2238-2247. doi:10.1038/leu.2015.125
151. Parker BS, Rautela J, Hertzog PJ. Antitumour actions of interferons: Implications for cancer therapy. *Nat Rev Cancer*. 2016;16(3):131-144. doi:10.1038/nrc.2016.14
152. Bruhns P. Properties of mouse and human IgG receptors and their contribution

to disease models. *Blood*. 2015;119(24):5640-5650. doi:10.1182/blood-2012-01-380121.5640
153. Shultz LD, Lyons BL, Burzenski LM, Gott B, Chen X, Chaleff S, Kotb M, Gillies SD, King M, Mangada J, Greiner DL, Handgretinger R. Human Lymphoid and Myeloid Cell Development in NOD/LtSz-scid IL2R null Mice Engrafted with Mobilized Human Hemopoietic Stem Cells. *J Immunol*. 2005;174(10):6477-6489. doi:10.4049/jimmunol.174.10.6477
154. Sockolosky JT, Dougan M, Ingram JR, Ho CCM, Kauke MJ, Almo SC, Ploegh HL, Garcia KC. Durable antitumor responses to CD47 blockade require adaptive immune stimulation. *Proc Natl Acad Sci*. 2016;113(19):E2646-E2654. doi:10.1073/pnas.1604268113
155. Purbhoo MA, Irvine DJ, Huppa JB, Davis MM. T cell killing does not require the formation of a stable mature immunological synapse. *Nat Immunol*. 2004;5(5):524-530. doi:10.1038/ni1058
156. Irvine DJ, Purbhoo MA, Krogsgaard M, Davis MM. Direct observation of ligand recognition by T cells. *Nature*. 2002;419(6909):845-849. doi:10.1038/nature01076
157. Sharma P, Allison JP. The future of Immune Checkpoint Inhibition. *Science (80-)*. 2014;348(6230).
158. Callahan MK, Wolchok JD, Allison JP. Anti-CTLA-4 antibody therapy: Immune monitoring during clinical development of a novel immunotherapy. *Semin Oncol*. 2010;37(5):473-484. doi:10.1053/j.seminoncol.2010.09.001
159. Kvistborg P, Philips D, Kelderman S, Hageman L, Ottensmeier C, Joseph-pietras D, Welters MJP, Burg S Van Der, Kapiteijn E, Michielin O, Romano E, Linnemann C, Speiser D, Blank C, Haanen JB, Schumacher TN. Anti – CTLA-4 therapy broadens the melanoma-reactive CD8 + T cell response. 2014;6(254):1-10.
160. Wolchok JD, Chiarion-Sileni V, Gonzalez R, Rutkowski P, Grob J-J, Cowey CL, Lao CD, Wagstaff J, Schadendorf D, Ferrucci PF, Smylie M, Dummer R, Hill A, Hogg D, Haanen J, Carlino MS, Bechter O, Maio M, Marquez-Rodas I, Guidoboni M, McArthur G, Lebbé C, Ascierto PA, Long G V., Cebon J, Sosman J, Postow MA, Callahan MK, Walker D, Rollin L, Bhore R, Hodi FS, Larkin J. Overall Survival with Combined Nivolumab and Ipilimumab in Advanced Melanoma. *N Engl J Med*. 2017:NEJMoa1709684. doi:10.1056/NEJMoa1709684
161. Roy S, Gupta P, Palit S, Basu M, Ukil A, Das PK. The role of PD-1 in regulation of macrophage apoptosis and its subversion by Leishmania donovani. *Clin Transl Immunol*. 2017;6(5):e137. doi:10.1038/cti.2017.12
162. Del Re M, Marconcini R, Pasquini G, Rofi E, Vivaldi C, Bloise F, Restante G, Arrigoni E, Caparello C, Bianco MG, Crucitta S, Petrini I, Vasile E, Falcone A, Danesi R. PD-L1 mRNA expression in plasma-derived exosomes is associated with response to anti-PD-1 antibodies in melanoma and NSCLC. *Br J Cancer*. March 2018. http://dx.doi.org/10.1038/bjc.2018.9.
163. Rosenberg JE, Hoffman-Censits J, Powles T, Van Der Heijden MS, Balar A V., Necchi A, Dawson N, O'Donnell PH, Balmanoukian A, Loriot Y, Srinivas S,

Retz MM, Grivas P, Joseph RW, Galsky MD, Fleming MT, Petrylak DP, Perez-Gracia JL, Burris HA, Castellano D, Canil C, Bellmunt J, Bajorin D, Nickles D, Bourgon R, Frampton GM, Cui N, Mariathasan S, Abidoye O, Fine GD, Dreicer R. Atezolizumab in patients with locally advanced and metastatic urothelial carcinoma who have progressed following treatment with platinum-based chemotherapy: A single-arm, multicentre, phase 2 trial. *Lancet*. 2016;387(10031):1909-1920. doi:10.1016/S0140-6736(16)00561-4

164. Antonia SJ, Villegas A, Daniel D, Vicente D, Murakami S, Hui R, Yokoi T, Chiappori A, Lee KH, de Wit M, Cho BC, Bourhaba M, Quantin X, Tokito T, Mekhail T, Planchard D, Kim Y-C, Karapetis CS, Hiret S, Ostoros G, Kubota K, Gray JE, Paz-Ares L, de Castro Carpeño J, Wadsworth C, Melillo G, Jiang H, Huang Y, Dennis PA, Özgüroğlu M. Durvalumab after Chemoradiotherapy in Stage III Non–Small-Cell Lung Cancer. *N Engl J Med*. 2017;377(20):1919-1929. doi:10.1056/NEJMoa1709937
165. Gaiser MR, Bongiorno M, Brownell I. PD-L1 Inhibition with Avelumab for Metastatic Merkel Cell Carcinoma. *Expert Rev Clin Pharmacol*. February 2018:null-null. doi:10.1080/17512433.2018.1445966
166. Wargo JA, Reddy SM, Reuben A, Sharma P. Monitoring immune responses in the tumor microenvironment. *Curr Opin Immunol*. 2016;41:23-31. doi:10.1016/j.coi.2016.05.006
167. Haanen JBAG. Converting Cold into Hot Tumors by Combining Immunotherapies. *Cell*. 2017;170(6):1055-1056. doi:10.1016/j.cell.2017.08.031
168. Sharma P, Hu-Lieskovan S, Wargo JA, Ribas A. Primary, Adaptive, and Acquired Resistance to Cancer Immunotherapy. *Cell*. 2017;168(4):707-723. doi:10.1016/j.cell.2017.01.017
169. Şenbabaoglu Y, Gejman RS, Winer AG, Liu M, Van Allen EM, de Velasco G, Miao D, Ostrovnaya I, Drill E, Luna A, Weinhold N, Lee W, Manley BJ, Khalil DN, Kaffenberger SD, Chen Y, Danilova L, Voss MH, Coleman JA, Russo P, Reuter VE, Chan TA, Cheng EH, Scheinberg DA, Li MO, Choueiri TK, Hsieh JJ, Sander C, Hakimi AA. Tumor immune microenvironment characterization in clear cell renal cell carcinoma identifies prognostic and immunotherapeutically relevant messenger RNA signatures [Genome Biology. 17, (2016) (231)] DOI: 10.1186/s13059-016-1092-z. *Genome Biol*. 2016;18(1):1-25. doi:10.1186/s13059-017-1180-8
170. Zuniga EI, Macal M, Lewis GM, Harker JA. Innate and Adaptive Immune Regulation During Chronic Viral Infections. *Annu Rev Virol*. 2015;2(1):573-597. doi:10.1146/annurev-virology-100114-055226
171. Woo SR, Corrales L, Gajewski TF. The STING pathway and the T cell-inflamed tumor microenvironment. *Trends Immunol*. 2015;36(4):250-256. doi:10.1016/j.it.2015.02.003
172. Woo SR, Fuertes MB, Corrales L, Spranger S, Furdyna MJ, Leung MYK, Duggan R, Wang Y, Barber GN, Fitzgerald KA, Alegre ML, Gajewski TF. STING-dependent cytosolic DNA sensing mediates innate immune recognition of immunogenic tumors. *Immunity*. 2014;41(5):830-842. doi:10.1016/j.immuni.2014.10.017

173. Corrales L, Glickman LH, McWhirter SM, Kanne DB, Sivick KE, Katibah GE, Woo SR, Lemmens E, Banda T, Leong JJ, Metchette K, Dubensky TW, Gajewski TF. Direct Activation of STING in the Tumor Microenvironment Leads to Potent and Systemic Tumor Regression and Immunity. *Cell Rep*. 2015;11(7):1018-1030. doi:10.1016/j.celrep.2015.04.031
174. Sagiv-Barfi I, Czerwinski DK, Levy S, Alam IS, Mayer AT, Gambhir SS, Levy R. Eradication of spontaneous malignancy by local immunotherapy. *Sci Transl Med*. 2018;10(426). doi:10.1126/scitranslmed.aan4488
175. Sade-Feldman M, Jiao YJ, Chen JH, Rooney MS, Barzily-Rokni M, Eliane JP, Bjorgaard SL, Hammond MR, Vitzthum H, Blackmon SM, Frederick DT, Hazar-Rethinam M, Nadres BA, Van Seventer EE, Shukla SA, Yizhak K, Ray JP, Rosebrock D, Livitz D, Adalsteinsson V, Getz G, Duncan LM, Li B, Corcoran RB, Lawrence DP, Stemmer-Rachamimov A, Boland GM, Landau DA, Flaherty KT, Sullivan RJ, Hacohen N. Resistance to checkpoint blockade therapy through inactivation of antigen presentation. *Nat Commun*. 2017;8(1). doi:10.1038/s41467-017-01062-w
176. Gettinger S, Choi J, Hastings K, Truini A, Datar I, Sowell R, Wurtz A, Dong W, Cai G, Melnick MA, Du VY, Schlessinger J, Goldberg SB, Chiang A, Sanmamed MF, Melero I, Agorreta J, Montuenga LM, Lifton R, Ferrone S, Kavathas P, Rimm DL, Kaech SM, Schalper K, Herbst RS, Politi K. *Impaired HLA Class I Antigen Processing and Presentation as a Mechanism of Acquired Resistance to Immune Checkpoint Inhibitors in Lung Cancer*. Vol 7.; 2017. doi:10.1158/2159-8290.CD-17-0593
177. Angell TE, Lechner MG, Jang JK, LoPresti JS, Epstein AL. MHC class I loss is a frequent mechanism of immune escape in papillary thyroid cancer that is reversed by interferon and selumetinib treatment in vitro. *Clin Cancer Res*. 2014;20(23):6034-6044. doi:10.1158/1078-0432.CCR-14-0879
178. Perea F, Sánchez-Palencia A, Gómez-Morales M, Bernal M, Concha Á, García MM, González-Ramírez AR, Kerick M, Martin J, Garrido F, Ruiz-Cabello F, Aptsiauri N. HLA class I loss and PD-L1 expression in lung cancer: Impact on T-cell infiltration and immune escape. *Oncotarget*. 2018;9(3):4120-4133. doi:10.18632/oncotarget.23469
179. Zaidi MR, Merlino G. The two faces of interferon-γ in cancer. *Clin Cancer Res*. 2011;17(19):6118-6124. doi:10.1158/1078-0432.CCR-11-0482
180. Bago JR, Okolie O, Dumitru R, Ewend MG, Parker JS, Werff R Vander, Underhill TM, Schmid RS, Miller CR, Hingtgen SD. Tumor-homing cytotoxic human induced neural stem cells for cancer therapy. *Sci Transl Med*. 2017;6510(February):1-14.
181. Roybal KT, Williams JZ, Morsut L, Rupp LJ, Kolinko I, Choe JH, Walker WJ, McNally KA, Lim WA. Engineering T Cells with Customized Therapeutic Response Programs Using Synthetic Notch Receptors. *Cell*. 2016;167(2):419-432.e16. doi:10.1016/j.cell.2016.09.011
182. Morsut L, Roybal KT, Xiong X, Gordley RM, Coyle SM, Thomson M, Lim WA. Engineering Customized Cell Sensing and Response Behaviors Using Synthetic Notch Receptors. *Cell*. 2016;164(4):780-791.

doi:10.1016/j.cell.2016.01.012
183. Eyquem J, Mansilla-Soto J, Giavridis T, Van Der Stegen SJC, Hamieh M, Cunanan KM, Odak A, Gönen M, Sadelain M. Targeting a CAR to the TRAC locus with CRISPR/Cas9 enhances tumour rejection. *Nature*. 2017;543(7643):113-117. doi:10.1038/nature21405
184. Ren J, Liu X, Fang C, Jiang S, June CH, Zhao Y. Multiplex genome editing to generate universal CAR T cells resistant to PD1 inhibition. *Clin Cancer Res*. 2017;23(9):2255-2266. doi:10.1158/1078-0432.CCR-16-1300
185. Dorfman JR, Zerrahn J, Coles MC, Raulet DH. The basis for self-tolerance of natural killer cells in beta2-microglobulin- and TAP-1- mice. *J Immunol*. 1997;159(11):5219-5225. http://www.ncbi.nlm.nih.gov/pubmed/9548460%5Cnhttp://www.jimmunol.org/content/159/11/5219.full.pdf.
186. Raulet DH, Vance RE. Self-tolerance of natural killer cells. *Nat Rev Immunol*. 2006;6(7):520-531. doi:10.1038/nri1863
187. Doorduijn EM, Sluijter M, Marijt KA, Querido BJ, van der Burg SH, van Hall T. T cells specific for a TAP-independent self-peptide remain naïve in tumor-bearing mice and are fully exploitable for therapy. *Oncoimmunology*. 2018;7(3). doi:10.1080/2162402X.2017.1382793
188. Reddehase MJ. Antigens and immunoevasins: Opponents in cytomegalovirus immune surveillance. *Nat Rev Immunol*. 2002;2(11):831-844. doi:10.1038/nri932
189. Verweij MC, Horst D, Griffin BD, Luteijn RD, Davison AJ, Ressing ME, Wiertz EJHJ. Viral Inhibition of the Transporter Associated with Antigen Processing (TAP): A Striking Example of Functional Convergent Evolution. *PLoS Pathog*. 2015;11(4):1-19. doi:10.1371/journal.ppat.1004743
190. Noriega V, Redmann V, Gardner T, Tortorella D. Diverse immune evasion strategies by human cytomegalovirus. *Immunol Res*. 2012;54(1-3):140-151. doi:10.1007/s12026-012-8304-8
191. Yura Y. Presage of oncolytic virotherapy for oral cancer with herpes simplex virus. *Jpn Dent Sci Rev*. 2017;53(2):53-60. doi:10.1016/j.jdsr.2016.10.001
192. Tomazin R, van Schoot NE, Goldsmith K, Jugovic P, Sempé P, Früh K, Johnson DC. Herpes simplex virus type 2 ICP47 inhibits human TAP but not mouse TAP. *J Virol*. 1998;72(3):2560-2563. http://www.pubmedcentral.nih.gov/articlerender.fcgi?artid=109564&tool=pmcentrez&rendertype=abstract.
193. Oosten LEM, Koppers-Lalic D, Blokland E, Mulder A, Ressing ME, Mutis T, van Halteren AGS, Wiertz EJHJ, Goulmy E. TAP-inhibiting proteins US6, ICP47 and UL49.5 differentially affect minor and major histocompatibility antigen-specific recognition by cytotoxic T lymphocytes. *Int Immunol*. 2007;19(9):1115-1122. doi:10.1093/intimm/dxm082
194. Garrido F, Aptsiauri N, Doorduijn EM, Garcia Lora AM, van Hall T. The urgent need to recover MHC class I in cancers for effective immunotherapy. *Curr Opin Immunol*. 2016;39:44-51. doi:10.1016/j.coi.2015.12.007
195. Cabrera T, Fernandez MA, Sierra A, Garrido A, Herruzo A, Escobedo A, Fabra

A, Garrido F. High Frequency of Altered HLA Class I Phenotypes in Invasive Breast Carcinomas. *Hum Immunol*. 1996;8859(96).
196. Sethumadhavan S, Silva M, Philbrook P, Nguyen T, Hatfield SM, Ohta A, Sitkovsky M V. Hypoxia and hypoxia-inducible factor (HIF) downregulate antigen-presenting MHC class I molecules limiting tumor cell recognition by T cells. *PLoS One*. 2017;12(11):1-18. doi:10.1371/journal.pone.0187314
197. Baker BM, Tortorella D. Dislocation of an endoplasmic reticulum membrane glycoprotein involves the formation of partially dislocated ubiquitinated polypeptides. *J Biol Chem*. 2007;282(37):26845-26856. doi:10.1074/jbc.M704315200
198. Czapski GA, Czubowicz K, Strosznajder RP. Evaluation of the antioxidative properties of lipoxygenase inhibitors. *Pharmacol Reports*. 2012;64(5):1179-1188. doi:10.1016/S1734-1140(12)70914-3
199. Mendoza MC, Er EE, Blenis J. The Ras-ERK and PI3K-mTOR pathways: Cross-talk and compensation. *Trends Biochem Sci*. 2011;36(6):320-328. doi:10.1016/j.tibs.2011.03.006
200. Manchado E, Weissmueller S, Morris JP, Chen CC, Wullenkord R, Lujambio A, de Stanchina E, Poirier JT, Gainor JF, Corcoran RB, Engelman JA, Rudin CM, Rosen N, Lowe SW. A combinatorial strategy for treating KRAS-mutant lung cancer. *Nature*. 2016;534(7609):647-651. doi:10.1038/nature18600
201. Hu D-E, Beauregard DA, Bearchell MC, Thomsen LL, Brindle KM. Early detection of tumour immune-rejection using magnetic resonance imaging. *Br J Cancer*. 2003;88(7):1135-1142. doi:10.1038/sj.bjc.6600814
202. Moore MW, Carbone FR, Bevan MJ. Introduction of soluble protein into the class I pathway of antigen processing and presentation. *Cell*. 1988;54(6):777-785. doi:10.1016/S0092-8674(88)91043-4
203. Hewitt EW, Gupta SS, Lehner PJ. The human cytomegalovirus gene product US6 inhibits ATP binding by TAP. *EMBO J*. 2001;20(3):387-396. doi:10.1093/emboj/20.3.387
204. Chew WL. Immunity to CRISPR Cas9 and Cas12a therapeutics. *Wiley Interdiscip Rev Syst Biol Med*. 2018;10(1):1-23. doi:10.1002/wsbm.1408
205. Charlesworth CT, Deshpande PS, Dever DP, Dejene B, Gomez-Ospina N, Mantri S, Pavel-Dinu M, Camarena J, Weinberg KI, Porteus MH. dentification of Pre-Existing Adaptive Immunity to Cas9 Proteins in Humans. *bioRxiv Prepr*. 2018.
206. Chaoul N, Fayolle C, Desrues B, Oberkampf M, Tang A, Ladant D, Leclerc C. Rapamycin impairs antitumor CD8p T-cell responses and vaccine-induced tumor eradication. *Cancer Res*. 2015;75(16):3279-3291. doi:10.1158/0008-5472.CAN-15-0454
207. Das K, Eisel D, Lenkl C, Goyal A, Diederichs S, Dickes E, Osen W, Eichmuller SB. Generation of murine tumor cell lines deficient in MHC molecule surface expression using the CRISPR/Cas9 system. *PLoS One*. 2017;12(3):e0174077. doi:10.1371/journal.pone.0174077
208. Campbell KS, Hasegawa J. Natural killer cell biology: an update and future directions. *J Allergy Clin Immunol*. 2013;132(3):536-544.

doi:10.1016/j.jaci.2013.07.006
209. Stern-Ginossar N, Mandelboim O. An integrated view of the regulation of NKG2D ligands. *Immunology*. 2009;128(1):1-6. doi:10.1111/j.1365-2567.2009.03147.x
210. Van Hall T, Wolpert EZ, Van Veelen P, Laban S, Van Der Veer M, Roseboom M, Bres S, Grufman P, De Ru A, Meiring H, De Jong A, Franken K, Teixeira A, Valentijn R, Drijfhout JW, Koning F, Camps M, Ossendorp F, Kärre K, Ljunggren HG, Melief CJM, Offringa R. Selective cytotoxic T-lymphocyte targeting of tumor immune escape variants. *Nat Med*. 2006;12(4):417-424. doi:10.1038/nm1381
211. Doorduijn EM, Sluijter M, Querido BJ, Oliveira CC, Achour A, Ossendorp F, Van Der Burg SH, Van Hall T. TAP-independent self-peptides enhance T cell recognition of immune-escaped tumors. *J Clin Invest*. 2016;126(2):784-794. doi:10.1172/JCI83671
212. Ataie N, Xiang J, Cheng N, Brea EJ, Lu W, Scheinberg DA, Liu C, Ng HL. Structure of a TCR-Mimic Antibody with Target Predicts Pharmacogenetics. *J Mol Biol*. 2016;428(1):194-205. doi:10.1016/j.jmb.2015.12.002
213. Cameron BJ, Gerry AB, Dukes J, Harper J V, Kannan V, Bianchi FC, Grand F, Brewer JE, Gupta M, Plesa G, Bossi G, Vuidepot A, Powlesland AS, Legg A, Adams KJ, Bennett AD, Pumphrey NJ, Williams DD, Binder-Scholl G, Kulikovskaya I, Levine BL, Riley JL, Varela-Rohena A, Stadtmauer EA, Rapoport AP, Linette GP, June CH, Hassan NJ, Kalos M, Jakobsen BK. Identification of a Titin-Derived HLA-A1 – Presented Peptide as a Cross-Reactive Target for Engineered MAGE A3 – Directed T Cells. *Sci Transl Med*. 2013;5(197):197ra103-197ra103. doi:10.1126/scitranslmed.3006034